National Library of Canada
Acquisitions and Bibliographic Services Branch
395 Wellington Street
Ottawa, Ontario
K1A 0N4

Bibliothèque nationale du Canada
Direction des acquisitions et des services bibliographiques
395, rue Wellington
Ottawa (Ontario)
K1A 0N4

Your file Votre référence

Our file Notre référence

NOTICE

The quality of this microform is heavily dependent upon the quality of the original thesis submitted for microfilming. Every effort has been made to ensure the highest quality of reproduction possible.

If pages are missing, contact the university which granted the degree.

Some pages may have indistinct print especially if the original pages were typed with a poor typewriter ribbon or if the university sent us an inferior photocopy.

AVIS

La qualité de cette microforme dépend grandement de la qualité de la thèse soumise au microfilmage. Nous avons tout fait pour assurer une qualité supérieure de reproduction.

S'il manque des pages, veuillez communiquer avec l'université qui a conféré le grade.

La qualité d'impression de certaines pages peut laisser à désirer, surtout si les pages originales ont été dactylographiées à l'aide d'un ruban usé ou si l'université nous a fait parvenir une photocopie de qualité inférieure.

Canada

EFFECTS OF CHEST WALL CONFIGURATION AND ELECTRODE POSITIONING ON HUMAN DIAPHRAGMATIC EMG

JENNIFER BECK

A thesis submitted to
the Faculty of Graduate Studies and Research
in partial fulfilment of the requirements for the degree of
Master of Science

Department of Physiology
and
Meakins Christie Laboratories
McGill University
Montreal, Quebec, Canada
October, 1994

ISBN 0-612-00002-8

Canada

ABSTRACT

The measurement and analysis of the human diaphragm electromyogram (EMGdi), as obtained with an esophageal electrode, requires objective control of the disturbances and filtering effects which can influence the signal. One issue of importance is that an increase in the muscle-to-electrode distance (MEdist) acts as a low-pass filter, filtering out the high frequency components of the EMG power spectrum (the MEdist filter). Due to the numerous factors which can influence the EMGdi, control of signal quality is also of utmost importance. The aims of this study were: (1) to evaluate the effect of the MEdist filter on EMGdi, as measured with a multiple array esophageal electrode, (2) to take advantage of the MEdist filter in order to locate the position of the diaphragm with respect to the electrodes, and (3) to evaluate the influence of changes in chest wall configuration on EMGdi center frequency (CF) values, while controlling for both signal quality and the MEdist filter.

Five normal male subjects performed static contractions of the diaphragm at seven pre-determined chest wall configurations. The EMGdi was measured with an array of eight steel rings mounted on a catheter, forming seven sequential pairs of electrodes, with an interelectrode distance of 10 mm. EMGdi signal quality was evaluated by computer algorithms. The pair of electrodes whose EMGdi signals (and power spectrums) were the least influenced by the MEdist filter was assumed to be closest to the diaphragm.

The results of the study indicated (1) EMGdi power spectrums and their associated CF values were strongly affected by the position of the diaphragm with respect to the multiple array esophageal electrode. CF decreased by approximately 1 Hz per mm displacement away from the diaphragm. (2) By controlling for the MEdist filter, there was no relationship found between changes in chest wall configuration and CF values. These data demonstrate that changes in chest wall configuration, and hence diaphragm length, do not influence the CF values of the EMGdi, if the distance between the electrodes and the diaphragm and signal quality are controlled for.

RESUMÉ

L'enregistrement de l'électromyogramme du diaphragme (EMGdi) humain, avec un électrode esophagien, demande le controle objectif des perturbances et des filtres qui puissent influencer le signal. Une affaire d'importance est qu'une augmentation de la distance entre le muscle et les électrodes (distME) est similaire à un filtre de type "low-pass", où les composantes de haute fréquence sont éliminées (filtre distME). En plus, à cause des nombreuses facteurs qui puissent influencer l'EMGdi, il est de la première importance que la qualité du signal soit controlée. Cette étude a été mise en oeuvre pour : (1) évaluer l'effet du filtre distME sur l'EMGdi avec un électrode esophagien composé d'une série d'électrodes, (2) prendre avantage du filtre distME pour déterminer la position du diaphragme par rapport aux électrodes, et (3) évaluer l'effet de la configuration de la cage thoracique sur la fréquence moyenne (FM) du spectre de fréquence de l'EMGdi, en controllant la qualité du signal et le filtre distME.

Cinq sujets masculins ont réalisé des contractions volontaires du diaphragme non-fatiguantes, dans sept différentes configurations de la cage thoracique. L'EMGdi a été enregistré grâce à un dispositif esophagien composée d'une séquence de sept paires d'électrodes annulaires, chaque électrode étant séparée d'une distance de 10 mm. La FM et le spectre de fréquence ont été calculés pour chaque paire d'électrodes. La qualité des signaux a été évalué avec des logiciels qui éliminent les segments d'EMG parasités. La paire d'électrodes qui était la moins influencée par le filtre distME a été nommée "la paire optimale", et a été présumée être la paire d'électrodes la plus proche du diaphragme.

Les résultats de cette étude indiquent: (1) les spectres de fréquence de l'EMGdi et les FM associées, sont extrèmement influencés par la position du diaphragme par rapport aux électrodes. FM diminua par 1 Hz par mm de déplacement des électrodes du diaphragme. (2) En controllant le filtre distME, les FM obtenues étaient comparables entre-elles.

Ces résultats indiquent que les changements de la configuration de la cage thoracique, et donc les changements de la longueur du diaphragme, n'influencent pas les valeurs de FM de l'EMGdi.

ACKNOWLEDGEMENTS

This work was carried out at Hôpital Notre-Dame de Montreal, in the department of Respiratory Physiology. To my supervisor, Dr. Alex Grassino, I express my sincere gratitude for his stimulating advice and constructive criticism, which has been of great value to me. What I have learned from Alex over the last three years will serve me well as I pursue a future career in science.

To Professor Lars Lindström, I am extremely grateful for his involvement in the project, as well as for providing me with the tools to accomplish this work.

The investigation has been made in close collaboration with Dr. Christer Sinderby, whom I cannot thank sufficiently for his constant, unselfish help and support. My thanks are due to Norman Comtois for helping me with the experiments, and for his support, both technical and emotional, throughout the last three years. I am especially grateful to Mr. Robert Thomson from the Meakins Christie Laboratories for constructing the multiple array esophageal electrode, and for repairing any of the equipment as was needed. Special thanks to Jan Weinberg from Stockholm, Sweden, and Dario Caldiroli, from Milan, Italy, who helped me in the early stages of the experiments.

I would like to express my thanks to those who patiently acted as experimental subjects. Thanks to Alain Comtois, Juan Galdiz, and Joaquim Gea for reviewing sections of the thesis. Finally, thank you to Belsis Diaz, Adriana Spahija, Igor Salazkin, Ercheng Zhu, and everyone in the pulmonary function lab for their patience, kind help and support.

TABLE OF CONTENTS

ABBREVIATIONS

AB	Abdomen
BIN	Belly-in
CF	Center frequency
CMAP	Compound muscle action potential
CSA	Cross-sectional area
CV	Conduction velocity of action potentials
DP	Drop in power ratio
ECG	Electrocardiogram
EMG	Electromyogram
EMGdi	Electromyogram of the diaphragm
EPP	End-plate potential
FFT	Fast Fourier transform
FRC	Functional residual capacity
IC	Inspiratory capacity
l_o	Optimal muscle length
M_n	Spectral moment of order n
MEdist	Muscle to electrode distance
MEdist filter	Muscle to electrode distance filter
MF	Median frequency
MUAP	Motor unit action potential
MUAPT	Motor unit action potential train
RC	Rib cage
RLX	Relaxation curve
RMS	Root-mean-square
SM	Signal to motion artifact ratio
SN	Signal to noise ratio
SR	Sarcoplasmic reticulum
TLC	Total lung capacity
ω	Power spectrum shape index

CHAPTER 1

INTRODUCTION

The electromyogram of the diaphragm (EMGdi) - the electrical activity manifested during diaphragmatic contractions - can be recorded via an esophageal electrode placed at the level of the gastro-esophageal junction. Development of diaphragmatic fatigue has been associated with a shift of the EMGdi power spectrum to lower frequencies, as observed experimentally in normal subjects (Bellemare & Grassino, 1982; Gross et al, 1979), and in patients with respiratory disorders (Bellemare & Grassino, 1983; Brochard et al, 1989; Muller et al, 1979). Due to a lack of standards in recording techniques (and the cumbersome analysis which is involved), EMGdi has not gained widespread use in the clinical setting. The work presented in this thesis is one step towards the development of an automatized method to accurately detect diaphragmatic fatigue. Due to the limited number of publications which specifically evaluate the methodological issues presented in this thesis, reference to parallel studies performed in our laboratory (although not yet peer reviewed) are included where appropriate.

In order for the EMGdi power spectrum to accurately reflect the development of diaphragmatic fatigue, all factors which influence it, physical as well as physiological, must be identified and controlled for. Previous reports have suggested that lung volume and chest wall configuration influence the EMGdi signal (Gandevia & McKenzie, 1986). The authors stated that esophageal recordings of EMGdi are unreliable as a method to evaluate diaphragmatic fatigue due to an "artifact" created by lung volume and chest wall configuration. The possibility that their results were due to changes in muscle-to-electrode distance cannot be excluded.

Signal theory predicts that an increase in distance between the muscle and the electrodes will filter the EMG signal in such a way that the high frequency components are filtered out, in a similar fashion to that of a low pass filter (Lindström, 1970). Increasing the muscle-to-electrode distance will therefore affect the power spectrum and its associated measurements. Hence, control of the muscle-to-electrode distance is crucial in the analysis

and interpretation of the EMGdi power spectrum.

The objectives of this study were 1) to take advantage of the muscle-to-electrode distance filter in order to locate the position of the diaphragm with respect to a multiple array esophageal electrode, and 2) to evaluate the effects of chest wall configuration on the EMGdi power spectrum, while controlling for the muscle-to-electrode distance. An important aspect of this study is the additional control for signal quality throughout the analysis.

A literature review relevant to this study is presented in chapters 2, 3 and 4. Chapter 2 is a brief review of the anatomy and physiology of skeletal muscle. Where appropriate, reference to the diaphragm is included. Chapter 3 is a description of the electromyogram in both the time and frequency domain, introduces concepts used in spectral analysis, and provides a review of the numerous physical and physiological factors which can influence the signal. Chapter 4 provides the background which is relevant to the methodology used in this study, and includes a brief description of the functional anatomy of the diaphragm, a description of the methods used to evaluate the chest wall and to record EMGdi, and the specific factors which have been suggested to influence esophageal recordings of EMGdi.

Chapter 5 is a presentation of the work completed for this thesis in a manuscript format, entitled "Effects of electrode positioning and chest wall configuration on the human diaphragm EMG". It includes sections for an introduction, methodology, results and a discussion.

Chapter 6 summarizes the conclusions from this study, and proposes some ideas for future work in the field of diaphragm electromyography, for the purpose of evaluating diaphragmatic fatigue.

CHAPTER 2

ANATOMY AND PHYSIOLOGY OF SKELETAL MUSCLE

Three different types of muscles can be characterized on the basis of their structural and contractile properties, namely skeletal muscle, smooth muscle, and cardiac muscle. As the diaphragm is morphologically and functionally a skeletal muscle, the following discussion will be devoted to this type of muscle; special reference to the diaphragm will be included where appropriate. This chapter includes a review of the anatomy and physiology of skeletal muscle which is relevant to the work presented in this thesis.

2.1. ANATOMY OF SKELETAL MUSCLE

2.1.1. Gross anatomy of skeletal muscle

Skeletal muscle is composed of individual muscle cells, or muscle fibers (Figure 2.1.A-C), which contract by converting chemical energy into mechanical energy. Each fiber is in turn made up of successively smaller sub-units, also illustrated in Figure 2.1., and are described in subsequent sections (Section 2.1.2.(i) through (iii)).

Bundles of muscle fibers are bound together in parallel by sheets of fascia to form the muscle (Fawcett, 1986). The fascia surrounding the entire muscle is the epimysium; the fascia which penetrates into the muscle and separates it into bundles, or fasciculi, is the perimysium; the endomysium is a thin extension of fascia which surrounds each individual muscle fiber. The different fascias join together at the ends of the muscle where they form tendons, attaching the muscle to bone. Blood vessels and nerves penetrate through these fascial sheaths in order to supply the individual muscle fibers. The capillary beds are located exclusively between the muscle fibers, and are the site for the exchange of energy substrates between the systemic blood supply and the muscle fibers (Enad et al, 1989).

Each muscle fiber is innervated by a branch of a motor neuron (Sherington, 1925). The motor neuron endings are concentrated in regions known as innervation zones (Goodgold &

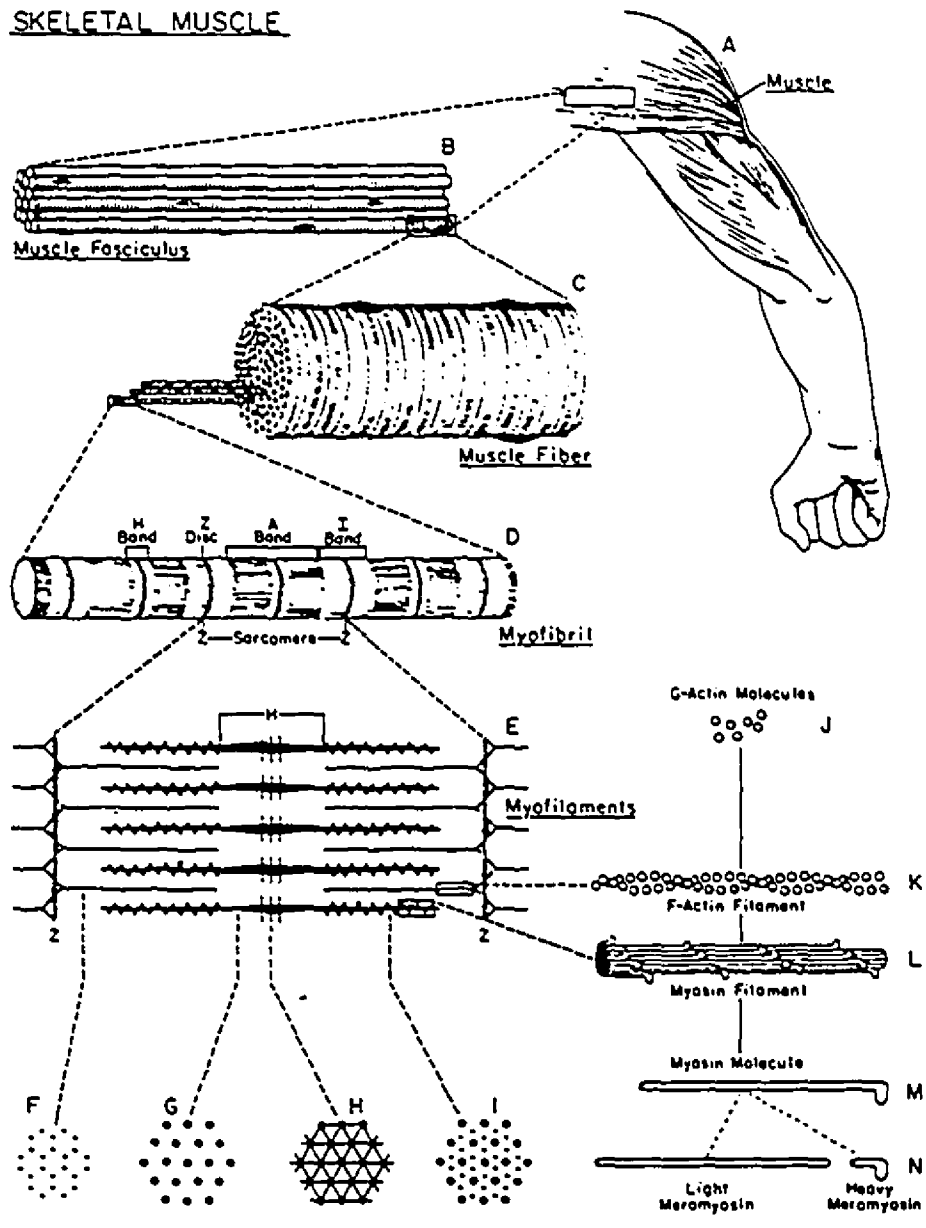

Figure 2.1. Diagram of the organization of skeletal muscle from the gross to the molecular level (From Fawcett, 1986)

Eberstein, 1983). Innervation zones were originally reported to lie near the central portion of the muscle (Coërs & Woolf, 1959), however, recent evidence suggests that the innervation zones can be scattered throughout the muscle (Masuda et al, 1983; Roy et al, 1986). It has been demonstrated with histochemical staining that the innervation zones in the rat diaphragm are organized in a single band, normal to the fiber orientation, along the whole surface of the muscle (Gordon et al, 1989). In contrast, several bands of innervation zones are present in the diaphragm of larger animals (Gordon et al, 1989). In humans, anatomical descriptions of the crural (and/or costal) diaphragm's innervation exist in the literature, but are limited to the point of insertion of the respective phrenic branches into the muscle. et al (1969) described a profuse and clear-cut innervation of the crural diaphragm which bounded the esophagus anterolaterally, more so on the left side than the right.

2.1.2. Anatomy of the muscle fiber

Muscle fibers are multinucleated cells, which have a diameter of 10-200 μm (depending on the species and the particular muscle examined), and a length of up to several cm (Fawcett, 1986). In humans, muscle fiber diameters range from 40 to 80 μm, as measured in 50 muscle sites in six normal male autopsy subjects (Polgar et al, 1973). In the human diaphragm, muscle fiber size was reported to be in the range of 55-60 μm in the costal portion, and 45-51 μm in the crural portion (Sanchez et al, 1985). In the canine diaphragm, muscle fiber diameters can range from 34 to 53 μm (Reid et al, 1987). As later described (see Chapter 3, Section 3.2.), fiber diameter plays an important role in muscle fiber action potential conduction velocity (Häkansson, 1957a,b).

(i) The sarcolemma:

The muscle fiber is bounded by a cell membrane, the sarcolemma, which is an excitable membrane similar to the nerve cell membrane, and is responsible for the selective permeability characteristics of the cell surface. The sarcolemma consists of an outermost basement membrane (basal lamina), and a lipid bilayer plasma membrane (Carpenter & Karpati, 1984).

The function of the basal lamina, composed mainly of collagen, is to provide external mechanical support for the fiber and to facilitate muscle fiber regeneration (Vracko, 1974). The main function of the plasma membrane, containing both sodium and potassium ion channels, is to conduct the wave of depolarization which initiates muscle contraction (Kirchberger, 1990).

(ii) Myofibrils, the transverse tubules, and the sarcoplasmic reticulum:

Muscle fibers can be further subdivided into a bundle of myofibrils, which are typically 1-2 μm in diameter (Fawcett, 1986) and extend the length of the muscle fiber (Figure 2.1.D). Myofibrils do not possess membranes but are separated by a surrounding network of tubes and sacs, which has two parts, the transverse tubules (T-tubules) and the sarcoplasmic reticulum (SR) (Figure 2.2.).

The T-tubules are tubular invaginations of the sarcolemma containing extracellular fluid (Peachey & Adrian, 1973), and are therefore a part of the fiber surface membrane. They serve to conduct the muscle fiber action potential (travelling along the membrane) into the interior of the muscle fiber. The myofibrils at the centre of the muscle fiber and those near the sarcolemma are thus activated almost simultaneously.

The SR is an intracellular membranous network of longitudinal tubules and sacs that run parallel to the myofibrils and terminate in chambers, or terminal cisternae, that abut the transverse tubule. The SR contains intracellular fluid, with a high concentration of calcium. The functions of the SR include the release of calcium during muscle contraction, and the re-uptake and storage of calcium during relaxation (Martonosi, 1982).

The three-component structure formed by the two terminal cisternae of the SR with the T-tubule is known as a triad. The triad is the site at which the electrical signal propagated along the T-tubule is converted into a signal for the release of calcium from the SR (Cullen & Landon, 1988). For further details on the function of the T-tubules and the SR, see Section 2.3.4.

(iii) Myofilaments and the sarcomere

Under the microscope, myofibrils can be seen to be composed of two types of

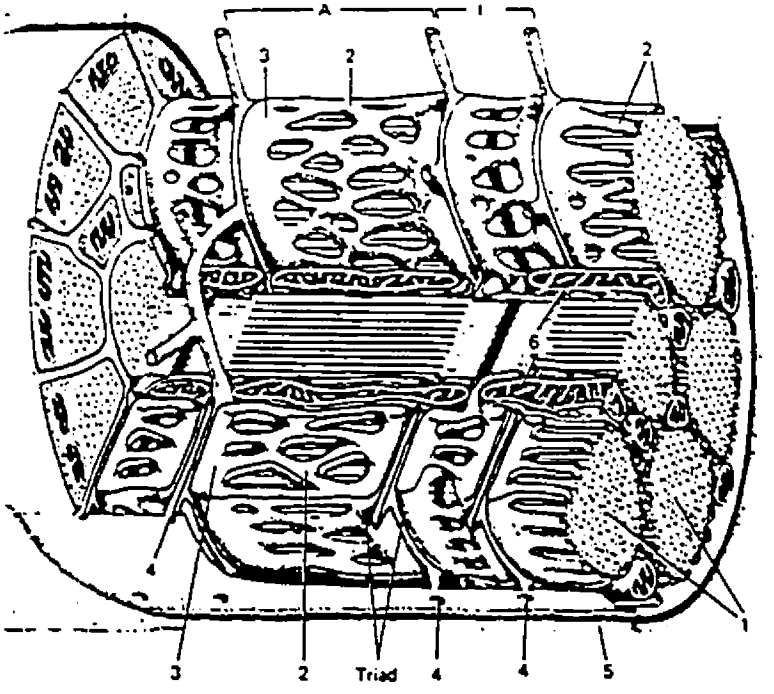

Figure 2.2. A single mammalian skeletal muscle fiber surrounded by its sarcolemma has been cut away to show individual myofibrils (1). The sarcoplasmic reticulum (2) with its terminal cisternae (3) surrounds each myofibril. The T-tubules (4) are also presented. A basal lamina (5) surrounds the sarcolemma. (From Ganong, 1991)

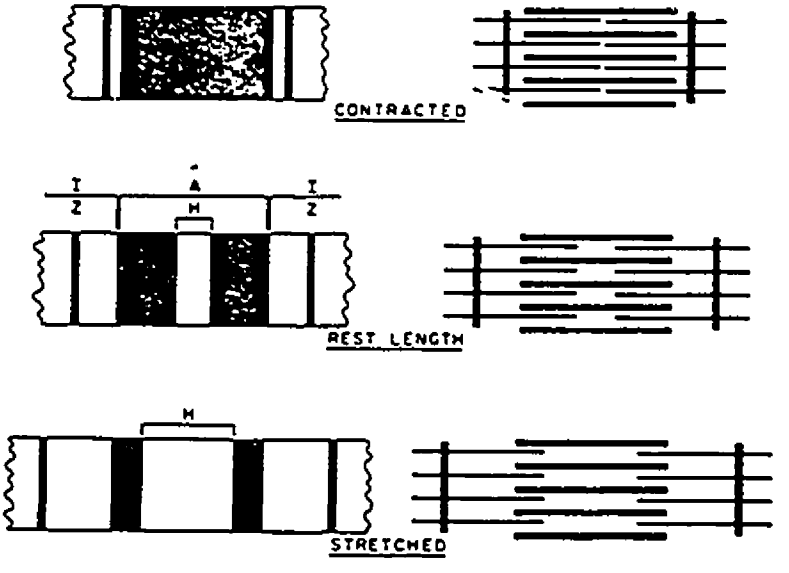

Figure 2.3. Left: A schematic representation of the changing appearance of the cross-striations in different phases in contraction. Right: The differing degrees of interdigitating thick and thin filaments corresponding to the different patterns of striations. (From Fawcett, 1986).

myofilaments (Figure 2.1.E), the thick and thin filaments (Fawcett, 1986). The thick filaments (10.7 nm in diameter) are mainly composed of bundles of myosin molecules (Figure 2.1.L). Each myosin molecule has a head region and a tail region (Figure 2.1.N). The thin filaments are chains of actin molecules existing in two forms: G-actin (Figure 2.1.J), and F-actin (Figure 2.1.K), a fibrous protein which is a polymer of G-actin. Actin molecules are associated with two other proteins, troponin, composed of three subunits, T, C, and I, and tropomyosin. Each troponin complex is bound to a tropomyosin molecule. While only actin and myosin are involved in tension generation, the troponin-tropomyosin complex are known to regulate the actin-myosin interaction, and hence are referred to as regulatory proteins (Kirchberger, 1990).

Myofibrils are composed of alternating transverse light (I band) and dark bands (A band) which are responsible for the striated appearance of skeletal muscle (Figure 2.1.D). The A bands (1.5-1.6 μm long) are formed by the lining up of the thick filaments (myosin), whereas the less dense I band is formed by an array of the thin filaments (actin, troponin, and tropomyosin) which do not overlap the thick filaments. The length of the I band is variable and depends on the state of contraction of the fiber. Crossing down the middle of each I band is a dense, fibrous Z-line, which contains the protein alpha-actinin (Masaki et al, 1967). The Z-lines divide the myofibrils into repeating segments, or sarcomeres. In the centre of the sarcomere is the H zone which is the region where, when the muscle is relaxed, the thin filaments do not overlap the thick filaments. A narrow dark band can be seen in the centre of the H zone; this is known as the M line (Knappeis & Carlsen, 1968), and is produced by linkages between adjacent thick filaments. The resting length of a sarcomere is in the range of 2.3-2.6 μm in many vertebrate skeletal muscles (Huxley, 1985). Sarcomeres are arranged in series to make up the length of the myofibril. In the costal part of the hamster diaphragm, approximately 5000 sarcomeres are needed to span the distance from the origin at the central tendon to the insertion on the costal margin (Farkas & Roussos, 1982; Kelsen et al, 1983).

A cross section through a myofibril in the region of the A band, where both thick and thin filaments overlap, shows a regular arrangement (Huxley & Brown, 1967). Each thick filament is surrounded by a hexagonal array of six thin filaments, and each thin filament is surrounded

by a triangular arrangement of three thick filaments (Figure 2.1.F-I).

2.1.3. Muscle fiber types

It is now generally accepted that muscle fibers can be divided into different types, based on their mechanical, morphological, and biochemical properties (Kandell & Schwartz, 1985). Important differentiating characteristics include enzymatic properties demonstrated by histochemical studies (Henneman & Olson, 1965), the velocity and force of contraction (and relaxation) (Peter et al, 1972), and the degree of fatigability (Burke et al, 1973; Edstrom & Kukelberg, 1968). Table 2.1. gives a summary of the fiber type classification systems, as well as the characteristics of the different types of fibers.

Muscle fibers can be divided into two types, slow (Type I) and fast (Type II). Slow (red) muscle fibers contract and relax slower than fast fibers, and generate low levels of force. Slow muscle fibers have a red appearance due to their high myoglobin content. According to Kimura (1983) and Guyton (1991), they are generally smaller in diameter than the fast fibers. However, in the canine diaphragm, the fiber diameters of the slow and fast fibers are not significantly different (Reid et al, 1987). In fact, there seems to be controversy in the literature concerning the size of muscle fibers in relation to their fiber type (Polgar et al, 1973; Sanchez et al, 1985). Slow fibers are highly vascularized, contain a lot of mitochondria, and utilize oxidative metabolism. They are therefore quite resistant to fatigue and are specialized for low tension, endurance-type contractions. Fast (white) muscle fibers, on the other hand, contract and relax rapidly following stimulation, and are capable of generating a large amount of force. These fibers are large in diameter (Guyton, 1986), are poorly vascularized, and rely on glycolysis for their energetic requirements. Hence, fast fibers are rapidly fatigable. The fast fatigable fibers (FF) are often referred to as Type IIB. A fast, fatigue-resistant fiber (FR), has also been described which depends on both oxidative and glycolytic metabolisms, and is often referred to as Type IIA.

In general, the velocity of contraction of a muscle fiber is dependent on the particular species of the contractile proteins (eg. type of myosin isoforms) (Pette & Vrbova, 1985). The

relaxation rate of the muscle fibers depends on the rate of calcium re-uptake by the SR following contraction. Fast muscle fibers have a more extensive SR than the slow ones (Eisenberg & Kuda, 1976), and therefore the relaxation times are shorter. The fatigability of a muscle fiber is dependent on its metabolic properties as well as the extent of its blood supply (Burke et al, 1973; Edstrom & Kukelberg, 1968).

The human diaphragm has a very heterogeneous fiber population, composed of approximately 55% S fibers, 21% FR fibers, and 24% FF fibers (Lieberman et al, 1973), as obtained from the costo-ventral portion of the diaphragm *in vivo* during surgery. The proportions of muscle fiber types in the diaphragm vary between the different mammalian species (Reid et al, 1987).

2.1.4. The motor unit

Skeletal muscle fibers are innervated by α-motor neurons originating in the anterior horn of the spinal cord. The axons of the α-motor neuron extend peripherally to the muscles, and the terminal branches reach the muscle fiber in a localized region known as the end-plate region. In 1925, Sherington coined the term "motor unit" to describe the smallest functional unit that can be controlled by the nervous system, and defined the motor unit as being a single motor neuron and the muscle fibers it innervates.

The actual number of muscle fibers innervated by a single motor neuron varies according to the function served by the muscle (Basmajian, 1973). Motor units that control fine movements (for example those of the eye muscles), consist of only a few muscle fibers, and are considered small motor units. In contrast, there are a few thousand fibers in the (large) motor units of postural muscles (for example the back muscles). The muscle fibers belonging to one motor unit are not localized to any one specific region of the muscle, but are rather intermingled throughout the muscle (van Harreveld, 1947; Norris & Irwin, 1961), as observed with staining procedures. The scattering of muscle fibers belonging to a given motor unit has been confirmed using single fiber electromyography (Ekstedt, 1964).

The muscle fibers within a given motor unit have the same histochemical and

mechanical properties (Edstrom & Kukelberg, 1968; Pette & Vroba, 1985; Salmons & Sreter, 1976). Furthermore, it is hypothesized that these properties are regulated by the activity pattern imposed on the motor unit by the motor neuron. As a result of the above, motor units are characterized, or classified, by the same criteria as muscle fibers. In 1974, Burke et al made detailed histochemical and mechanical studies of the motor units of the cat hindlimb muscle. On the basis of twitch contraction time, twitch relaxation time, and a fatigue index (ratio of the final to initial force after three minutes of intermittent tetanic stimulation), most motor units could be separated into the three groups: FF (fast-twitch, fatigable), FR (fast-twitch, fatigue-resistant), and S (slow-twitch, fatigue-resistant). An unclassified motor unit type, designated Type FI, with a fast twitch and an intermediate fatigue resistance, has since proven to appear consistently in cat hind-limb muscles (Clamann, 1993). The fatigability of a motor unit has been shown to be correlated with the metabolic properties of the muscle fibers which make it up (Burke et al, 1973; Edstrom & Kukelberg, 1968). It should be noted, however, that muscle fiber typing distinctions appear to be more clearly apparent in animals than in human muscles, and therefore, motor unit classification in humans is more complex (Basmajian & De Luca, 1985).

2.2. PHYSIOLOGY OF SKELETAL MUSCLE

2.2.1. Sliding filament model of muscle contraction

Huxley & Hanson (1954) and Huxley & Nierdergerke (1954) examined single muscle fibers at the microscopic level during their relaxed state, during contraction, and during a stretched state, and observed that as the fiber became shorter, the thick and thin filaments slid past each other, but their individual lengths did not change (Figure 2.3.). This explains why the width of the A band remains constant during a contraction, corresponding to the constant length of the thick filaments. In contrast, these same authors observed that the widths of both the I band and the H zone decreased during shortening, as the thin filaments moved past the thick filaments. These observations of the changes in banding pattern during a contraction led to the sliding filament theory of contraction which states that muscle shortening results from

the relative movement of the thick and thin filaments past each other.

2.2.2. Crossbridge theory of contraction

The sliding filament model, although accepted as a valid one, does not reveal how tension is developed and how the sarcomere shortens. A possible explanation for this was provided by Huxley in 1957, who observed "crossbridges" projecting from the surface of the myosin molecules towards the actin filaments. It is now known that each crossbridge consists of the globular heads of the myosin (S_1 subfragment) and an α-helical tail (S_2 subfragment) by which the crossbridges attach to the thick filament (Elliot & Offer, 1978). It was subsequently proposed that these crossbridges could provide the necessary physical link between the two sets of filaments and that the sliding force was produced by a change in the conformation of the crossbridges while they were attached to the actin filament. It is now generally believed that the crossbridges go through a cyclic interaction with actin in which they first attach to actin, then swing on actin, causing the interacting filaments to slide, and then detach, ready for another attachment cycle further along the actin filament (Huxley & Simmons, 1971). These events are collectively known as crossbridge cycling, the rate of which is dependent on such factors as temperature and type of myosin isoform (Close, 1972). Subsequent experiments over the last three decades, by a variety of techniques, have confirmed the validity of the crossbridge theory of contraction (Huxley, 1985).

2.2.3. Excitation-contraction coupling

Traditionally, excitation-contraction coupling was originally defined as the process linking electrical excitation (depolarization) of the muscle membrane to contraction. More recently, the term has been used to describe coupling between depolarization of the T-tubule membrane and calcium release from the SR (Rios & Pizarro, 1991). A detailed description of the steps involved in the excitation-contraction process can be found below (steps 2.3.4.-2.3.6.).

2.3. EVENTS OCCURRING DURING A MUSCLE CONTRACTION

The initiation and execution of muscle contraction occurs in the following sequential steps:

2.3.1. When the motor nerve is stimulated, an action potential travels along the nerve to the nerve terminal where the transmitter, Acetylcholine (Ach), is released as equalized multimolecular "packets", or quanta (Katz, 1966). At rest, these packets are liberated at a frequency of approximately one per second. These spontaneously released packets Ach act on a local area of the muscle fiber membrane, the end plate region, and initiate minute transient non-propagated depolarizing potentials, the so-called miniature end-plate potentials (Fatt & Katz, 1952). When an action potential in the motor nerve arrives at the nerve endings, they are almost instantaneously depolarized and a large number of Ach packets are immediately liberated into the synaptic cleft. The number of packets which are liberated by a single nerve action potential has been estimated to be about one hundred (Del Castillo & Katz, 1954).

2.3.2. Ach acts post-synaptically on the end-plate region of the muscle to open multiple Ach-gated protein channels (or Ach receptors) located in the muscle fiber membrane. Opening of Ach-gated channels in the membrane increases the permeability of the motor end plate to sodium and potassium ions, producing a local depolarization, the end-plate potential (EPP).

2.3.3. If the EPP depolarizes the muscle membrane to its threshold potential, an action potential will be initiated which will propagate along the length of the muscle cell membrane, in the same way that action potentials travel along nerve membranes (see Chapter 3, Section 3.2.4.). Ach is meanwhile hydrolyzed into choline by the enzyme acetylcholinesterase. Choline is taken up by ne nerve terminals and used to re-synthesize Ach via the enzyme acetyltransferase (Slater & Harris, 1988).

There are three important differences between EPPs and muscle fiber action potentials triggered by the EPP (Wray, 1988). The EPP can only be recorded in the region of the end-plate since its amplitude dissipates passively within a few mm from the postsynaptic region (Fatt & Katz, 1951). This is unlike the muscle action potential which is propagated with a constant amplitude along the entire fiber membrane. Secondly, the EPP is a graded potential,

whose amplitude depends on the amount of Ach released from the nerve terminal; the action potential, on the other hand, is an all-or-nothing regenerative response. Thirdly, channels are opened chemically at the end-plate (Anderson & Stevens, 1973) whereas the channels producing the muscle action potential are opened by electrical changes in the membrane (Hodgkin & Huxley, 1952).

2.3.4. The muscle fiber action potential depolarizes the T-tubules and travels deeply within the muscle fiber. This is not a simple spread of electrical activity from the surface action potential, but rather an inward transmission via the same process which occurs during propagation of the action potential along the membrane (Constantin, 1970). This depolarization causes the release of calcium ions from the lateral sacs of the sarcoplasmic reticulum. The mechanism of this communication between the T-tubules and the SR is still unknown (Rios & Pizarro, 1991), but some of the answers that have been proposed include: a) the electrical transmission through an ionic pathway between the T-tubule lumen and the SR (via Ryanodine sensitive receptors) (Mathias et al, 1981), b) calcium-induced calcium release (Frank, 1958), c) a mechanical mechanism (Chandler et al, 1976), and d) the release of inosotol tri-phosphate (IP_3) as a second messenger at the T-tubule-SR junction (Vergara et al, 1985; Volpe et al, 1985). Following release from the SR, calcium diffuses to the thick and thin filaments.

2.3.5. When the concentration of free calcium ions in the vicinity of the contractile elements reaches 10^{-6} M (resting concentration is 10^{-8} M), calcium binds to troponin C on the thin filaments, causing tropomyosin to move away from its blocking position, and uncovers the crossbridge binding sites on actin (Weber & Herz, 1963).

2.3.6. Before contraction begins, the heads of the myosin crossbridges bind to ATP. The ATP-ase activity of myosin cleaves the ATP, leaving ADP and Pi bound to the myosin head. This generates an "energized" myosin molecule. The myosin head then binds to actin (and releases Pi), and then moves the actin filament relative to the fixed myosin (and releases ADP). The product of this step, is the so-called rigor complex, in which the actin-myosin linkage is inflexible.

2.3.7. ATP then re-binds to the myosin bridge, breaking the actin-myosin bond and allowing

the crossbridge to dissociate from actin. Cycles of crossbridge interaction continue as long as the concentration of calcium remains high enough to inhibit the action of the troponin-tropomyosin system.

2.3.8. As acetylcholinesterase breaks down Ach in the neuromuscular junction, Ach concentrations drop and less Ach binds to the receptors in the end plate region of the muscle fiber. When the receptor sites no longer contain bound Ach, the ion channels in the end plate close and the depolarized end plate returns to its resting potential.

2.3.9. Calcium concentration levels fall as the ions are actively transported back into the lateral sacs of the SR. This is an energy requiring step which requires ATP. (Hence, both contraction and relaxation are ATP requiring events). Removal of calcium ions restores the inhibitory action of the troponin-tropomyosin system, and in the presence of ATP, actin and myosin remain in the inactive dissociated state.

2.4. THE GRADATION OF MUSCLE FORCE

An increase in muscle force can be accomplished either by changing the number of active motor units (recruitment), and/or by increasing the discharge frequency of those motor units already firing (rate coding) (Freund, 1983).

Motor units are hypothesized to be recruited according to Henneman's "size principle" (Henneman, 1957), which describes that motor units are recruited in an orderly fashion according to the size of the motor neurons. The cause of this size principle is that the small motor units are driven by small motor neurons, which are more excitable than the larger ones, and are therefore excited first. Large motor units are innervated by large motor neurons and become activated at progressively higher levels of contraction (Kandel & Schwartz, 1985).

The size principle predicts that the recruitment order of motor units correlates with the maximum tension generated by these motor units (Henneman, 1957). The tension generated by a motor unit depends on: the number of muscle fibers innervated by a motor neuron, the cross-sectional area of the fibers within the motor unit, and the specific tension (force per cross-sectional area) of the fibers within the unit. Hence, recruitment of small motor units (small

number of fibers with small diameters) will result in low levels of tension. The larger type FF and FR motor units generate higher levels of force, and are thus progressively recruited as the demand for muscle force increases. The size principle also ensures that motor units are usually recruited in order of increasing fatigability, with type S, type FR, and the type FF units being added sequentially, to optimize the total work output during prolonged or repetitive contractions.

Some authors agree, however, that modifications of the order of recruitment are possible (Wyman et al, 1974). Sypert & Munson (1981) proposed that, although several factors can influence the order of motor unit recruitment, the essential determinant is motor unit type. In muscles in which a range of movements is possible, the order of recruitment may depend on the task (Denier van der Gon et al, 1982), as a consequence of the differing descending inputs to the motor neurons for each task.

In the cat diaphragm, motor units have been shown to be recruited according to Henneman's size principle during normal breathing (Dick et al, 1987). On the other hand, Sieck (1991) proposed that, regardless of whether recruitment of diaphragm motor units follows the size principle, the recruitment order is dependent on motor unit type. It was hypothesized that the number of motor units recruited during any specific behavior of the diaphragm depends on the forces required by that behavior, the duration of the force output, and the contractile properties of each motor unit type (Sieck & Fournier, 1989).

In comparison to voluntary activation of muscle, during direct (submaximal) electrical stimulation of a muscle (or the nerve), the order of recruitment is observed to be reversed, and is dependent on the voltage and the frequency of the stimulation (Clamann et al, 1974; Merletti et al, 1992; Stephens et al, 1978). Large motor units are generally recruited first during electrical stimulation, whereas small motor units are generally recruited first during voluntary "stimulation". Perhaps this is because motor unit activity is synchronous with electrical stimulation, in contrast to being asynchronous during voluntary activation (Merletti et al, 1992).

The force output of a muscle can also be graded by increasing the firing rate of the motor neurons (see force-frequency relationship, Section 2.5.2.). Essentially, if a motor unit is

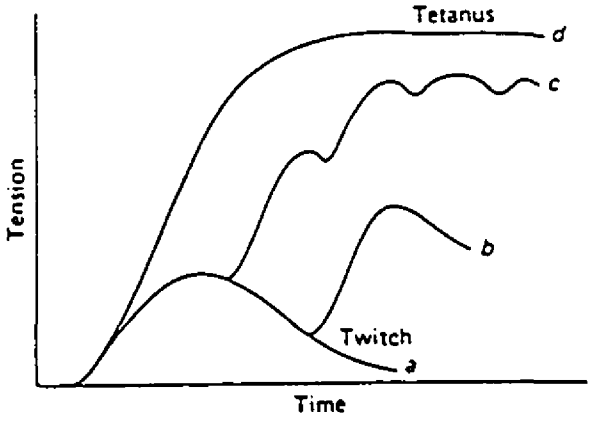

Figure 2.4. The force-frequency relationship. a) response to a single stimulus, producing a twitch; b) response to two stimuli, showing mechanical summation; c) response to a train of stimuli, showing an unfused tetanus; d) response to a train of stimuli at a higher firing rate, showing a maximal fused tetanus. (From Keynes & Aidley, 1991)

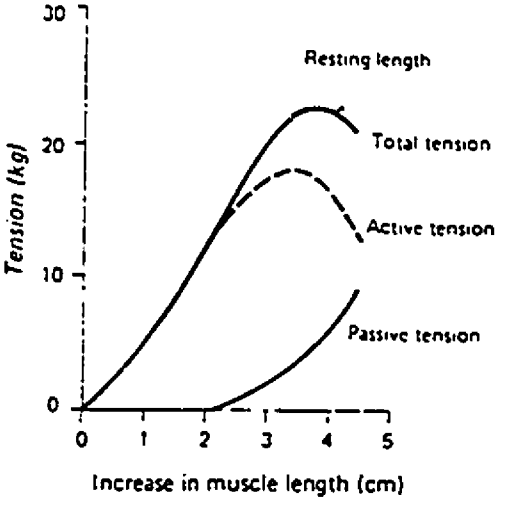

Figure 2.5. Length-tension relationship for the human triceps muscle. The passive tension curve measures the tension exerted by this skeletal muscle at each length when it is not stimulated. The total tension curve represents the tension developed when the muscle contracts isometrically in response to a stimulus. The active tension is the difference between the two. (From Ganong, 1991)

stimulated with a brief electrical pulse, the unit responds with a twitch of a given tension, and as the frequency of stimulation increases, the tension developed by the muscle fibers within the motor unit increases in a sigmoid fashion (Figure 2.4.).

Recruitment has been reported to be the dominant strategy to increase muscle force for low levels of contraction, whereas at intermediate and high force levels, the increase in firing rate becomes the dominant mechanism (Milner-Brown & Stein, 1975). However, the relative contributions of rate coding and motor unit recruitment in the gradation of muscle force probably depend on the muscle and its function. For example, the biceps and deltoid muscles are known to recruit motor units throughout the complete force range while the firing rate of the active units is continuously increasing (Basmajian & De Luca, 1985; De Luca et al, 1982; Kukulka & Clamann, 1981). The first dorsal interosseous muscle, on the other hand, is known to recruit all of its motor units by the time 50% of maximal tension is generated, although the motor unit discharge rate continues to increase until 100% of the force is developed (De Luca et al, 1982).

2.5. SKELETAL MUSCLE MECHANICS

2.5.1. Single muscle twitches

The mechanical response of a muscle to a single action potential in a muscle cell is known as a muscle twitch. Following excitation of the muscle, there is an interval of a few milliseconds (the latent period), before the tension begins to increase. During this period, the processes associated with excitation-contraction coupling occur. Following the latent period, an increase in tension occurs (contraction period) which then decays more slowly (the relaxation period). The precise velocity of contraction varies greatly between species, and between muscle within a given species. Muscles composed primarily of slow muscle fibers develop and dissipate tension slowly, ie. long contraction and relaxation periods, whereas the converse is true for muscles composed mainly of fast fibers. The time course of the muscle twitch also depends on a number of other factors including whether the stimulus was provided

under isometric (same length) or isotonic (same force) conditions, temperature, fiber type, and crossbridge cycling rate, the dynamics of calcium release and re-uptake, and the mechanical properties of the muscle fibers and their attachments (Keynes & Aidley, 1991).

2.5.2. Force-frequency relationship

If the muscle is stimulated repetitively at a sufficiently low frequency, it responds with one twitch (of a specific tension) per stimulus. As stimulus frequency increases, the upstroke of one twitch adds to the tail of the preceding twitch (unfused tetanus) (Figure 2.4.). Eventually, the response to repeated stimuli rises smoothly to a plateau. This is known as the tetanic force, and is generally about five times greater than the isometric (same length) twitch tension produced by a single stimulus (see Section 2.9.2.). The frequency of stimulation that just produces tetanus is known as the tetanizing frequency and increasing the stimulation rate above this does not result in higher (tetanic) forces. The differences in force development during a twitch and during a tetanus are due to the elastic component of the muscle which is stretched and thus slows down the rate of tension development when a muscle becomes active. There is not enough time in a twitch for maximum tension to be achieved before activation declines. A.V. Hill (1949) showed that if the muscle is quickly stretched when it is activated, enough to eliminate the effect of the series elastic component, the force produced by the twitch is equal to that produced in tetanus.

The frequency required for fused tetanus is an inverse function of the contraction time of the muscle, and the relationship is thus different for slow and fast muscles (Rack & Westbury, 1969). Slow muscles will show summation at lower frequencies of stimulation than fast muscles and consequently higher relative tension at a given frequency of stimulation. Compared to fast muscles, the maximum isometric tension development of slow muscles will occur at a lower stimulation frequency. The observation of rightward shifts in the force-frequency curve has been used as a method to evaluate limb muscle fatigue (Edwards, 1981), fatigue of the sternomastoid (Moxham et al, 1980), and the diaphragm (Aubier et al, 1981).

Within a given species, *in vitro* diaphragm strips have been shown to generate higher

relative forces at a given level of stimulation frequency, as compared to other respiratory muscles (Farkas & Rochester, 1988; Farkas & De Troyer, 1987). In humans, the shape of the diaphragm force-frequency curve (as evaluated by transdiaphragmatic pressure) produced by transcutaneous stimulation of the phrenic nerve *in vivo*, is almost identical to the relationship measured for isolated diaphragm bundles *in vitro* (Aubier et al, 1981; Moxham et al, 1981).

2.5.3. Length-tension relationship

The resting *in situ* length is defined as the maximal length at which a relaxed or passive muscle fails to exert a force. When a resting muscle is stretched beyond its resting length, it exerts a passive tension which increases exponentially as a function of increasing muscle length (Banus & Zeltin, 1938; Geffen, 1964; Ralston et al, 1947; Stolov & Weiplepp, 1966; Walker, 1960). In whole muscle, much of this passive tension is due to connective tissue acting in parallel, but cross-bridges may also contribute (Hill, 1967). The length-tension curve for the contractile component of muscle is obtained by subtracting the initial passive tension from the total tension during isometric contractions over a wide range of muscle lengths (Figure 2.5.). During tetanic stimulation, there is an optimal muscle length (l_o), usually between 100% and 120% of the resting in situ length, at which isometric tension is maximal (Bahler et al, 1967, 1968; Geffen, 1964; Ralston et al, 1947; Walker, 1960).

Studying the length-tension relation using single muscle fibers, however, creates problems because the sarcomeres at the ends of the fiber are shorter than those in the middle (Huxley & Peachey, 1961), and when the fiber is stimulated with the tendons fixed, these end regions shorten further, stretching the middle and generating tension (Zierler, 1973). Gordon, Huxley and Julian (1966) devised an electromechanical feedback system (an optical servomechanism) that maintains the sarcomere lengths in the middle of the muscle fiber constant during a contraction, and eliminates the unwanted contributions from sarcomeres at the ends of the fiber. They published length-tension curves from frog muscle fibers and correlated length-tension parameters with sarcomere lengths and the extent of overlap of thick and thin filaments, assuming the sliding filament theory of contraction to be valid. Their results

are summarized in Figure 2.6. The fall of tension on the right-hand side of the figure (the descending limb) can be explained by the decrease in overlap between the thick and thin filaments. The tension over this range of sarcomere lengths was found to be directly proportional to the degree of overlap. The curve plateaus between sarcomere lengths 2.0 μm and 2.25 μm, and over this range, tension and the overlap of thick and thin filaments are maximal. The fall in tension on the left-hand side of the graph (ascending limb) was attributed to interference with crossbridge formation by "double overlap" of actin filaments at the center of the sarcomere and, at very short lengths, meeting of thin filaments on the opposite Z-line. It has been suggested that the decrease in force along the ascending limb (lengths less than l_o) of the length-tension relationship is not so much due to a decrease in myofilament overlap as to a length-dependent alteration in the activation of crossbridges by calcium (Lopez et al, 1981; Ridgway & Gordon, 1975).

The *in vitro* length-tension curves for the diaphragm muscle in different species are consistent with results reported for intact limb muscles (McCully & Faulkner, 1983). Attempts to estimate the force-length relationship of the human diaphragm *in vivo* have not been successful (McKenzie & Gandevia, 1991) due to the complex changes in diaphragm and rib cage geometry which occur with changes in lung volume. Supramaximal stimulation of the phrenic nerves in human subjects reveals a decline in transdiaphragmatic pressure (as an indirect measure of diaphragmatic force) as the muscle shortens above functional residual capacity, consistent with ascending limb of the length-tension curve (Hubmayr et al, 1989).

2.5.4. Force-velocity relationship

If a muscle at l_o is attached to a load and stimulated, it will shorten and move the load. The velocity with which it begins to shorten is a function of the load imposed on the muscle. The relationship has a characteristic hyperbolic relationship, extending from zero velocity at a load equal and opposite to the maximum isometric tetanic tension, to a maximum velocity of shortening at zero load (Hill, 1938). The maximal velocity of shortening is not affected by the number of active crossbridge, but rather seems to be determined by the crossbridge cycling

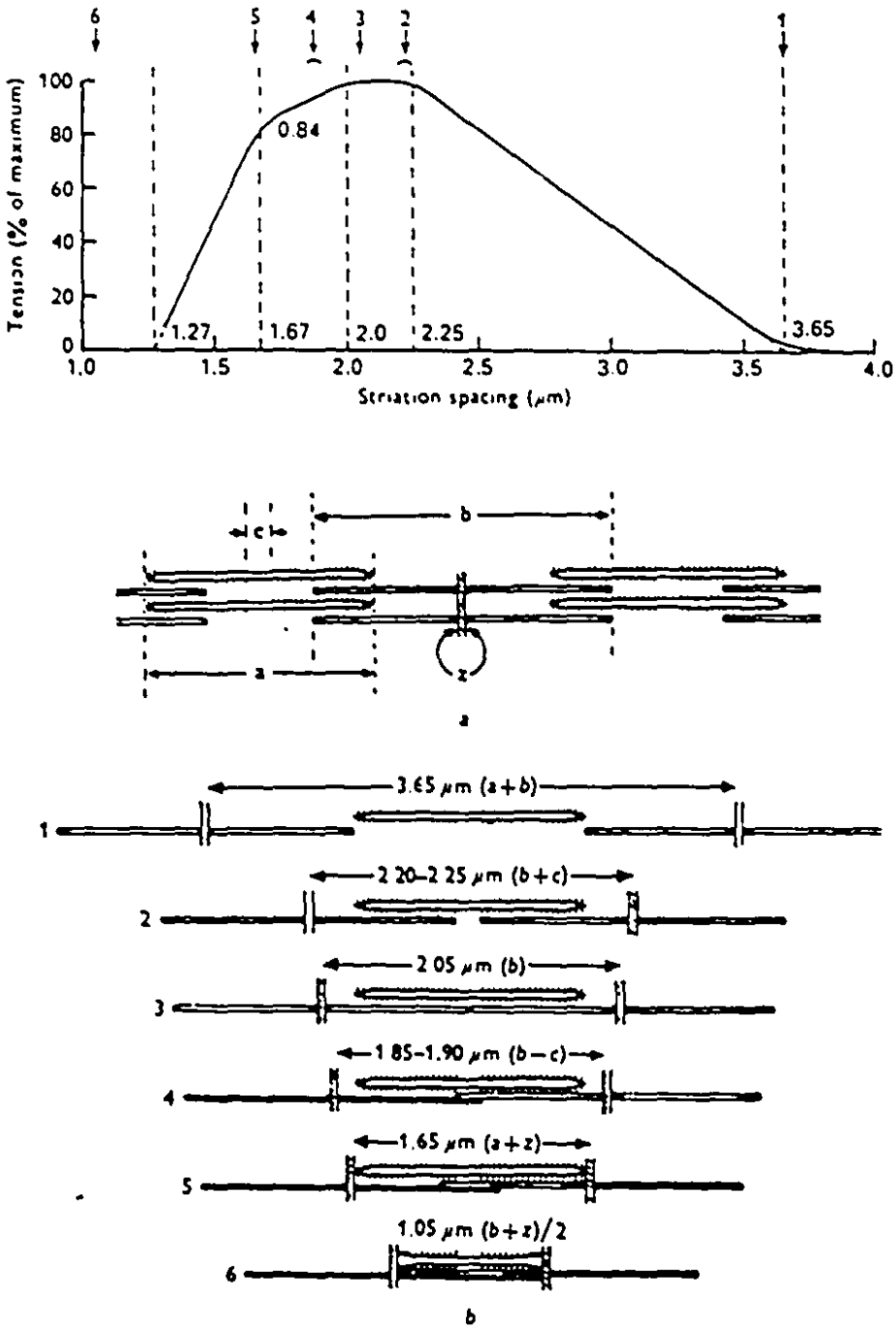

Figure 2.6. Above: Length-tension curve from part of a single muscle fiber. The arrows along the top show the various critical stages of overlap that are displayed below. Below: Critical stages in the increase in overlap between thick and thin filaments as the sarcomere shortens (From Gordan et al, 1966).

rate (Vander et al, 1985).

A.V. Hill (1938) produced a mathematical formula to describe the shape of the force-velocity relationship:

$$(P+a)V = b(P_o-P),$$

where V is the velocity of shortening, P is the load, P_o is the isometric tension, and a and b are constants (Close, 1972). The maximum velocity of shortening occurs when the muscle contracts against no load (P=0). As the load increases, shortening will take place as long as the load remains less than P_o. Once $P=P_o$ the velocity of shortening drops to zero.

The maximum speed of shortening is higher for fast mammalian muscle than for slow muscle (Close, 1972). In addition, when both the tension and the velocity are normalized to the maximum value, slow muscles show greater curvature for the relationship than fast muscles do. The force velocity curves for the diaphragm are similar in shape to those reported for limb muscles (Edwards & Faulkner, 1986; Luff, 1981; Sharp & Hyatt, 1986) and in accordance with their other characteristics, are located midway between curves of predominantly fast and slow limb muscles.

The purpose of this chapter was to provide the reader with some of the general concepts about skeletal muscle activation and contraction. The muscle under investigation in this study is the diaphragm, which as demonstrated above, is morphologically and functionally a skeletal muscle. The diaphragm has an intermediate fiber type distribution, which makes it well suited for endurance-type activity. However, the diaphragm, like other skeletal (limb) muscles, is also prone to fatigue. Fatigue can be evaluated by electromyography, the topic of the next chapter (Chapter 3).

TABLE 2.1. Types of muscle fibers

1. Commonly used classifications:

Fiber types (ref)	Type I	Type IIA	Type IIB
Twitch and fatigue characteristics (ref)	slow (S)	fast resistant (FR)	fast fatigue (FF)
Twitch and enzymatic properties (ref)	slow oxidative (SO)	fast oxidative-glycolytic (FOG)	fast glycolytic (FG)

2. Properties of muscle fibers:

Resistance to fatigue	high	high	low
Oxidative enzymes	high	high	low
Phosphorylase (glycolytic)	low	high	high
Adenosine triphosphate	low	high	high
Twitch velocity	low	high	high
Twitch tension	low	high	high

Adapted from Kimura (1983)

CHAPTER 3

ELECTROMYOGRAPHY

Electromyography is the study and recording of the electrical activity of a muscle. This thesis focuses on esophageal recordings of the diaphragm electromyogram, which is a surface recording of the crural diaphragm's electrical activity. The following chapter begins with a brief description of electromyogram (EMG) recording techniques, and is followed by a general description of how the muscle fiber action potential, and thus how the EMG signal, is generated. A more detailed description of the characteristics of the EMG signal in the frequency domain is then provided. There are numerous factors which can influence the EMG signal, both physical and physiological, and these are described in detail.

3.1. RECORDING TECHNIQUES

3.1.1. Intracellular recording techniques

Intracellular recordings of the electrical activity of single muscle fibers reflect the potential difference between the inside of the fiber with respect to the outside of the fiber (Nastuk & Hodgkin, 1950). With this technique, micropipette electrodes are used, consisting of fine glass tubing (diameter <1 μm) filled with a 3 Molar potassium chloride solution. For *in vitro* measurements, the isolated muscle tissue is placed in a bath containing a physiological salt solution, and the voltage difference between one electrode placed inside the muscle fiber, and a second electrode placed in the bath, is recorded. Intracellular recordings have been attempted *in vivo*, but are proven to be difficult because contraction or slight movement of the muscle fiber results in a breakage of the microelectrode tip. Hence, intracellular recordings are usually limited to *in vitro* preparations (Goodgold & Eberstein, 1983).

3.1.2. Extracellular recording techniques

Extracellular recordings of the muscle's electrical activity can be obtained either by (1)

electrodes placed on the surface of the muscle, or on the skin overlying the muscle, (surface electrodes), or by (2) electrodes inserted into the muscle (intramuscular electrodes). Extracellular recordings can be applied either *in vitro* or *in vivo*.

Depending on how the signals are referenced, extracellular recordings can be either monopolar or bipolar. In a monopolar configuration, the voltage recorded by one "active" electrode is measured relative to a "reference" electrode located in an environment which is either electrically silent, or contains signals which are unrelated to those being detected. In a bipolar recording, two detection surfaces are located on or in the muscle of interest, and the voltage difference between the two recording points is obtained. The bipolar configuration reduces disturbances in the signal because the influences common to both electrodes are "subtracted out", or rejected (common mode rejection).

The specificity of the electrodes is mainly determined by (1) the distance between the electrodes (Koh & Grabiner, 1992; Lynn et al, 1978; Zipp, 1982), and (2) the size of the electrodes (Ekstedt & Stålberg, 1973; Fuglevand et al, 1992; Gath & Stålberg, 1976). As a general rule, the smaller the interelectrode distance and the smaller the electrodes, the higher the specificity (Lynn et al, 1978). The type of electrode that is chosen to detect the EMG signal depends on the purpose of the investigation, i.e. if the signal of interest is the motor unit action potential (MUAP) from single motor units, or the global EMG signal, which reflects the activity from many muscle fibers. To measure the electrical activity from single muscle fibers, or from a small number of motor units, thin intramuscular electrodes, such as needles or wires, are preferable (Basmajian & De Luca, 1985; Stålberg, 1966). Surface electrodes are usually used to detect EMG signals from numerous motor units, and are used most effectively when investigating superficial muscles, (or when the muscle is directly accessible *in situ*).

3.2. GENERATION OF THE ACTION POTENTIAL

3.2.1. The resting membrane potential

The electrical potential difference (the "potential") between the inside and the outside

of an excitable cell (nerve or muscle fiber) depends on the ionic concentration gradients across the membrane and on its relative permeability to the ions present. At rest, muscle fibers actively maintain their intracellular environment at a potential of about -80 to -90 mV with respect to the extracellular environment. Voltage and time-dependent channels in the muscle fiber membrane regulate the conductance of sodium (Na^+) and potassium (K^+) ions across the membrane. The channels for K^+ are open, whereas those controlling the movement of Na^+ are closed. In addition, a Na^+/K^+ pump located within the muscle fiber membrane actively pumps Na^+ ions out of the cell and K^+ ions into the cell, thereby creating the electro-chemical gradient that produces the resting membrane potential, as quantified by the Goldman equation (Goldman, 1943).

3.2.2. The end-plate potential

As described in the previous Chapter (Section 2.3.), the arrival of a nerve impulse at the neuromuscular junction causes the release of acetylcholine (Ach) from the motor nerve terminal, which binds post-synaptically to Ach receptors in the motor end plate region. A conformational change within the receptor opens the acetylcholine-gated ion channels, permitting Na^+ ions to enter the muscle cell, carrying with them a large amount of positive charge. This creates a local voltage change across the muscle fiber membrane known as the end-plate potential.

3.2.3. The action potential

When the end-plate potential reaches a certain "threshold" voltage, the voltage dependent Na^+ channels open, causing the membrane to become extremely permeable to Na^+. Na^+ ions flow into the cell due to the Na^+ concentration gradient across the muscle fiber membrane. The influx of Na^+ further depolarizes the membrane, thereby opening additional Na^+ channels, which allows more Na^+ ions to enter the cell. Thus, a self-generating process (the "Hodgkin-Huxley cycle") is established between depolarization and sodium permeability (Hodgkin & Huxley, 1952). As the depolarization continues, there is an inactivation of the Na^+

channels, as well as a delayed opening of K^+ channels. With the Na^+ channels closed, and the K^+ channels open, K^+ ions diffuse to the exterior of the cell, repolarizing the membrane. Because the inactivation of the K^+ channels is a relatively slow process, K^+ ions continue to diffuse out of the muscle cell well beyond the resting membrane potential. This hyperpolarization of the membrane continues until the K^+ channels become completely inactivated, after which the resting membrane potential is re-established. The whole series of events, depolarization due to the inward flow of Na^+ ions, and repolarization due to the outward flow of K^+, constitutes the action potential.

3.2.4. Propagation of the action potential

Once an action potential has been initiated at one point along the cell membrane (the "active" region), a local current loop is set up (Figure 3.1.). Current flows from (1) the active region (positively charged) through the intracellular fluid longitudinally, to the adjacent negatively charged inactive regions. (2) Current then flows across the membrane to the extracellular fluid. (3) Extracellular current flows longitudinally along the muscle fiber membrane, and the loop is completed by the flow of current across the membrane into the cell, back to the starting point (Clark & Plonsey, 1968). When current flows from inside the cell to the outside (step 2), the membrane is depolarized. When the depolarization reaches threshold, an action potential is generated, giving rise to a new local current loop. The action potential is thus self-propagating, moving along the whole length of the muscle fiber, and does not decrease in amplitude (Goodgold & Eberstein, 1983).

3.2.5. Single muscle fiber action potentials

Depolarization of the muscle fiber membrane, accompanied by the movement of ions, generates an electric field outside the muscle fiber. A pair of extracellular recording electrodes can detect this electrical field, producing a change in voltage (the EMG signal), whose time course is known as the muscle fiber action potential. If the two electrodes are placed in the direction of the muscle fiber axis, the muscle fiber action potential is essentially a bi-phasic

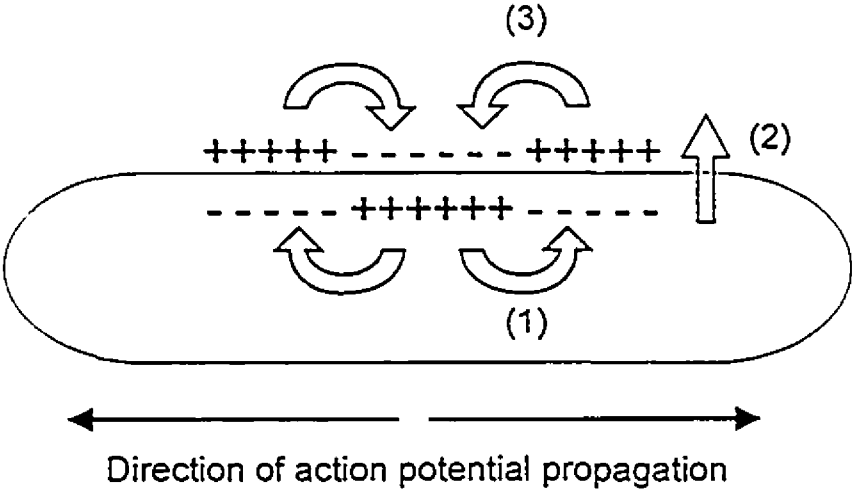

Figure 3.1. Illustration of the propagation of the action potential along a nerve or fiber membrane. Arrows indicate the direction of current flow. See text for details. (Adapted from Kimura, 1983)

waveform.

In humans, muscle fiber action potentials move physically down the muscle fiber membrane at a velocity of 2 to 6 m/s (Stålberg, 1966). The velocity at which the action potential moves along the muscle fiber membrane is known as the muscle fiber action potential conduction velocity, and will hereafter be referred to as CV.

Although the action potentials from a single fiber are identical in terms of shape and amplitude (i.e. it is an "all or nothing" phenomena), the shape and amplitude of the recorded action potential will depend on such factors as the orientation of the recording electrodes with respect to the active muscle fibers, the distance between the muscle fiber and the electrodes, the filtering properties of the electrodes, and the CV of the signal along the fiber membrane (Lindström, 1973).

3.3. SINGLE MOTOR UNIT ACTION POTENTIAL

The motor unit action potential (MUAP) constitutes the spatial-temporal summation of the individual muscle fiber action potentials from a given motor unit (Broman & Lindström, 1974). A graphic representation of the summation of single fiber action potentials is presented in Figure 3.2 (from Basmajian & De Luca, 1985). The integer n represents the total number of muscle fibers of one motor unit that are sufficiently near to the recording electrode to be detected. The action potentials associated with each muscle fiber and the resultant MUAP, h(t), are presented at the right side of the figure. The shape of the MUAP is not a simple biphasic wave because the action potentials arise from different fibers which are spatially dispersed within the muscle, and hence, do not travel under the electrodes at the same time (Basmajian & De Luca, 1985). In addition, differences in the lengths of the motor neuron terminal branches, and possible fiber to fiber differences in CV will affect the arrival times of the action potentials at the electrodes (Merletti et al, 1992). Essentially, the shape and amplitude of the MUAP is dependent on the geometrical arrangement of the active muscle fibers with respect to the electrode site, the distance between the muscle fibers and the electrodes, the filtering properties of the electrodes, the CVs along the fiber membranes, and the number of fibers

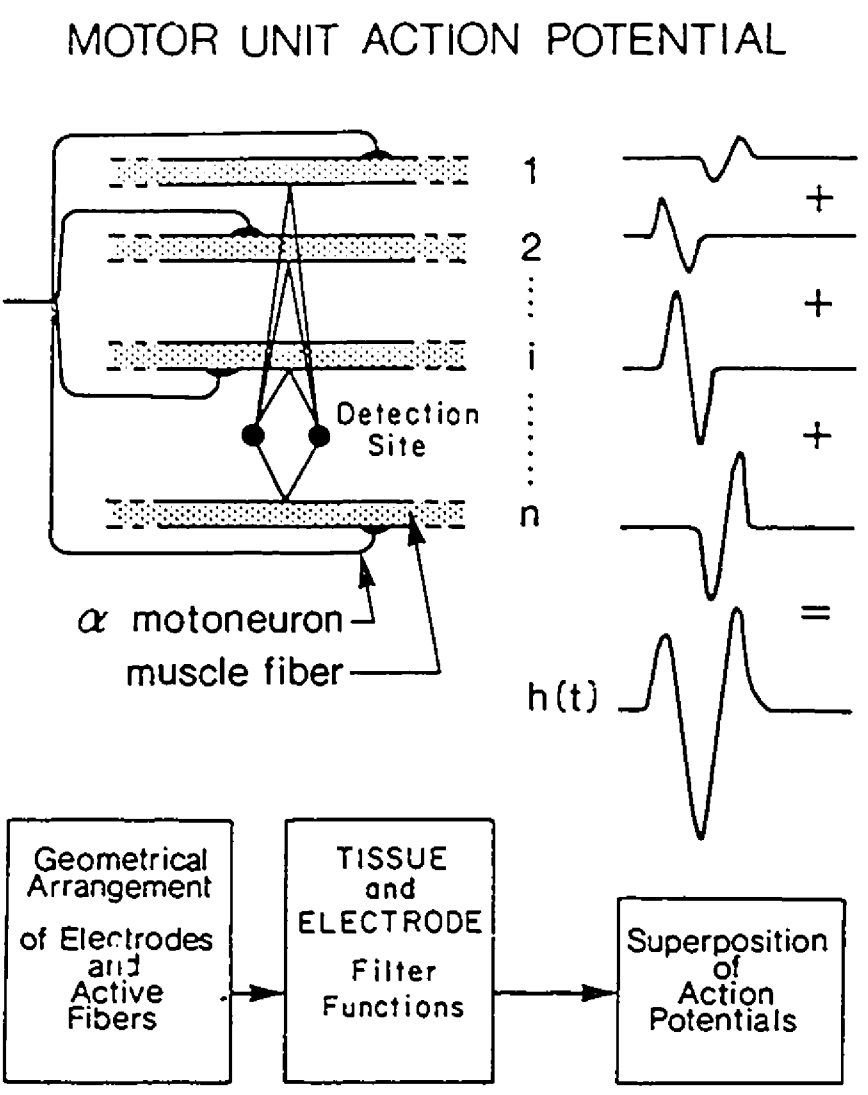

Figure 3.2. Schematic representation of the generation of the motor unit action potential. (From Basmajian & De Luca, 1985)

within the motor unit (Broman & Lindström, 1974; Lindström, 1973).

3.4. SUMMATION OF MOTOR UNIT SIGNALS - THE INTERFERENCE PATTERN EMG

The consequence of a MUAP, following a few milliseconds delay, is a mechanical twitch of the muscle fibers in the motor unit. In order to sustain a voluntary contraction, the motor units fire repeatedly. The resulting sequence of MUAPs is known as a motor unit action potential train (MUAPT). The EMG signal recorded during voluntary contractions represents the linear, temporal and spatial summation of asynchronously firing MUAPTs (Lindström & Broman, 1974). When single MUAPs can no longer be distinguished, the signal is referred to as an interference pattern EMG.

A simplified schematic representation of the summation of motor unit signals is presented in Figure 3.3. (from Basmajian & De Luca, 1985). As described in Section 3.3., the location of the active motor units with respect to the recording site determines the waveform of the MUAPs, h(t). The integer p in Figure 3.3. represents the total number of MUAPTs which contribute to the potential field at the recording site. The superposition of the MUAPTs at the recording site forms the physiological EMG signal $m_p(t,F)$, and is a function of both contraction time, t, and force, F. The physiological signal is not observable.

The physiological signal is influenced by electrical noise, n(t), and the filtering properties of the recording electrodes and the equipment, r(t). The resulting signal is the observed EMG signal m(t, F), and can be described by the following equation:

$$m(t,F) = \sum_{i=1}^{p} u_i(t,F),$$

where i = the ith MUAPT, and the other variables are as described above.

The observed interference pattern EMG is thus a function of the number of active motor units, their firing rates and/or synchronization, the shape of the MUAPs (in turn dependent on distance and electrode filtering), and cancellation of opposite phase potentials (Lindström & Broman, 1974; Lindström & Kadefors, 1974). For a more detailed mathematical description

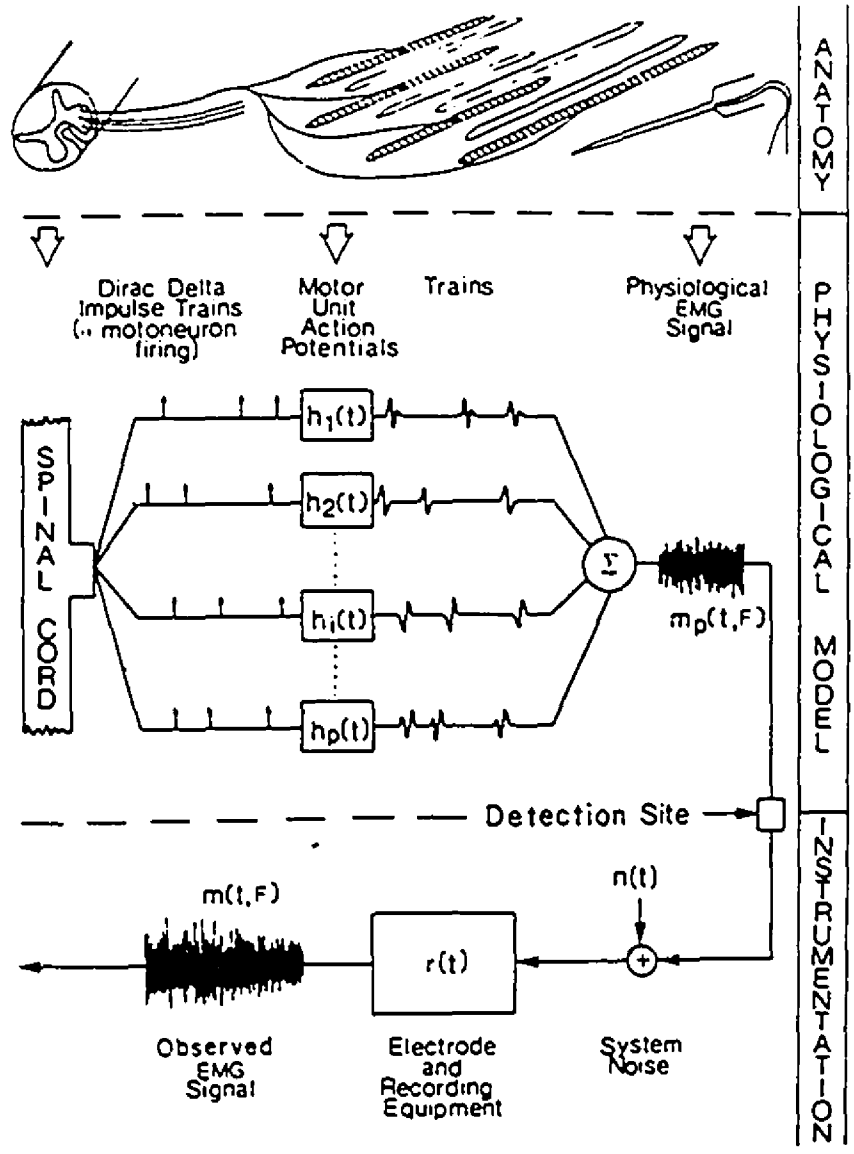

Figure 3.3. Schematic representation of the model for the generation of the interference pattern EMG. (From Basmajian & De Luca, 1985)

of the interference pattern EMG, the reader is referred to the original works by Broman & Lindström (1974), Lindström (1973), Lindström & Broman (1974), and Lindström & Kadefors (1974).

3.5. ANALYSIS OF THE INTERFERENCE PATTERN EMG

3.5.1. Time domain

The "raw" surface EMG signal, whether monopolar or bipolar, represents changes in the muscle's electrical activity as a function of time, and is therefore referred to as a time domain signal (Figure 3.4. top). At minimal levels of contractions, isolated MUAPs can be distinguished and analyzed by such time domain measurements as rise time, duration, the number of phases, amplitude, and total power (area) (Daube, 1981).

With increasing levels of contraction, new motor units are recruited and/or the firing rate of already active motor units increases. The resulting interference pattern EMG can be analyzed by such measurements as amplitude and total power, which are generally accepted to be related to the tension exerted by the muscle (Lippold, 1952; Milner-Brown & Stein, 1975). Other useful information can be obtained by counting the number of zero crossings (Hägg, 1981) or the number of turns in the signal (Willison, 1964). These measurements are related to the frequency content of the signal, and have been shown to provide information regarding muscle fatigue (Hägg, 1992).

The power of the EMG signal is intimately related to its frequency characteristics (Lindström & Kadefors, 1974), and the frequency characteristics are in turn related to the CV, the filtering properties of the electrodes, the distance to the muscle, and noise (Lindström & Pétersen, 1983). These factors are difficult to evaluate in the time domain, and since modern technology allows for frequency domain analysis of the EMG signal, frequency domain analysis is preferable.

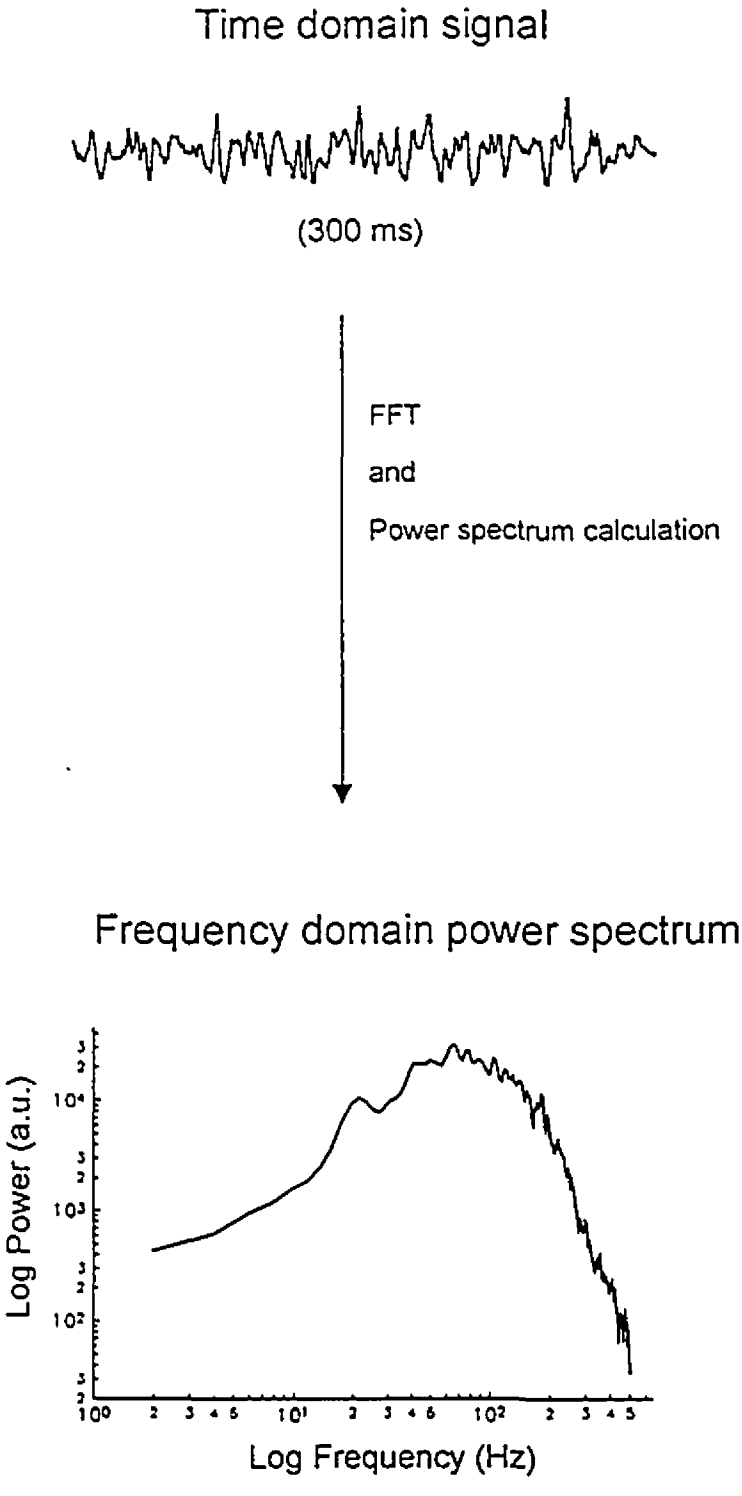

Figure 3.4. Top: Time domain signal of diaphragm EMG as obtained with an esophageal electrode (300 ms sample). Bottom: Power spectrum of the transformed signal. (Data obtained from the present study).

3.5.2. Frequency domain

Transformation between the time domain and the frequency domain is usually performed by a discrete Fourier transform, the fast Fourier transform (FFT) (Cooley & Tukey, 1965). The FFT components, both real and imaginary, are squared, and their product is calculated, giving the power spectrum of the EMG signal (Figure 3.4. bottom). The power spectrum represents the power of the signal, or the strength of its components, plotted as a function of frequency (Lindström & Magnusson, 1977).

Mathematically, the power spectrum $W(\omega)$ can be written as the squared absolute value of the Fourier amplitude (Φ) described by the following formula (Lindström & Pétersen, 1983):

$$W(\omega) = \lim_{T \to \infty} (1/2T) \left| \Psi(i\omega)\Psi(-i\omega) \right|$$

where, the spectral amplitudes $\Psi(i\omega)$ are obtained with a Fourier transformation of the time dependent signal $\Phi(t)$:

$$\Psi(i\omega) = \int_{-T}^{+T} \Phi(t)\exp(-i\omega t)dt.$$

The power of the signal, P, can be calculated according to the formula:

$$P = (1/\pi) \int_{0}^{\infty} W(\omega)d\omega.$$

Based on these computations, Lindström and Broman (1974) have shown that the power spectrum of randomly and temporally summated motor unit signals reflects the properties of the individual motor units' power spectrum (Figure 3.5, spectrums A and B). For the EMG signal composed of motor unit potentials of different shapes, the observed power spectrum represents a weighted mean of the spectra from the contributing units.

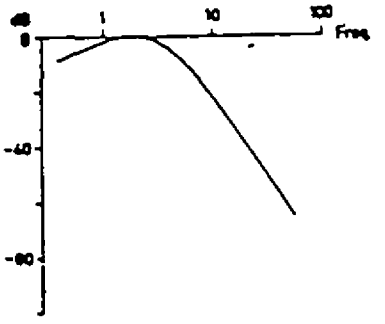

Power spectrum A: Computer generated motor unit action potential and its power spectrum

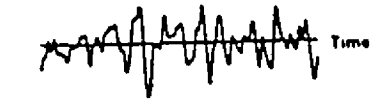

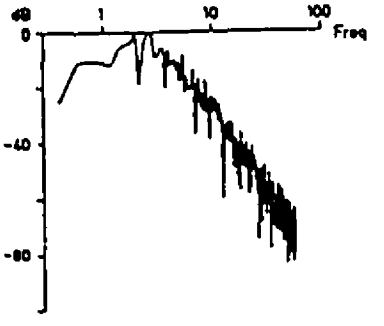

Power spectrum B: Random summation of the above motor unit action potential

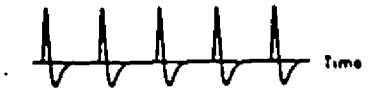

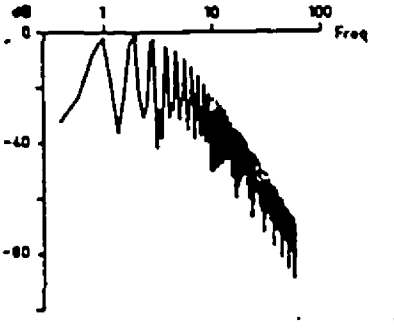

Power spectrum C: Temporal summation of the above motor unit action potential

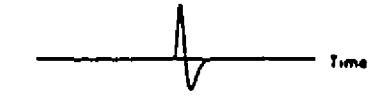

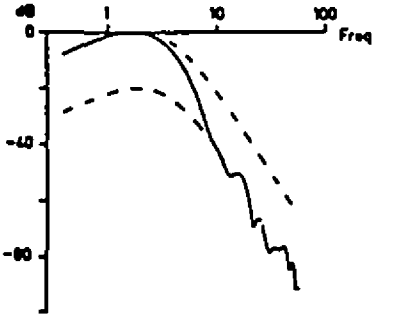

Power spectrum D: Spatial summation of the above motor unit action potential

Figure 3.5. Examples of motor unit spectrums and summation effects
(From Lindström and Magnusson, 1977)

Numerical quantification of the power spectrum is possible by calculating the spectral moments of the spectrum (Lindström & Pétersen, 1983). Spectral moments (M) of order n are defined as:

$$M_n = \sum_{0}^{f} \text{power} * (\text{frequency})^n,$$

where f is the highest frequency in the power spectrum. Note that spectral moments of increasing order are more sensitive to high frequency noise as the frequency values are raised to higher powers.

The moment of order zero, M_0, represents the total power of the EMG signal. This quantity, and the RMS value ($M_0^{1/2}/n$, where n is the number of points in the sample), theoretically represents the force output of the muscle (Lindström & Kadefors, 1974). However, both the RMS (and the total power) depend on a number of parameters such as the electrode-to-muscle distance, the number of fibers in the motor unit, the CV, and others (see Section 3.7. and 3.8.) (Lindström & Kadefors, 1974).

In comparison to measuring the power of the signal in the time domain, frequency domain calculations of power can be performed for different frequency bands of the spectrum, and thus, artifactual influences occurring at particular frequencies (eg. 60 Hz influence from the power line) can be distinguished, and eliminated. It is also possible to calculate the power ratio between pre-determined high and low frequency bands of the power spectrum (the H/L ratio), in order to get an index of the distribution of power for different frequency bands.

Quantification of the distribution of power in the spectrum can be obtained by calculating the frequency which divides the power spectrum into two parts of equal power. This is known as the median frequency (MF), and is mathematically described as:

$$MF = M_0/2$$

The frequency-distribution of power in the spectrum can also be evaluated by calculating the ratio of M_1 to M_0, which is known as the center frequency (CF) (also known as the mean or centroid frequency), and is defined as:

$$CF = M_1/M_0.$$

where,
$$M_0 = \sum_{0}^{f} \text{power} * (\text{frequency})^0,$$

and,
$$M_1 = \sum_{0}^{f} \text{power} * (\text{frequency})^1,$$

In a study evaluating the statistical properties of spectral moments and spectral estimates, it was reported that the CF was the most reliable measure to quantify the spectrum because of its stability and sensitivity with respect to spectral shifts during fatigue (Hary et al, 1982). Empirical studies by Schweitzer et al (1979) have confirmed this theory. This is in contrast to the conclusion of Stulen & De Luca (1981) who deduced that the MF is a better estimate than the CF, since it is less sensitive to noise interference.

All mathematical formulas and expressions proposed by Lindström (1970) to model the EMG power spectrum contain the quotient ω/v, where ω is the angular frequency (or 2π times frequency), and v is the conduction velocity (or CV) of the action potential. This states that any change in CV must be accompanied by a translation of the spectrum along the frequency axis (Lindström, 1970), and hence CF and MF values are related to CV. Experimentally, the relationship between CF/MF and CV has been demonstrated (Arendt-Nielsen et al, 1984; Arendt-Nielsen & Mills, 1985; Eberstein & Beattie, 1985; Roy et al, 1986; Sadoyama et al, 1983; Sinderby, unpublished observations; Zwarts et al, 1987).

Spectral analysis of surface EMG therefore provides direct information concerning the

physiological properties of the muscle fiber membrane. However, there are a number of factors, both physical and physiological, which can modify the signal, and subsequent calculations of CF/MF, as described in Sections 3.6. and 3.7.

3.6. PHYSICAL FACTORS INFLUENCING THE EMG POWER SPECTRUM

The factors which influence the power spectrum can be described as a cascaded chain of filter functions, each describing one particular physical or physiological phenomenon (Figure 3.6.), and are described below (3.6.1.-3.6.5.) and in the following section (3.7.).

3.6.1. Bipolar electrode transfer function

For bipolar electrodes which are lined up parallel to the direction of the muscle fibers and which have an interelectrode distance of 2d, the bipolar electrode transfer function (F_{bipol}) is calculated to be (Lindström, 1973):

$$F_{bipol} = \sin^2(\omega d/CV)$$

(A transfer function is an expression linking the output of an instrument to its input). The influence of the bipolar electrode transfer function on the EMG power spectrum is presented in Figure 3.7. (middle and right panels), and demonstrates that the filter function behaves as a differentiating filter that adds a positive slope of 6 dB/octave to the spectrum in the low frequency region, i.e. acting as a high-pass filter. In addition, due to the difference in arrival time of the signal at the two detection sites, so-called "dips" are introduced into the power spectrum at frequencies where the sine function is equal to zero, that is, at:

$$\omega = n\pi(CV)/d,$$

where n = an integer (dip of order n), and d is half the interelectrode distance. The positions of these dips are dependent upon the interelectrode distance and the CV along the muscle fiber

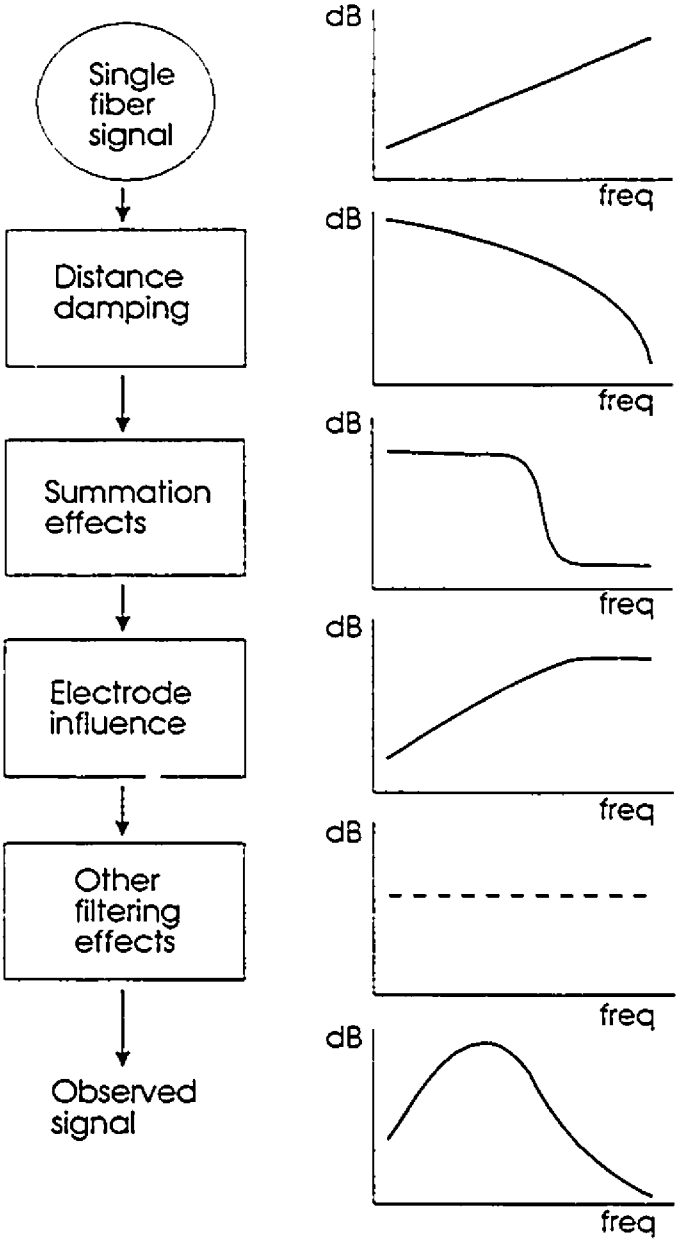

Figure 3.6. Successive modifications of the EMG signal (single fiber potential) through cascaded filter functions modeling various physiological and physical processes. (Adapted from Lindström & Pétersen, 1983).

membrane. Given the interelectrode distance (2d), we can determine the CV from the following formula:

$$CV = 2df_{dip}$$

where f_{dip} = the frequency at which the first dip occurs in the power spectrum. In experiments performed on the biceps brachii, Lindström and Magnusson (1977) used dip analysis and found CVs in the range of 3.5-4.8 m/s, which were in agreement with previously published values of 2.8-5.9 m/s, as measured directly by needle electrodes (Buchtal et al, 1955; Stålberg, 1966).

The use of "dip analysis" in determining CV was later criticized because of the difficulties in observing distinct dips in the power spectrum (Arendt-Nielsen & Zwarts, 1989; De Luca, 1984; Lynn, 1979; Lynn et al, 1978). However, if the required methodology is adhered to, namely that the electrodes should be placed along the muscle fiber direction and in a region free of innervation zones (Lindström, 1970), the presence of dips is easily discernible, as is demonstrated in Figure 3.7. (left panel) for the canine costal diaphragm.

3.6.2. Interelectrode distance

3.6.2.(i) Effects of interelectrode distance on the bandwidth of the signal

The effect of changing the interelectrode distance between a bipolar pair is a change in the bandwidth of the detected EMG signal (Basmajian & De Luca, 1985; Fuglevand et al, 1992; Kadefors et al, 1969; Lynn et al, 1978; Parker & Scott, 1973; Sinderby et al, 1993b; Zipp, 1978). The bandwidth of the signal is defined as "the range of frequency between the high and low 3 dB (or 6 dB) points". A reduction in the interelectrode distance acts as a high-pass filter, resulting in an increase in the bandwidth of the signal. Figure 3.8.A demonstrates the effect of changing the interelectrode distance on the bandwidth of the costal diaphragm EMG power spectrum.

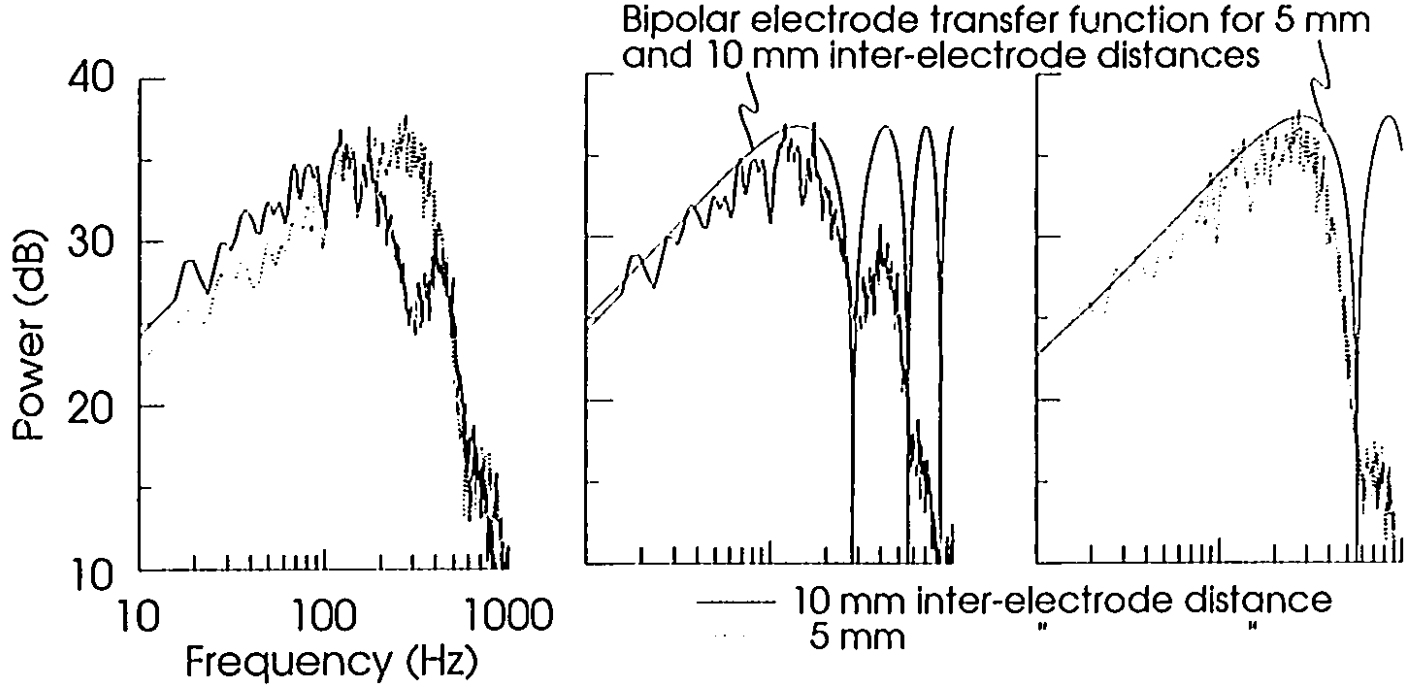

Figure 3.7. Bipolar electrode transfer function for 5 and 10 mm interelectrode distance (solid lines, mid and right panels). (From Sinderby et al, 1993b)

3.6.2.(ii) Effects of interelectrode distance on the position of the dips in the spectrum

Changing the interelectrode distance will affect the frequencies at which power spectral dips occur, providing CV remains constant, and if the electrodes are placed along the muscle fibers and in an area free of innervation zones (Lindström, 1973). According to the formula $v = 2df_{dip}$, (see Section 3.6.1.) reductions in the interelectrode distance will place the dips at higher frequencies, until they surpass the frequency range of the spectrum, at which point they can no longer be observed (i.e. the dips fall into the region of high frequency noise) (Figure 3.8.B). Hence, changes in interelectrode distance will alter the shape and frequency-distribution of the power spectrum (Sinderby et al, 1993b).

3.6.2. (iii) Effects of interelectrode distance on calculations of CF/MF and RMS

Because the frequency-distribution of power is altered with variations in interelectrode distance, calculations of spectral estimates such as CF, and MF are also influenced. A tendency for increasing MF values with reductions in interelectrode distance has been observed in the biceps brachii (Gerdle et al, 1990), and in the triceps brachii and anconeus muscles (Bilodeau et al, 1990). In these studies, however, the orientation of the electrode with respect to fiber direction and innervation zones was not controlled (see Sections 3.6.3. and 3.6.5.). Experiments in which electrode positioning was well controlled reveal a strong effect of changes in interelectrode distance on CF/MF (Figure 3.8.C). As a general rule, high-pass filtering of the signal due to decreasing the interelectrode distance will enhance the high frequency components of the signal, and thus CF and MF values will be higher.

It has been observed that CF/MF values can actually increase with increases in interelectrode distance (>15 mm). This has been attributed to the presence and positions of numerous dips in the power spectrum (Figure 3.8.B). In addition, the relationship between CF/MF and CV is weakened for interelectrode distances greater than 10 mm (Sinderby, unpublished observations).

The effect of interelectrode distance on CF/MF is critical in experiments in which wires

Figure 3.8.(A) Effects on bandwidth

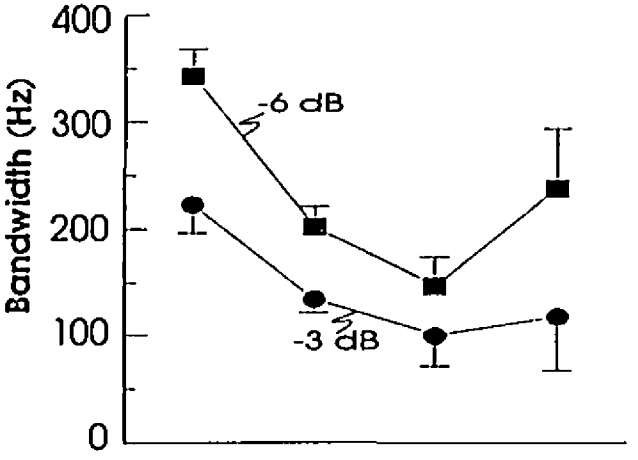

Figure 3.8.(B) Effects on dips

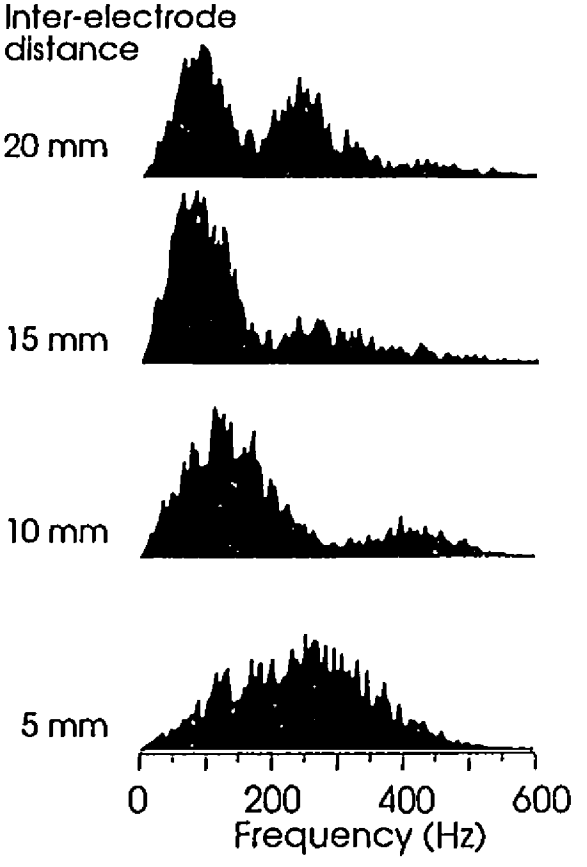

Figure 3.8.(C) Effects CF and MF values

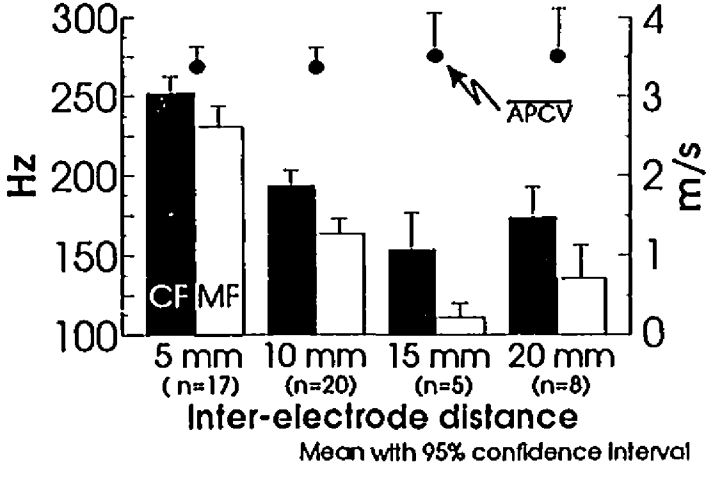

Figure 3.8. Effects of interelectrode distance on EMG power spectrum

are attached or inserted in two points along the muscle. During muscle shortening, the separation between the two electrodes decreases, thus influencing the power spectrum and subsequent calculation of CF/MF. This increase in CF/MF observed may be misinterpreted as being due to the shortening of the muscle (i.e. a length effect), rather than an interelectrode distance effect.

A consistent finding is the relationship between the interelectrode distance and the total power, or RMS, of the EMG signal. In experiments performed on the biceps, Lindström & Kadefors (1974) found that the power of the EMG signal (RMS) was proportional to the interelectrode distance, and that the RMS level reached an asymptotic value as the spacing was increased. This observation has been confirmed by other investigators for other muscles (Andreassen & Rosenfalck, 1978; Gath & Stålberg, 1976; Gerdle et al, 1990; Moller, 1966; Parker & Scott, 1973; Vigreux et al, 1979), and for studies in nerves (Buchtal & Rosenfalck, 1966; Palacios et al, 1993; Varguese & Rogoff, 1983; Winkler et al, 1991). Lynn et al (1978) have demonstrated that most of the increase in power with increasing inter-electrode distance occurs in the low frequency range of the spectrum.

3.6.3. Electrode orientation

In theory, calculations of spectral estimates such as CF and MF have a direct relationship with CV (Lindström, 1970), when a bipolar configuration is used. This relationship holds true when the electrodes are placed parallel to the direction of the muscle fibers, and outside the innervation zones. If the electrode orientation with respect to the fiber direction is not maintained, calculations of CV can be misinterpreted (Lindström, 1970; Lynn, 1979; Sadoyama et al, 1985).

In esophageal recordings of the diaphragm EMG (in humans), the direction of the (crural) muscle fibers with respect to the esophageal electrodes is not known, and therefore, no deductions about CV can be made. However, during the development of fatigue (where CV is known to decrease), spectral shifts and decreases in CF/MF have clearly been demonstrated for muscles in which the fiber direction was not known, such as the diaphragm (Gross et al,

1979; Bellemare & Grassino, 1982). Hence, mis-orientation of the electrodes does not exclude measurements of CF/MF in terms of evaluating fatigue, although absolute measurements of CV cannot be determined.

3.6.4. Distance dependent filtering function

Lindström and Magnusson (1977) demonstrated that the electrical field generated by the muscle decreases with increasing observation distance, in such a way that the high frequency components are more strongly damped than those of low frequency. CF and MF values, as well as RMS are thus reduced as the electrodes are placed further away from the muscle.

Mathematically, the electric field outside the muscle fiber is described by Lindström (1970) by modified Bessel functions of the second kind and order zero, Ko, which gives the power spectrum distance dependent filtering function:

$$\text{Distance filtering} = Ko^2(\omega h/v)/Ko^2(\omega a/v)$$

and is plotted in logarithmic scales in Figure 3.9.

The distance dependent filter has the character of a low-pass filter, the cut-off frequency of which is inversely proportional to the observation distance. This filter influences both the signal amplitude and the signal shape, causing the fast variations to disappear earlier than the slow ones, as one moves away from the signal source. If the electrode is placed in the vicinity of an innervation zone, or near the tendinous portion of the muscle, the filter function described above is modified (De Luca, 1984; Lindström & Pétersen, 1983).

Experimentally, it has been demonstrated that increasing the radial distance between the active muscle fibers and the electrode results in an increase in attenuation of the signal's peak-to-peak amplitude (Andreassen & Rosenfalck, 1978; Ekstedt, 1964; Fuglevand et al, 1992; Gath & Stålberg, 1976; Gath & Stålberg, 1978; Gydikov & Gatev, 1982; Håkansson, 1957b; Lynn et al, 1978; Morimoto et al, 1980; Stålberg, 1966). Several authors have shown

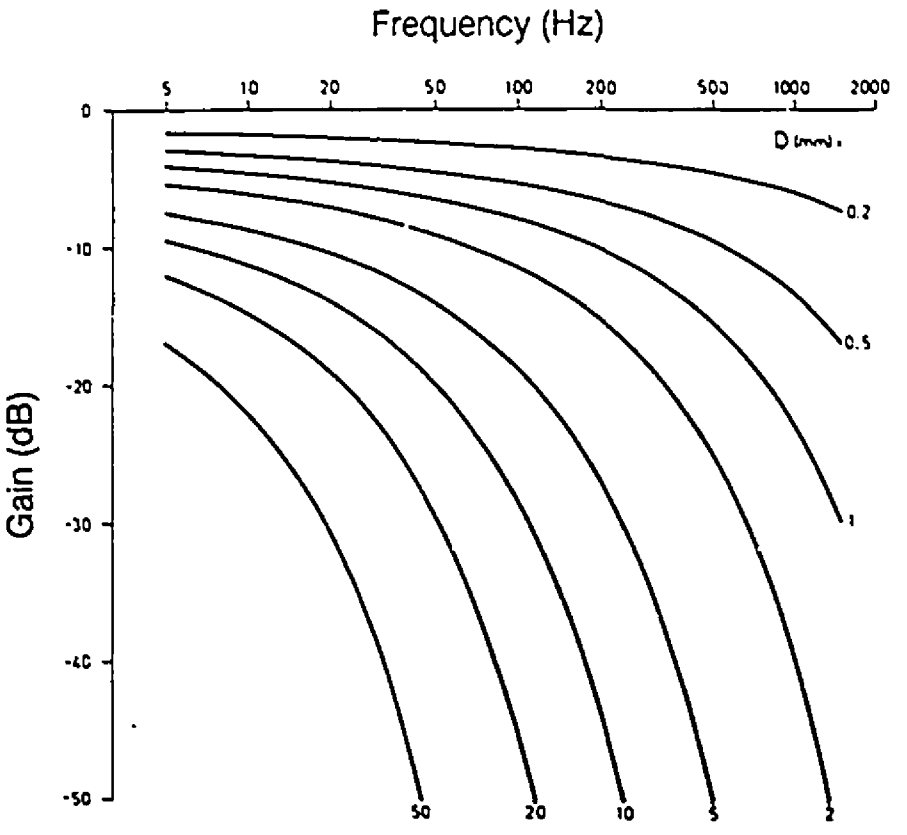

Figure 3.9. Logarithmic plot of the distance dependent filtering function. The parameter D indicates the distance from an active fiber to the detection electrode. (From Lindström, 1970)

that the peak to peak amplitude of the potentials (from single muscle fibers) decreases inversely with the radial distance raised to some power, for example n=1.3 (Håkansson, 1956, 1957b), or n=2.4 (Buchtal et al, 1957).

Studies concerning the effect of distance filtering on the frequency content of the EMG power spectrum are few. Gath and Stålberg (1978) found that the attenuation of the action potential peak-to-peak amplitude with radial distance is exponential, and the steepness of the decline depends on the frequency content of the signal. Gydikov and Gatev (1982) demonstrated an increase in duration of a single muscle fiber action potential as the radial distance increased, implying a reduction in the signal's frequency content. With respect to interference pattern EMG, it has been described that the peak of the power spectrum moves to lower frequencies with increasing distance between the electrodes and the muscle fiber (Andreassen & Rosenfalck, 1978; Gath & Stålberg, 1978; Lateva et al, 1993), but no comment was made regarding CF or MF values. Most recently, De la Barrera & Milner (1994) demonstrated a significant, inverse correlation between MF values obtained from the biceps brachii, and skinfold thickness, but a description of the power spectrums was lacking.

3.6.5. Innervation zone

Bipolar electrodes positioned directly over an innervation zone will produce a complex interference pattern (Basmajian & De Luca, 1985; Desmedt, 1958; Lindström, 1973), and will strongly affect the power spectrum (Lindström, 1973).

The mathematical expression which describes the power spectrum obtained with electrodes overlying an innervation zone shows a very complicated oscillating pattern, the derivation of which is beyond the scope of this thesis (Lindström, 1973). However, the innervation zone effect can be reduced to a simplified model, and is described by:

$$\text{Innervation zone factor} = \sin(\omega z/v)$$

where z is the distance between the center of the total innervation zone and the center point

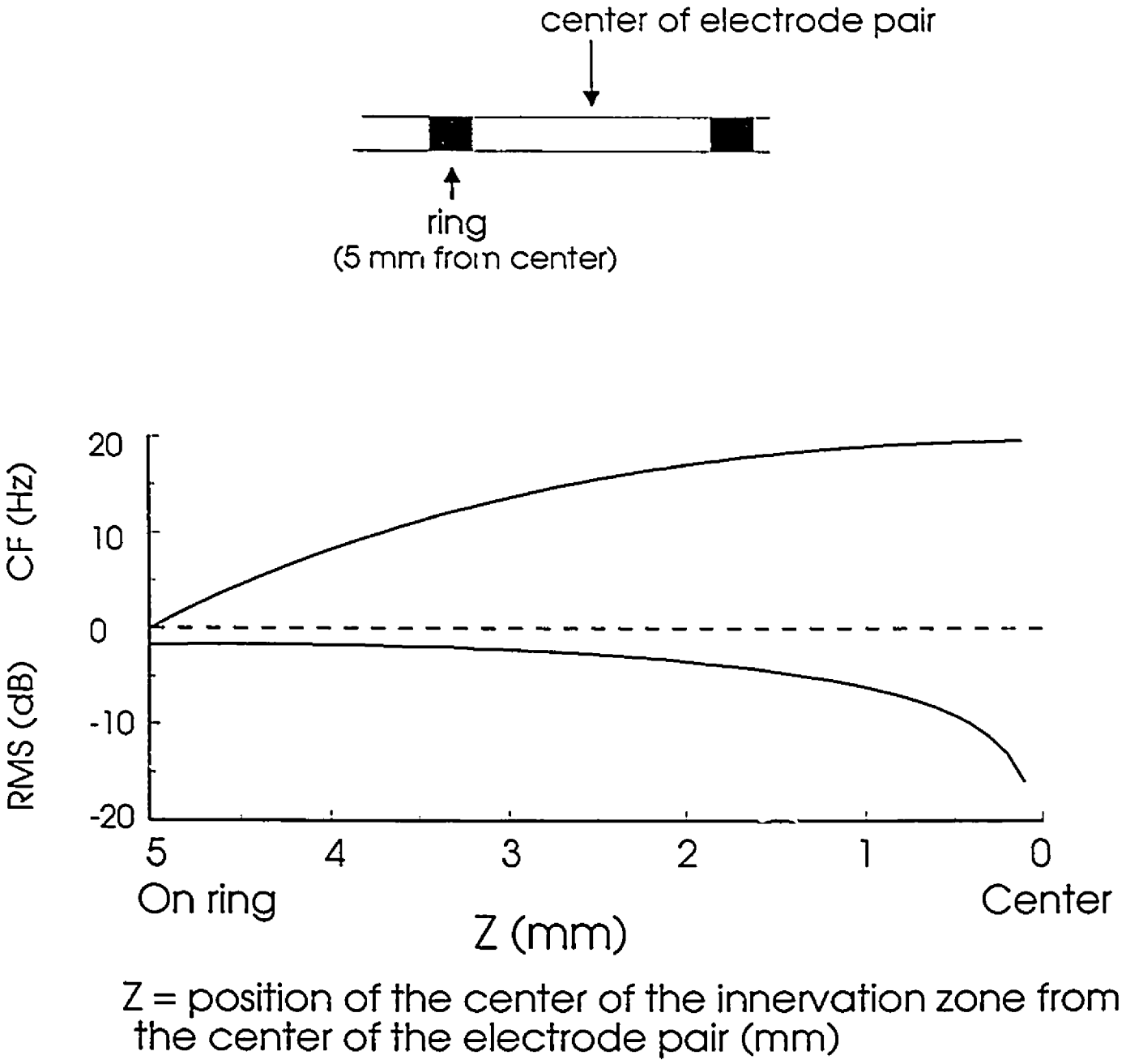

Figure 3.10. Effect of innervation zone on CF and RMS according to Lindström model (personal communication)

between the two electrodes (Lindström, personal communication). This factor is added to the previously described sine function describing the bipolar electrode transfer function (see Section 3.6.1.). According to mathematical predictions, bipolar EMG recordings obtained with electrodes overlying an innervation zone are predicted to be reduced in total power, and to have a broadened power spectrum with enhanced contributions in the high frequency range. This indicates that spectral estimates, such as the CF and MF, will increase when the electrode pair lies over an innervation zone, and that RMS values will decrease. The above innervation zone factor is presented graphically in Figure 3.10.

Studies on limb muscles have demonstrated that EMG signals obtained by bipolar surface electrodes are influenced by the underlying innervation zones (Buchtal & Rosenfalck, 1955; Hilfiker & Meyer, 1984; Lindström & Kadefors, 1974; Masuda et al, 1983a,b; Morimoto et al, 1980; Roy et al, 1986; Saitou et al, 1991). Morimoto et al (1980) found that when one of the electrodes from a bipolar electrode pair was positioned directly over an end-plate, action potentials were steeper and shorter in duration near the innervation zone than at a distance from them. In a later study, it was observed that when the innervation zone was located just under the center of the bipolar electrode pair, the amplitude of the signals was clearly reduced (Masuda & Sadoyama, 1986; Morimoto, 1986). This is similar to the findings of Lindström & Kadefors (1974), in which a 10 dB decrease in power was observed at the innervation zone when an electrode pair was moved along the muscle from one end to the other. In agreement with Lindström's predictions, Roy et al (1986) and Saitou et al (1991) found that measurements of MF were consistently highest at the region of the innervation zone of the tibialis anterior, and the biceps brachii, respectively. The technical conclusion is therefore that when bipolar surface electrodes are used for measurement, the innervation zone should be avoided.

3.7. PHYSIOLOGICAL FACTORS WHICH INFLUENCE THE EMG POWER SPECTRUM

3.7.1. Muscle length

Based on the cable theory of electric propagation, Hodgkin & Rushton (1946) predicted

that the CV of fibers with identical membranes and cellular composition should vary as the square root of the fiber diameter, i.e. $v = k\sqrt{r}$, where v is the conduction velocity, r is the radius of the fiber, and k is a constant. *In vitro* studies in both nerves and skeletal muscle fibers have confirmed that when fibers of different diameters were evaluated, the CV was found to be directly proportional to the fiber diameter, i.e. $v = kr$ (Håkansson, 1956; Katz, 1948).

Based on the assumption and the experimental verification that the volume of a muscle fiber remains constant during length changes (Elliot et al, 1963, 1967), stretching of a muscle fiber will result in a decrease in muscle fiber diameter. In 1946, Hodgkin & Rushton hypothesized that a reduction in diameter (due to lengthening of the fiber), will result in an increase in intracellular resistance, and hence will reduce CV. Later, Hodgkin (1954) proposed that when a fiber is stretched, the increase in intracellular resistance caused by the reduced diameter could be compensated by a decrease in surface area (per unit length) produced when the membrane "unfolds". (This "unfolding model" is based on the assumption that both the surface area and the volume of the muscle fiber, or at least their ratio, remain constant during stretching). According to this model, Hodgkin (1954) predicted that CV remains constant during stretching of a muscle fiber. The unfolding of the muscle fiber membrane with passive stretch of the muscle was later demonstrated *in vitro* (Dulhunty & Franzini-Armstrong, 1975), and it was shown that the foldings in the membrane, or caveolae, provide the membrane necessary for the maintenance in surface area.

Studies on single muscle fibers *in vitro*, under well controlled experimental conditions, have demonstrated that CV does not change with moderate changes in muscle length (Håkansson, 1957; Martin, 1954; Oetlicker & Schumperli, 1982). In fact, under conditions of extensive stretching of muscle fibers, it has been reported that CV can actually increase (Håkansson, 1957; Inoue, 1955; Oetlicker & Schumperli, 1982).

In vivo experiments performed on whole limb muscles with bipolar surface EMG electrodes have demonstrated that CF/MF and CV values can either increase (Bazzy et al, 1986; Inbar et al, 1987; Kappert et al, 1989; Okada, 1987; Shankar et al, 1989), remain unchanged (Saitou et al, 1991; Sato, 1982), or decrease (Petrofsky et al, 1982; Shankar et al,

1989) with muscle shortening. With respect to muscle lengthening, Morimoto (1986) found a decrease in CV. Experiments performed with needle electrodes have as well provided conflicting results, and have showed that CV can increase (Trontjel, 1993), (Kossev et al, 1992), or remain unchanged (Gydikov & Kosarov, 1973) with muscle length.

In general, surface recording studies pertaining to muscle length and its effect on the EMG power spectrum should be interpreted with caution. As stated at the onset of this chapter, numerous physical factors can influence the frequency content of the EMG signal, particularly when bipolar surface electrodes are used, the most important being the position of the electrodes with respect to the innervation zone (see Section 3.6.5.). Surface electrodes placed on the biceps will move with respect to the underlying innervation zone as the muscle changes in length and thus will lead to erroneous measurements of CF and/or MF values (Saitou et al, 1991). In addition, the changes in skin thickness which occur with changes in muscle length, will alter the electrode-to-muscle distance (De la Barrera & Milner, 1994) and will filter the signal as previously described (Section 3.6.4.). Lastly, studies in which the interelectrode distance is not kept constant cannot be considered reliable as the EMG power is significantly influenced by changes in interelectrode distance (Section 3.6.2.). The above can be exemplified by an *in vivo* study in our laboratory in which signal quality, electrode positioning, and distance filtering were controlled for (Sinderby et al, 1993c). The results indicated a tendency for a 10 % increase in CV with 50% shortening of the diaphragm from FRC, as determined by extrapolation of the obtained data (Sinderby et al, 1993c).

In summary, well controlled studies *in vitro* and *in vivo* indicate that there are minor or no changes in CV with changes in muscle length, and that studies in which the methodology is not controlled, can show a variety of results.

3.7.2. Muscle force

The effects of muscle force on the EMG power spectrum can be described in terms of the complicated, interacting effects of motor unit summation, recruitment according to the "size principle", and motor unit firing rate, which are described in 3.7.2.(i) through (iv). The last

subsection (v) will deal with the "global" effect of force on CF/MF/CV.

3.7.2.(i) Motor unit summation effects

As previously described (section 3.3), the interference pattern EMG's power spectrum obtained during moderate to high levels of contraction is determined by the summation (random, temporal and/or spatial) of individual motor unit signals.

Random summation (Figure 3.5.B.): Computer simulations of the EMG power spectrum have demonstrated that the power spectrum of randomly summated signals contains fluctuations, but overall, has the same shape as that of the single motor unit power spectrum. The power spectrum of randomly summated signals thus reflects the properties of the individual components (Lindström & Broman, 1974).

Temporal summation (Figure 3.5.C.): Temporal summation of signals (signals arriving at a regular time sequence) also yields an EMG signal whose power spectrum's shape is similar to that of the single motor unit spectrum. In this case, the power spectrum is characterized by a number of peaks which occur at frequencies which are equal to the firing rate of the individual signal and its harmonics (Lindström & Pétersen, 1981; Van Boxtel & Schomaker, 1984).

Spatial summation (Figure 3.5.D.): In the case of spatial summation, where the individual motor unit signals are synchronized with relatively small time differences, the power spectrum's shape is altered considerably (Lindström & Pétersen, 1983). At low and high frequencies, the shape of the spectral curve follows that of the individual motor unit spectrum. The position of the curve is, however, shifted upwards in the low frequency range by an amount proportional to the number of active motor units. The energy of the power spectrum drops at higher frequencies, the relative amount depending also on the number of active units.

3.7.2.(ii) Recruitment according to the size principle

It has been hypothesized that the progressive recruitment of larger motor units can account for the increases in CF/MF/CV observed during the gradation of muscle force (Andreassen & Arendt-Nielsen, 1987; Arendt-Nielsen et al, 1984; Broman et al, 1985;

Gantchev et al, 1992; Masuda & DeLuca, 1991; Roy et al, 1986; Sadoyama et al, 1983; Solomonow et al, 1990), regardless of the type of summation.

It is generally accepted that during voluntary muscle contraction, the recruitment of motor units progresses according to a "size principle", from small units to large units (Henneman, 1957). As previously described (see section 3.4.2.), fibers of larger diameter have higher CVs, supporting the above suggestion that the increase in CF/MF/CV with force is due to the recruitment of larger motor units. Andreassen & Arendt-Nielsen (1987) found that the CV of a single motor unit was related to the contractile properties of the unit (rise time, twitch force, one half relaxation time), and hence, that CV could be considered a size principle parameter. It has been demonstrated experimentally with both surface (Masuda & DeLuca, 1991) and needle recordings (Gantchev et al, 1992) that motor units with higher recruitment thresholds have higher CVs. According to Gantchev et al (1992), CV in itself cannot be regarded as a size principle parameter because the recruitment threshold-CV relationship was found to be non-linear. On the other hand, a strong correlation between CF and fast-twitch fiber content (type II fibers) has been demonstrated (Gerdle et al, 1988b; Moritani et al, 1985), supporting the statement by Andreassen & Arendt-Nielsen (1987) that CV is a size principle parameter.

3.7.2.(iii) Effects of increasing firing rate

It has been shown *in vitro* that the excitability of a nerve or a muscle membrane is affected by the preceding action potential (Hanson, 1974; Homma et al, 1983). Stålberg (1966) demonstrated an increase in CV with decreasing spike interval in *in situ* human single muscle fibers. The signals were recorded with a multielectrode needle during both electrically evoked and voluntary muscle activation, and he defined the term "velocity recovery function" to describe the changes in CV with firing rate.

The same increase in CV with motor unit firing rate has been found by various authors using surface electrodes (Gydikov et al, 1976; Morimoto & Masuda, 1984; Nishizono et al, 1979; Sadoyama & Masuda, 1987), and concentric needle electrodes (Fuglsang-Frederiksen

& Ronager, 1988). In contrast, others have demonstrated that firing rate has no effect at all on CF/MF/CV values with electrical stimulation (Solomonow et al, 1990), under conditions of voluntary activation (Kossev et al, 1991), or with computer simulations of the EMG power spectrum (Hermens et al, 1991; Rourke et al, 1984). Sadoyama & Masuda (1987) presented a study in which they found that the change in CV within the individual motor units was smaller than the overall change in the average CV for the full range of the contraction force. They suggested that the increases in CV observed within the motor unit due to increased firing rate alone, are not sufficient to account for the increase in the average CV, and thus the effect of recruitment of additional motor units with higher CVs should not be discounted. In fact, Moritani & Muro (1987) concluded that the linear increase in the CF of the EMG power spectrum with increasing force in the biceps brachii was due to a combination of both an increase in firing rate, and the progressive recruitment of additional motor units.

3.7.2.(iv) Recruitment related distance filtering theory

Another explanation for the increase in CF/MF/CV with increasing levels of force includes the decreased influence of distance dependent filtering during the recruitment of larger, more superficial motor units, as seen in the biceps (Hagberg & Ericson, 1982; Hagberg & Hagberg, 1988).

3.7.2.(v) Effect of "global" force on CF/MF/CV

Studies evaluating the effect of muscle force on the EMG power spectrum have provided conflicting results. Experiments performed with surface electrodes have indicated that the CF/MF, or average CV can either increase in a linear (Bilodeau et al, 1990; Broman et al, 1985; Gerdle et al, 1990; Moritani & Muro, 1987) or curvilinear fashion (Arendt-Nielsen et al, 1984; Gantchev et al, 1992; Hagberg & Ericson, 1982; Hagberg & Hagberg, 1988; Komi & Vitasalo, 1976; Masuda & DeLuca, 1991; Naieje & Zorn, 1982; Palla & Ash, 1981; Sadoyama et al, 1983; Van Boxtel & Schomaker, 1984; Zwarts et al, 1988), or can remain unchanged with increasing levels of contraction (Bazzy et al, 1986; Bigland-Ritchie et al, 1981; Bilodeau et al, 1990;

Eberstein & Beattie, 1985; Gerdle et al, 1988a; Kaiser & Pétersen, 1963; Lindström & Pétersen, 1981; Merletti et al, 1984; Petrofsky & Lind, 1980a,b; Sato, 1976; Seki et al, 1991; Sollie et al, 1985a,b; Tarkka, 1984; Vitasalo & Komi, 1978). Studies reporting the curvilinear relationship between force and CF/MF/CV show inconsistencies with respect to the range of % maximal voluntary contraction (MVC) where CF/MF/CV was found to increase, and then plateau. In one study, CF was even found to decrease with increasing levels of force (Westbury & Shaughnessy, 1987). It must be mentioned however, that factors such as summation effects, recruitment, and firing rate were not evaluated in these studies. As well, the effect of fatigue on CF/MF/CV must be taken into consideration in studies evaluating the EMG at high levels of contraction.

The discrepancies between different studies may in part be due to differences in electrode size and inter-electrode spacing, as suggested by Bilodeau et al (1990). Moritani & Muro (1987) saw an increase in CF with force using small electrodes (4 mm) and a smaller inter-electrode distance of 6 mm, but no relationship with larger electrodes (10 mm), and an inter-electrode distance of 40 mm. Hagberg & Ericson (1982), using an inter-electrode distance of 20 mm, observed an increase in CF up to about 25-30% of MVC, while Petrofsky & Lind (1980a), using a 40 mm inter-electrode distance did not find any relationship at all. This seems to support the above suggestion that electrode size and spacing may be related to the differences between studies, however, it should also be pointed out that the muscles investigated in these studies were different.

Differences in muscle type alone could account for the discrepancies, as suggested by Moritani et al (1985). As described in Chapter 2, Section 2.4., different muscles have different recruitment threshold levels (and ranges of increasing firing rate), thereby providing one possible factor behind the different results in force-CF/MF/CV relationships reported in the literature. In addition, it has been suggested that the type of contraction (ramp vs. step) may influence the force- CF/MF/CV relationship (Bilodeau et al, 1991).

It is also possible that the different observations concerning the force-CF/MF/CV relationship are due to inaccurate positioning of the electrodes with respect to the muscle fiber direction and the innervation zones. In studies where the cross-correlation method is used to

calculate the average CV (Andreassen & Arendt-Nielsen, 1987; Broman et al, 1985; Sadoyama & Masuda, 1987), accurate electrode orientation with respect to the fiber direction is crucial, and if altered, will result in over-estimations of the average CV (see Section 3.6.3.). CV/CF/ MF measurements are also highly sensitive to electrode positioning with respect to the innervation zone. In most studies, the position of the end-plate region is seldom, if ever, mentioned. Komi and Viitasalo (1976) and Viitasalo and Komi (1977) found a consistent decrease in the MF with contraction strength for the rectus femoris muscle when the electrodes were placed over the motor point of the muscle. When the electrodes were placed distally from the motor point, a curvilinear relationship between CF and force was obtained.

In general, none of the above theories (Sections 3.7.2.(i)-(iv)) can fully support or reject the effects of muscle force on the EMG power spectrum. This is due to the different methods used and the different muscles under investigation.

3.7.3. Cross-talk

Cross-talk is defined as the signal generated by a given muscle and detected on the surface of, or inside a different muscle (Merletti et al, 1992), and was first described by Denny-Brown (1949) who showed that electrical activity can be recorded from inactive or denervated muscle, which was simply acting as a conductive tissue.

Cross-talk signals from distant sources are distance filtered (see Section 3.6.4.), and hence, are signals with the high frequency components filtered out. Thus, the EMG power spectrum influenced by cross-talk will have an enhanced contribution of power in the low frequency range. This has been demonstrated experimentally in the canine diaphragm under control conditions (where the intercostals were contaminating the diaphragm signal), in comparison to conditions under spinal anesthesia, which abolished all non-diaphragm related EMG activity (Sinderby et al, 1994). The results showed an increase in CF values by up to 100 Hz from before to after spinal anesthesia, while CV remained constant. The increase in CF values following spinal anesthesia was mainly due to a reduction in low-frequency power (originally due to the low-frequency cross-talk signals from the abdominal, intercostal, and

other chest wall muscles) (Figure 3.11.).

Under conditions where anesthesia of "cross-talk" muscles is not appropriate, the influence of cross-talk can be reduced by altering the specificity of the (bipolar) electrodes, namely by changing their size (Ekstedt & Stålberg, 1973; Gath & Stålberg, 1976), or the interelectrode distance (Koh & Grabiner, 1992; Zipp, 1982; Lynn et al, 1978). Other electrode arrangements have been proposed to reduce the influence of cross-talk such as the double differential technique (Broman et al, 1985; De Luca & Merletti, 1988; Koh & Grabiner, 1992; Koh & Grabiner, 1993; Reucher et al, 1987b), and the branched electrode technique (Gydikov et al, 1984; Koh & Grabiner, 1993).

With respect to esophageal recordings of the diaphragm electromyogram, there are no reports indicating that cross-talk from other muscles (besides the esophagus) influences the signal. Anatomically, the gastroesophageal junction is located in a region which is unlikely to receive cross-talk signals from other muscles (Petit et al, 1960).

3.7.4. Muscle temperature

Muscle temperature increases during exercise, and was reported to be due to the increase in blood flow to the muscle (Clarke et al, 1958; Humphreys & Lind, 1963), and to metabolic heat production (Edwards et al, 1975). It has been determined that the CV of a nerve action potential slows by 4% for each 4°C fall in temperature (Cummins & Dorfman, 1981). The propagation velocity of the muscle fiber action potential is also highly dependent on muscle temperature (Roberts, 1969), due to its dependence on the excitability of the muscle fiber membrane. Fink and Luttgau (1976) have shown that the membrane potential in skeletal muscle depends to a large extent on muscle temperature, just as is predicted for nerve fibers by the Nernst equation (Ganong, 1991).

The influence of muscle temperature (10-40°C range) on the frequency content of the EMG signal, and on CV has been described by a number of investigators (Bigland-Ritchie et al, 1981; Gydikov & Kosarov, 1973; Håkansson, 1956; Holewijn, 1991; Jarcho et al, 1954; Merletti et al, 1984; Morimoto et al, 1980; Mucke & Heuer, 1989; Petrofsky & Lind, 1979, 1980b;

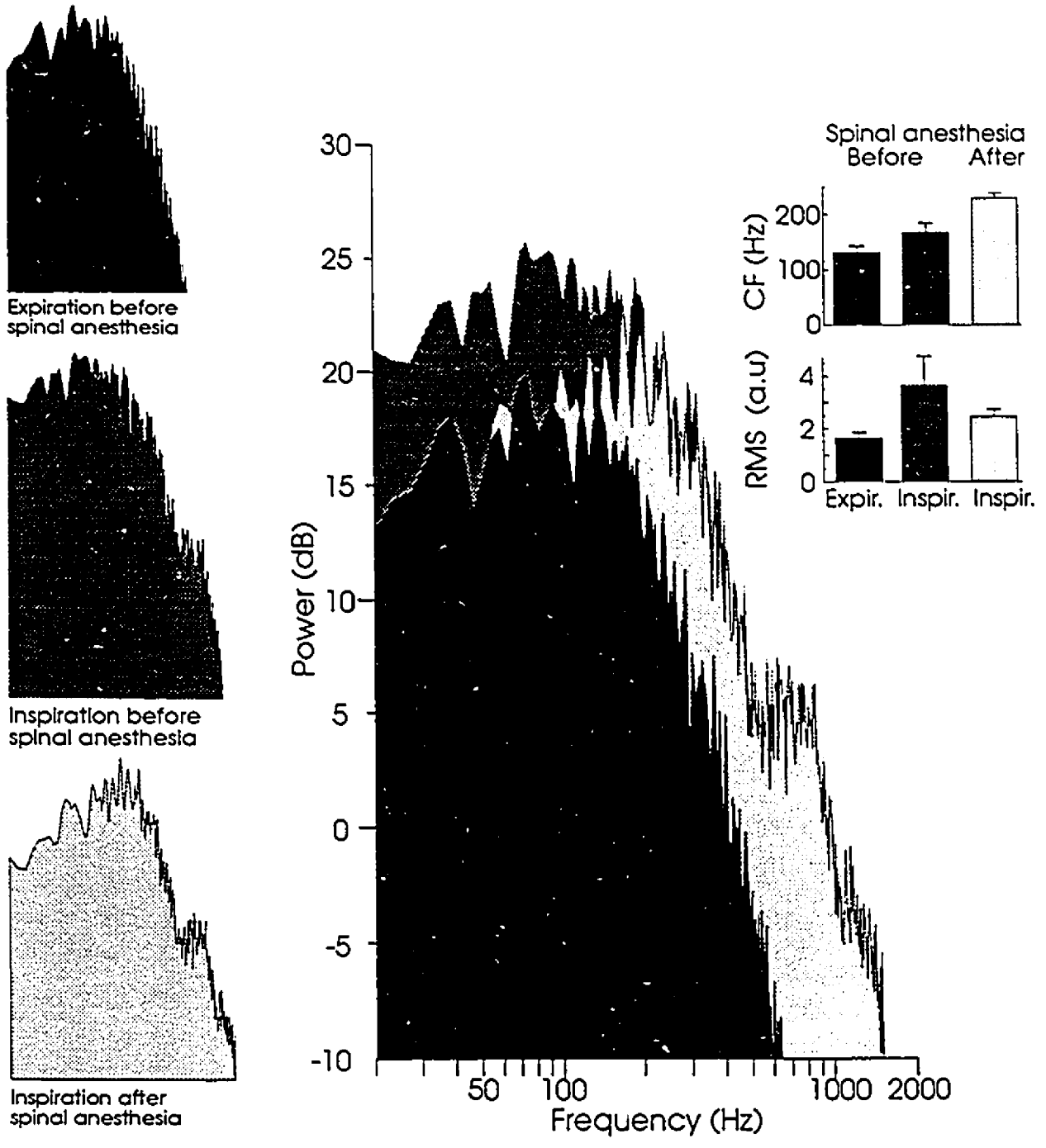

Figure 3.11. Effect of cross talk on EMG power spectrum and CF values (From Sinderby et al, 1994).

Stålberg, 1966). CF/MF were found to increase when the muscle was heated (Mucke & Heuer, 1989; Petrofsky & Lind, 1980b), and to decrease with muscle cooling (Holewijn, 1991; Merletti et al, 1984; Petrofsky & Lind, 1980b). The relationship between CF and temperature seems to no longer hold true for temperatures greater than 35°C (Mucke & Heuer, 1989). An increase in action potential duration was also reported (Petrofsky & Lind, 1980b) with muscle cooling, and it was suggested that this is due to a reduction in CV. The reduction in CV due to muscle cooling has been verified *in vitro* (Buchtal & Engbaek, 1963; Håkansson, 1956; Jarcho et al, 1954).

3.7.5. Fatigue

The concept of muscle fatigue is complex, and includes both physiological and psychological aspects. Edwards (1981) defined muscle fatigue as "the failure to maintain a required or expected force". Muscle contraction is produced by a chain of events at different levels of the nervous system, from the brain to the contractile proteins in the muscle cell, and fatigue can thus originate from any of these levels. "Central fatigue" involves fatigue of any level proximal to the neuromuscular junction, and has been attributed to such factors as lack of motivation, damage to the centers for motor control, spinal cord and motor neurons. "Peripheral fatigue" includes fatigue produced at the neuromuscular junction (neuromuscular fatigue), at the sarcolemma, during excitation-contraction coupling, or in the contractile mechanism of the muscle cell (Bigland-Ritchie, 1981).

Empirically, frequency analysis of the EMG signal during sustained contractions reveals that the signal is altered long before the mechanical manifestations of fatigue are evident. As early as 1912, Piper noticed that the properties of the EMG signal were altered during a sustained muscular contraction, and described a "slowing" of the signals when the muscle was close to failing during an endurance test. With the advent of computer technology, it became possible to scrutinize the effects of localized muscle fatigue on the EMG signal, by observing how the power spectrum of the signal is altered. The effect of localized muscle fatigue on the EMG power spectrum is characterized by (1) a loss of high frequency power, and

2) an increase in low frequency power. These events have been referred to as a "spectral shift" to lower frequencies, or a "spectral compression" (Merletti et al, 1992). Numerous investigators have observed a spectral shift during sustained contractions in limb muscles (Arendt-Nielsen et al, 1984; Arendt-Nielsen & Mills, 1985; Bigland-Ritchie et al, 1981; Broman et al, 1985; Gath & Stålberg, 1975; Hagberg & Ericson, 1982; Häkkinen & Komi, 1983; Kadefors et al, 1968; Kaiser & Pétersen, 1963; Kogi & Hakamada, 1962; Lindström et al, 1974, 1977; Petrofsky & Lind, 1980b; Sadoyama & Miyano, 1981; Sato, 1965; Stulen & De Luca, 1981), and in the diaphragm (Gross et al, 1979; Bellemare & Grassino, 1982).

All mathematical formulas proposed by Lindström (1970) to model the EMG power spectrum contain a linear relationship between the angular velocity (or 2π times frequency) and CV, stating that any change in CV must be accompanied by a shift of the power spectrum along the frequency axis, and a concomitant change in the frequency parameters such as CF and MF (Lindström, 1970). Hence, based on mathematical theory, it is accepted that the occurrence of spectral shifts to lower frequencies is due to a reduction in CV. As early as 1970, Lindström suggested that the reduction in CV is due to a "localized ischemic muscle fatigue", which alters the metabolic and thermal properties of the muscle cell, and hence affects the excitability of the muscle fiber membrane, and its CV.

Experimentally, investigators have shown a decrease in CV during sustained contractions by using the so-called "dip technique" (Lindström et al, 1970; Broman, 1977; Sinderby, unpublished obsevations), and by measuring the time delay between two simultaneously measured signals (Arendt-Nielsen et al, 1984; Arendt-Nielsen & Mills, 1985; Brody et al, 1991; Eberstein & Beattie, 1985; Sadoyama & Miyano, 1981; Sinderby et al, 1994). With respect to frequency parameters, a reduction in both CF (Alfonsi et al, 1991; Béliveau et al, 1991; Körner et al, 1984; Lindström et al, 1977; Lindström & Magnusson, 1977; Petrofsky & Lind, 1980b; Naije & Zorn, 1981; Sadoyama & Miyano, 1981; Sinderby et al, 1994), and MF (DeLuca, 1984; Stulen & De Luca, 1981; Vestergaard-Poulsen et al, 1992) has been observed during sustained contractions. An example of the drop in CF (measured with an esophageal electrode) observed during fatiguing contractions of the human diaphragm is presented in

Figure 3.12.

A linear relationship between CV and CF/MF has been reported during fatiguing contractions (Eberstein & Beattie, 1985; Arendt-Nielsen et al, 1984; Arendt-Nielsen & Mills, 1985; Roy et al, 1986; Sadoyama et al, 1983; Sinderby et al, 1994; Zwarts et al, 1987). Others have demonstrated that the relationship does not exist (Naeje & Zorn, 1982) or is non-linear (Yaar & Niles, 1992).

Again, one should consider that CV and the spectral shifts are very sensitive to errors in methodology. Roy et al (1986) showed that the outcome of the correlation between CV and MF (during fatigue) was directly dependent on the position of the electrodes with respect to the innervation zone. Sinderby et al (1993b) demonstrated that the relationship between CF and CV during fatigue disappears when interelectrode distances >10 mm are used.

A number of explanations have been proposed to account for the decrease in CV during sustained contractions, and are more or less based on the idea that muscle perfusion is reduced during contraction. Körner et al (1984) demonstrated that intramuscular pressure is a significant determinant of whether localized muscle fatigue will occur, due to the impaired perfusion of the muscle during contraction. A decrease in muscle perfusion will not only result in hypoxemia, and hence production of lactic acid via anaerobic metabolism, but will also reduce the washout of various metabolites (such as hydrogen, sodium and potassium ions), which could affect membrane excitability (Kahn & Monod, 1989) and CV.

It has been reported that reductions in CV and spectral shifts may be due to: (1) a decrease in intracellular pH (Brody et al, 1991; Vestergaard-Poulsen et al, 1992), (2) accumulation of lactic acid (Alfonsi et al, 1991; Horita & Ishiko, 1987; Mortimer et al, 1970; Tesch et al, 1983), and (3) accumulation of metabolites such as sodium and potassium ions (Bigland-Ritchie, 1979; Jones et al, 1979; Mills & Edwards, 1984). *In vitro* studies have confirmed that CV is affected by both intracellular pH, and the extracellular concentration of potassium (Juel, 1988). For an in depth review of the cellular mechanisms of muscle fatigue, the reader is referred to the most recent work by Fitts (1994). In general, it is still not known which specific factors are the most responsible for the reduction of CV seen with fatigue.

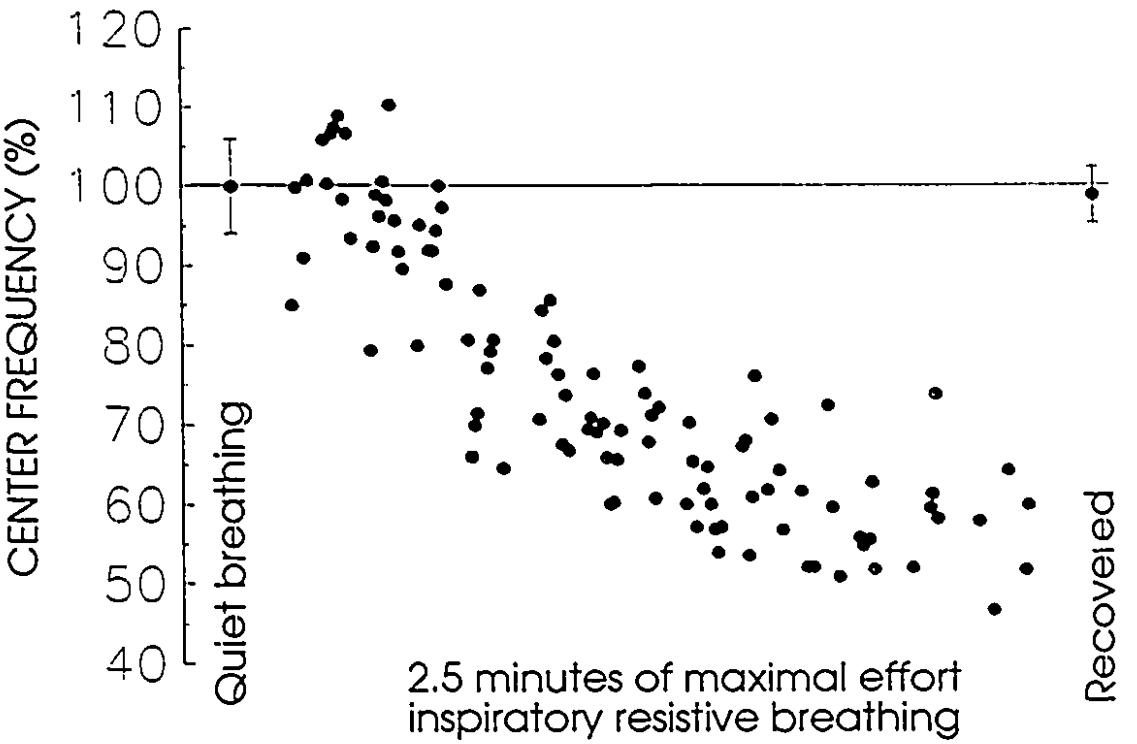

Figure 3.11. Example of the decrease in CF values of EMGdi (esophageal electrode) observed during maximal effort resistive breathing (From Sinderby et al, 1993a).

Other explanations, besides a reduction in CV, have been offered to explain the findings of a spectral compression including, (1) synchronization (Agarwal & Gottlieb, 1975; Bigland-Ritchie et al, 1981; Buchtal & Madsen, 1950; Chaffin, 1973; Fex & Krakau, 1957; Kadefors et al, 1968; Kwantny et al, 1970; Lippold et al, 1960; Person & Kudina, 1968; Person & Mishin, 1964; Sato, 1965; Scherrer & Bourguignon, 1959; Blinowska et al, 1980; Jones & Lago, 1982; Lago & Jones, 1977), (2) decrease in the mean firing rate (DeLuca, 1979; DeLuca, 1984; Fuglsand-Frederiksen & Ronager, 1988; Gerdle et al, 1990; Yaar & Niles, 1992; Van Boxtel & Schomaker, 1984), (3) recruitment and de-recruitment of motor units with different CVs (Kadefors et al, 1968; Kondo, 1960; Merletti et al, 1992, Sadoyama & Miyano, 1981).

It should be mentioned that any investigator applying spectral parameters and/or CV values as indicators of local muscle fatigue should be aware of all the factors which can influence the EMG signal (Sections 3.6. and 3.7.). It cannot be emphasized enough that in order to determine the cause of the spectral shift, the factors affecting the spectrum must be taken into account before any physiological interpretations can be made.

CHAPTER 4

THE DIAPHRAGM

This chapter provides the background which is relevant to the methodology used in this thesis. As the focus of this thesis is mainly the study of the electromyogram of the diaphragm (EMGdi), a detailed description of the other respiratory muscles, their mechanics, and interaction is not provided, however, the reader is referred to several recent works for a complete review (De Troyer, 1991; De Troyer & Estenne, 1988; De Troyer & Loring, 1986; Rochester, 1992).

The diaphragm is the principle muscle of inspiration. It is functionally a skeletal muscle, but is unique from most other skeletal muscles in that it contracts rhythmically throughout an individual's life (Derenne et al, 1978). The diaphragm is also different from most skeletal muscles in that it can either contract voluntarily, or it can be automatically driven by the lower respiratory centers (Derenne et al, 1978; De Troyer et al, 1983). In addition, it has been demonstrated that the diaphragm has other functions which are not related to respiration including, the maintenance of posture (Sinderby, 1991), defecation, and parturition (Grassino et al, 1991).

4.1. FUNCTIONAL ANATOMY OF THE DIAPHRAGM

The diaphragm separates the thoracic and abdominal cavities, its convex upper aspect facing the thorax, and its concave inferior surface directed towards the abdomen (De Troyer, 1991) (Figure 4.1., top panel). The periphery of the diaphragm consists of muscle fibers attached to the various bony structures of the rib cage and the spine, which converge into a tendinous sheet, the central tendon. While the diaphragm was originally considered to contract as a single unit (Sant'Ambrogio et al, 1963), more recent studies have suggested that the diaphragm can be regarded as two separate muscles, the costal portion and the crural portion (Roussos & Macklem, 1982), based on different segmental innervations (Lardau et al, 1962), different actions (De Troyer et al, 1981), and different embryological origins (Langman,

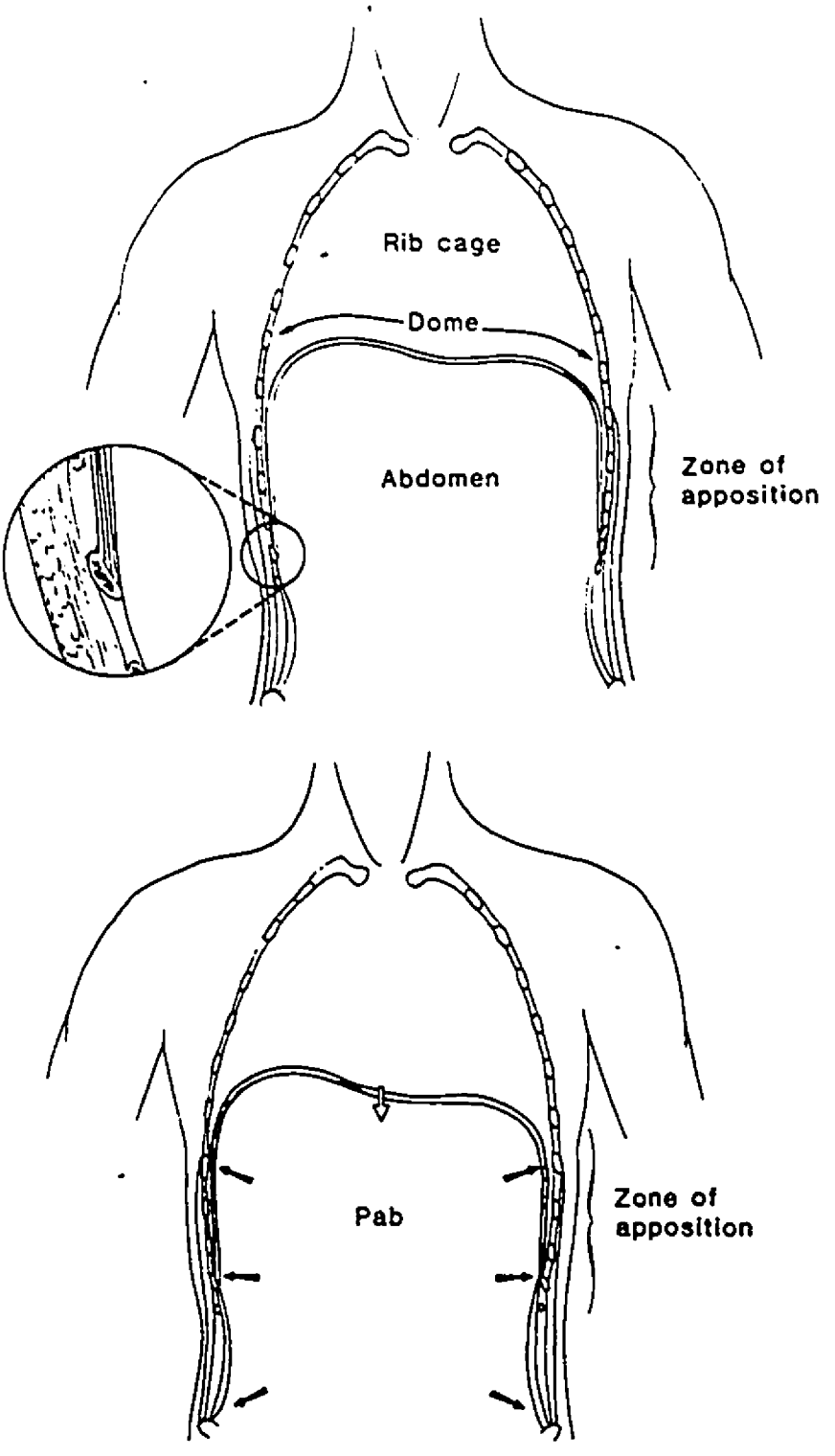

Figure 4.1. Top: Functional anatomy of the diaphragm. Note the orientation of the costal diaphragmatic fibers (inset). Bottom: Appositional component of diaphragm action. Descent of the diaphragmatic dome during inspiration (open arrow) causes an increase in abdominal pressure that is transmitted through the apposed diaphragm to expand the lower rib cage (bold arrows). (From De Troyer & Estenne, 1988).

1978).

Anatomically, the muscle fibers of the diaphragm can be divided into three main components - sternal, costal, and lumbar (or crural). The sternal portion arises from the back of the xiphoid process of the sternum (Figure 4.2.). The costal portion has its origin from the internal surfaces of the lower six ribs (Figure 4.1., top panel). The costal fibers run cranially, and are apposed directly to the inner aspect of the lower rib cage. The crural fibers arise from the ventrolateral aspects of the first three lumbar vertebrae on the right side, and from the first two lumbar vertebrae on the left (see Section 4.2. for a more detailed description of the crural diaphragm anatomy).

Functionally, the diaphragm can be considered as an elliptical cylinder capped by a dome (De Troyer, 1991; De Troyer & Estenne, 1988; De Troyer & Loring, 1986). The dome of the diaphragm is mainly composed of the central tendon while the cylindrical portion corresponds to the portion of the costal fibers which are directly apposed to the rib cage (Figure 4.1., top panel), and constitutes the so-called "zone of apposition" (Mead, 1979; Mead & Loring, 1982). With an increase in tension and shortening of the muscle fibers in the zone of apposition, the axial length of this area is reduced and the dome of the diaphragm descends relative to its costal insertions. The size and shape of the diaphragmatic dome, however, remain relatively constant during inspiration. Thus, the most prominent change in diaphragmatic shape is a piston-like axial displacement of the dome related to the shortening of the apposed muscle fibers (Mead & Loring, 1982).

During inspiration, the diaphragm contracts and exerts a force on the central tendon such that the dome of the diaphragm descends. This causes an expansion of the thoracic cavity and displaces the abdominal contents caudally. Thus, contraction of the diaphragm results in a fall in pleural pressure and an increase in lung volume (if the airways are open), and at the same time produces an increase in abdominal pressure which results in an outward motion of the abdominal wall (Figure 4.1., bottom panel).

Contraction of the diaphragm has three main actions on the rib cage: (1) During inspiration, the section of the rib cage above the area of apposition is influenced by the

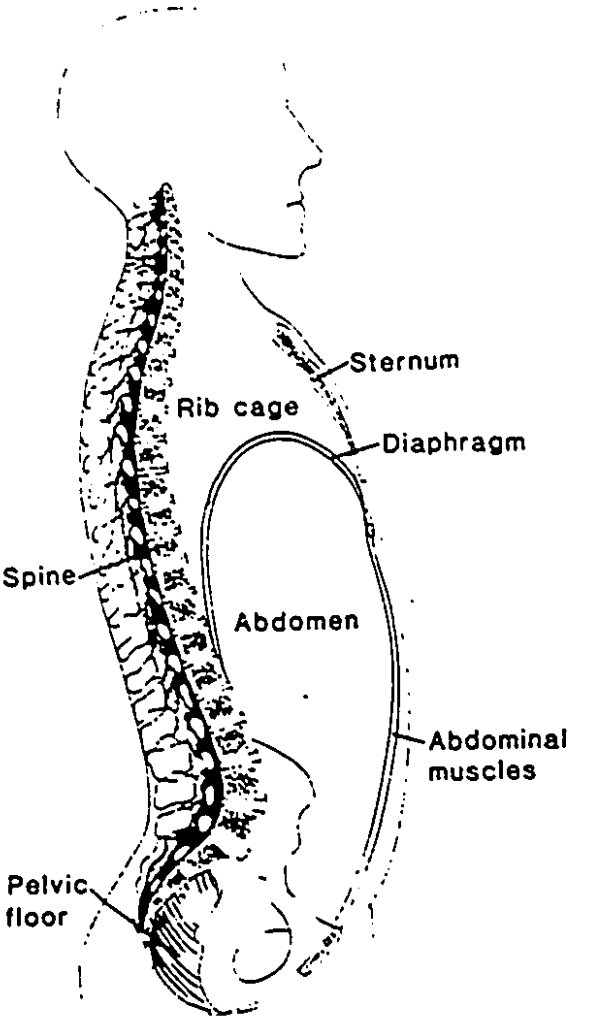

Figure 4.2. Illustration of the sternal insertion of the diaphragm. (From De Troyer & Estenne, 1988)

negative pleural pressure, which has an expiratory effect on the upper rib cage (Mortola & Sant'Ambrogio, 1978). (2) The lower rib cage in the area of apposition is exposed to the positive abdominal pressure, which expands the lower rib cage (appositional force) (De Troyer et al, 1982). (3) The diaphragm also exerts a direct force at the site of its insertions onto the lower six ribs (insertional force) (De Troyer et al, 1982), lifting the lower rib cage upwards and outwards (bucket handle motion). Because the crural diaphragm lacks attachments to the rib cage, the insertional force only applies to the costal portion of the diaphragm (De Troyer, 1991). Contraction of the crural portion of the diaphragm results in descent of the diaphragmatic dome, and hence contributes to the expiratory effect of the negative intra-pleural pressure and to the inspiratory effect of abdominal pressure i.e. the appositional force (De Troyer, 1991). The net action of the diaphragm on the rib cage therefore depends on the balance between the insertional and appositional forces that tend to expand the rib cage, and the expiratory action produced by the decrease in pleural pressure (Loring & Mead, 1982).

4.2. ANATOMY OF THE ESOPHAGEAL HIATUS IN RELATION TO THE CRURAL DIAPHRAGM

The complexities associated with esophageal recordings of EMGdi lie in the complicated anatomy of the crural diaphragm, and the surrounding esophageal structures. For this reason, the following description of the anatomy of the esophageal hiatus in relation to the crural diaphragm is provided.

The esophageal hiatus of the diaphragm is a muscular tunnel approximately 2-3 cm long, lying at the level of the tenth thoracic vertebra (Edwards, 1961; Skinner, 1972; Testut, 1921). The tunnel causes the esophagus to be oblique and oval in shape, and to angle slightly to the left and anteriorly as it passes through the diaphragm. Within the hiatus, the phrenoesophageal membrane anchors the esophagus to the diaphragm (Carey & Hollinshead, 1955). It has been noticed that the muscle fibers of the crural diaphragm bounding the esophageal opening, are more tightly applied to the esophagus on the right side than on the left side (Shehata , 1966). A narrow gap (2 to 3 mm) exists on the left side of the esophagus

between it and the less tightly applied crus.

As mentioned in the previous section (Section 4.1.), the muscles of the crural portion of the diaphragm arise posteriorly from the lateral aspects of the first three lumbar vertebrae on the right side, and from the first two lumbar vertebrae on the left. The muscles originating from the lumbar vertebrae form two distinct muscle bundles, the right and the left crura (Carey & Hollinshead, 1955), whose fiber direction is initially vertical (or cephalad), and then becomes more horizontal as the muscles pass anteriorly towards the central tendon.

From their origin, the right and left crura pass superiorly and medially past either side of the aorta, to form the margins of the esophageal hiatus (Figure 4.3.). With respect to the arrangement of the left and right crura in forming the hiatus, a variety of anatomic variations exist (Botros et al, 1990; Collis et al, 1954; Listerud et al, 1961; Pataro et al, 1961). In the most common pattern, the right crus divides into two unequal portions (a thick right and a thin left portion), to make up the margins of the hiatus (Figure 4.3., type A). The left portion of the right crus passes caudally across the left crus around the esophageal opening, and the right crus passes around the right side of the esophagus. However, this most frequent pattern has been reported to be present in only about 46% (Collis et al, 1954), 41% (Pataro et al, 1961), and 62% (Botros et al, 1990) of cadavers examined. In 10% of cadavers studied, both crura (left and right) provided equal contributions to the hiatus (Botros, 1990) (Figure 4.3., type B). The left crus can be dominant in 2% of cases (Botros et al, 1990). A common variation has been described in which a band of muscle from the left crus passes to the right side of the hiatus, and is commonly referred to as the muscle of Low (Low, 1907).

Regardless of the arrangement of the crus muscles around the esophagus, they usually continue as a band approximately 3-4 cm wide around the hiatus before inserting into the central tendon. Computed tomography scanning has revealed that the right crus is generally longer and thicker than the left, and that the thickness of both the right and the left crus (in cross section) is variable with respiration (Williamson et al, 1987). It has also been demonstrated that the thickness of the crural diaphragm, as measured by computerized tomography, does not change with age in the adult life (Caskey et al, 1989).

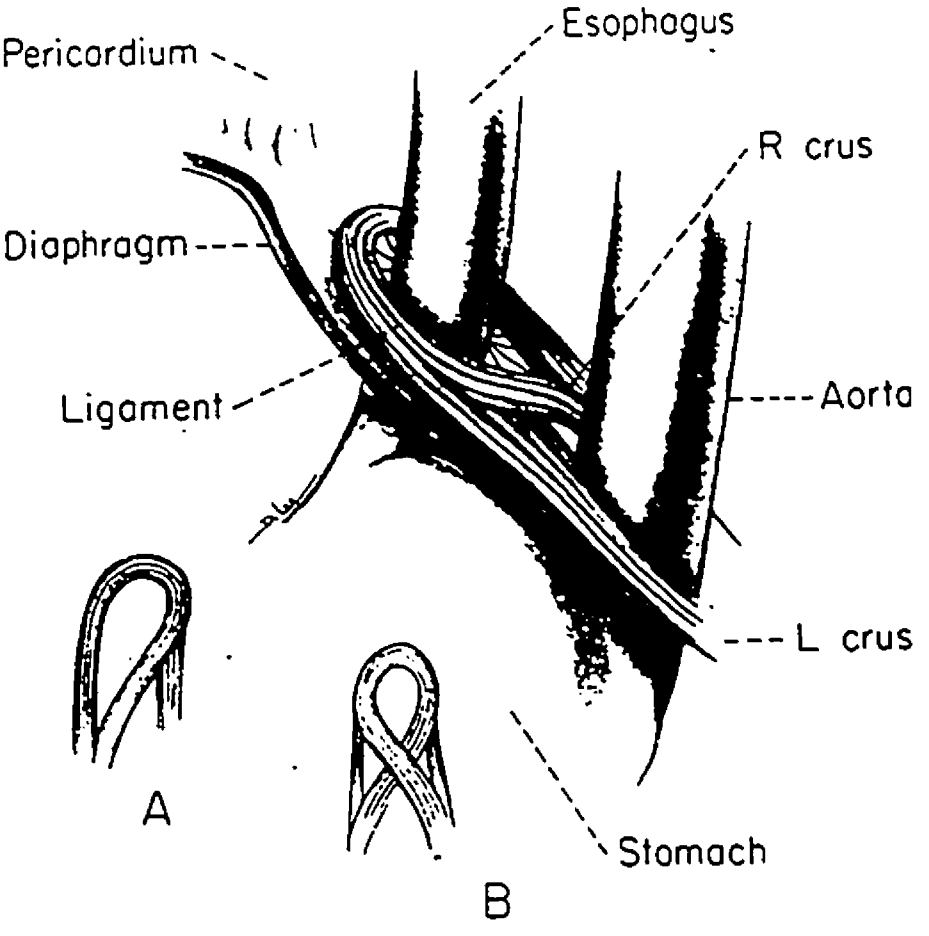

Figure 4.3. Crura of the diaphragm. A, most common anatomic variation. B, next most common variation. (From Payne & Spencer, 1974).

4.3. EVALUATION OF DIAPHRAGMATIC AND CHEST WALL CONFIGURATION BY THE METHOD OF KONNO AND MEAD

The purpose of this study was to determine the effect of diaphragm configuration on EMGdi. In this work, diaphragm configuration was evaluated by the configuration of the chest wall.

The chest wall can be considered to consist of the rib cage (RC) and the abdomen (AB), separated by the diaphragm (De Troyer, 1991). Numerous models have been applied to study the mechanics of the chest wall (Campbell, 1958; Konno & Mead, 1967; Macklem et al, 1978; Newman et al, 1984; Rahn et al, 1946). In the present study, the method of Konno and Mead (1967) was chosen, and will thus be the focus of this discussion.

4.3.1. Konno and Mead diagram

Konno and Mead (1967) hypothesized that the chest wall moves with two degrees of freedom, and that changes in lung volume can be accommodated by displacing the RC and/ or the AB. Since the diaphragm is a common wall for the AB and the RC, its own configuration (shape and radii of curvature) is set by the relative configurations of each of these compartments (Grassino et al, 1978).

Chest wall configuration and hence, diaphragm configuration, may be described in terms of RC and AB antero-posterior diameters, or in terms of their cross-sectional areas (CSA). The CSA of the RC and the AB can be measured by Respiratory Inductance Plethysmography via Respitrace® bands (Sackner et al, 1980). The transducers of the Respitrace® bands consist of coils of Teflon-insulated wire situated in a zig-zag pattern within an elastic band. One band is placed around the RC at the level of the sternum, whereas the other band is placed around the AB midway between the lower ribs and the iliac crest. The self-inductance of the coil is proportional to the CSA enclosed by the coil. Hence, a relative change in RC and AB CSA can be measured by the changes in self-inductance of the coils in each of the bands. The method of Konno and Mead involves the expression of chest wall

configuration by plotting RC CSA (y axis) versus AB CSA (x axis), as measured by the Respitrace® bands (Figure 4.4.).

4.3.2. Unique points on the Konno and Mead diagram

Each combination of RC and AB CSA (i.e. each point on the Konno and Mead diagram) represents a unique chest wall configuration and therefore, represents a unique diaphragm configuration (Figure 4.4.). The points indicated TLC, FRC, and RV represent the RC and AB CSAs obtained when these lung volumes were held by relaxing against a closed airway. The points that are in between represent intermediary lung volumes, and their respective CSA dimensions.

At a given lung volume, the Konno and Mead diagram may be used to infer changes in diaphragm length. For example, at FRC (point a, Figure 4.4.) with the muscles relaxed, the diaphragm has a particular length and configuration. Compression of the abdomen against a closed glottis ("belly-in maneuvre") results in a decrease in AB CSA (leftward movement in the Konno and Mead diagram). This inward displacement of the AB results in an increase in abdominal pressure which is transmitted to the undersurface of the diaphragm, hence lengthening it, and altering its shape. This causes an outward displacement of the RC, and hence an increase in RC CSA (upward movement on the Konno and Mead diagram) (see point b, Figure 4.4.).

The Konno and Mead diagram was used in the present study to qualitatively determine changes in the configuration of the diaphragm. With practice, a well-trained subject who views the Konno and Mead display can proceed to a particular point in the diagram, "relax" his diaphragm at that point (against a closed glottis), and produce an inspiratory effort without departing from that point. This thesis presents data obtained during such static maneouvers. In order to standardize, or "calibrate" the different configurations, the relaxation curve and isovolume maneouvres were repeated throughout the test (see below).

4.3.3. The relaxation curve

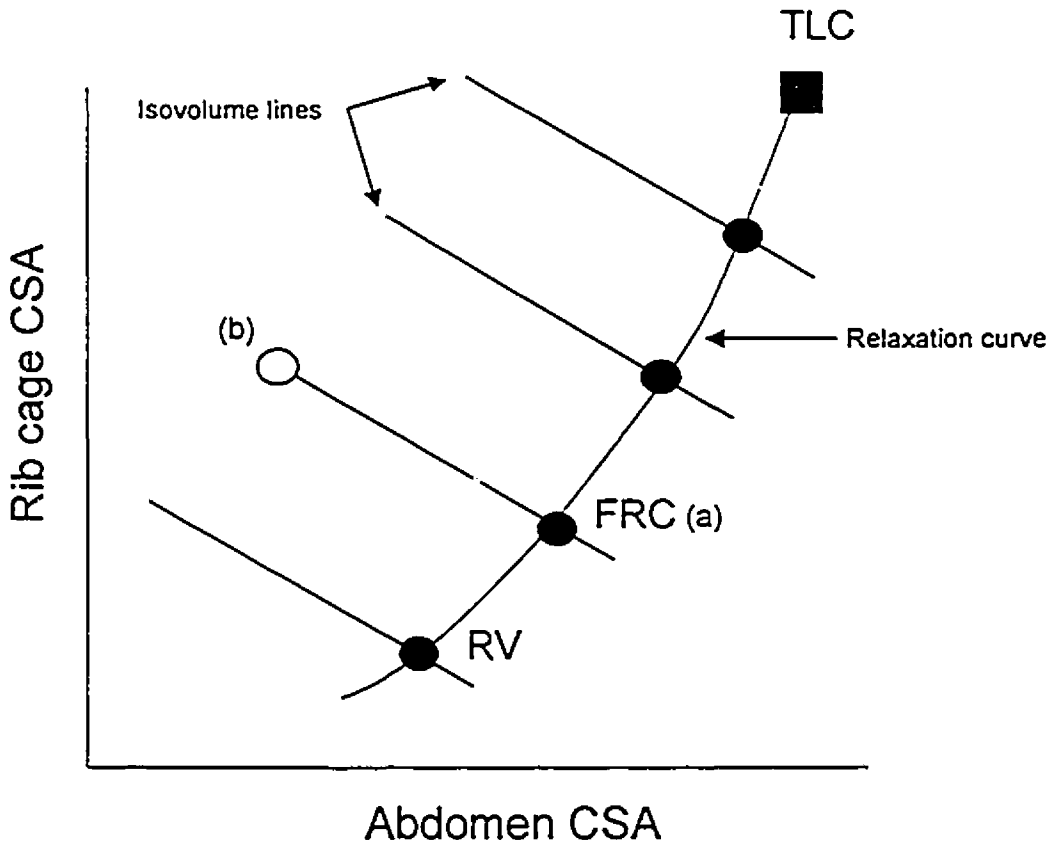

Figure 4.4. Konno and Mead diagram

(Adapted from Fitting and Grassino, 1986)

To obtain the relaxation characteristics, or relaxation curve, of the chest wall, subjects usually perform a slow deflation from total lung capacity (TLC) to functional residual capacity (FRC), through pursed lips. To obtain the relaxation curve of the chest wall below FRC, the subject expires actively to residual volume (RV), and lets his muscles passively relax from RV to FRC. The relaxed chest wall can then be represented in terms of the unique cross sectional areas of the RC and the AB (Figure 4.4.), for all lung volumes. The displacements of the RC and AB during quiet breathing in the upright posture generally occur on or close to the relaxation curve (Grassino et al, 1991).

4.3.4. The isovolume line

Konno and Mead observed that at a given lung volume (iso-volume), and with a fixed posture, it was still possible to change the configuration of the chest wall. At a constant volume and with a closed glottis, inward displacement of the AB (the belly-in maneuvre) results in an outward displacement of the RC (see above). When during such "iso-volume" maneuvers, the CSA of the RC is measured, and displayed on the y axis of an oscilloscope against the CSA of the AB on the x axis, there are reciprocal changes which result in a negatively sloped line, the iso-volume line (Figure 4.4.). If these iso-volume maneuvers are repeated at different lung volumes, further lines are produced, and are parallel to each other. All points along an isovolume line represent the different configurations that the chest wall can have at that particular lung volume.

4.4. ELECTROMYOGRAPHY OF THE DIAPHRAGM IN HUMANS

The electromyogram of the diaphragm in humans can be recorded via needle electrodes (Bolton et al, 1992; Goodgold, 1984; Koepke et al, 1958; Koepke, 1960; Newsom Davis, 1967; Saadeh et al, 1987; Taylor, 1960), skin surface electrodes on the lower rib cage (Aldrich et al, 1983; Banzett et al, 1981; Gross et al, 1979; Tusiewicz et al, 1977), and esophageal electrodes (Bellemare & Grassino, 1982; Gross et al, 1979; Schweitzer et al, 1979).

The simplest and most non-invasive manner in which to record the electrical activity of

the diaphragm in humans, is to use skin surface electrodes placed on the chest. It is customary to obtain EMGdi from the 6th, 7th, 8th, or 9th intercostal space, on or between the mid-axillary and mid-clavicular lines (Aldrich et al, 1983; Banzett et al, 1981; Cohen et al, 1982; Gross et al, 1979; Tusiewicz et al, 1977). This permits recording of the costal and sternal regions of the diaphragm, but activity from other respiratory and postural muscles can interfere with the signals recorded from the diaphragm. Various studies have shown that the amplitude of the EMGdi, as recorded with surface electrodes, is dependent on electrode positioning (Lansing & Savelle, 1989).

In the past, and again most recently, needle electromyography of the human diaphragm has been described (Bolton et al, 1992; Bolton, 1993; Draper; 1957; Goodgold, 1984; Saadeh, et al 1987). In the method reported by Goodgold (1984), the needle is inserted into the diaphragm at the xiphoid process; in that described by Saadeh et al (1987), the needle was inserted more laterally under the costal margin. In both cases, the needle was inserted through the thick abdominal wall and angulated upward under the costal margin, and thus required an unusually long needle as well as manual compression of the abdominal viscera. Bolton et al (1992), had difficulties in locating the diaphragm with these methods, and described a method which was simpler, and safer. It consists of introducing the needle electrode through any interspaces between the anterior axillary and medial clavicular lines. The needle is inserted just above the costal margin, where there is an approximately 1.5 cm distance between the pleura at the lower costal cartilage upon which the diaphragm inserts. Thus, the needle does not traverse either the pleural space or the lung. Although considered as a viable technique, needle electromyography of the diaphragm is unpleasant, the needles can be displaced by large tidal volumes, abdominal viscera such as the liver may be punctured, and action potentials can be excited through damage to the muscle (Lourenço & Mueller, 1967). Therefore, the technique has not gained widespread use.

Esophageal electrodes have been used to record the EMGdi in humans for over three decades (Agostini et al, 1960; Bellemare & Grassino, 1982; Cohen et al, 1982; Gross et al, 1979; Schweitzer et al, 1979). In general, electrodes are mounted onto a catheter which is then

passed through the nose, swallowed into the esophagus, and positioned at the level of the esophageal hiatus. Past studies have implied that the electrical activity recorded with esophageal electrodes is mainly from the crural portion of the diaphragm (Agostoni et al, 1960; Delhez & Petit, 1966; Draper, 1959; Lourenço & Mueller, 1967; Petit et al, 1960).

Until the early 1980's, the electrodes usually consisted of one pair of electrodes, with an interelectrode distance of 20 mm mounted on a catheter (Agostini et al, 1960; Delhez, 1965; Draper, 1957; Gross et al, 1979; Lourenco & Mueller, 1967; Petit et al, 1960). Other interelectrode distances have also been used (Aldrich et al, 1983; Schweitzer et al, 1979). More recently, several investigators have designed multiple electrode arrays consisting of three (Gandevia & McKenzie, 1986; Önal et al, 1979), five (Kim et al, 1978), and seven pairs of electrodes (Daubenspeck et al, 1989), at various interelectrode distances. Önal et al (1981) and Javaheri et al (1987) later designed a single gastro-esophageal catheter which could simultaneously measure EMGdi, and esophageal and gastric pressures. Esophageal electrodes are considered non-invasive, and as long as the catheter is relatively thin and flexible, subjects and patients tolerate the electrode quite well.

There are no reports in the literature comparing the reliability of the three different EMGdi recording techniques. It is difficult to compare the use of needle electrodes with surface or esophageal recordings of EMGdi, mainly because the former record specific information about the activity of individual motor units within the pick-up area of the electrodes, whereas the latter record the electrical activity of the diaphragm more "globally". Only a few studies exist which compare surface electrodes to esophageal electrodes during voluntary activity of the diaphragm (Gross et al, 1979; Repko et al, 1989; Sharp et al, 1993). Repko et al (1989) simultaneously measured the EMGdi center frequency (CF) values with surface electrodes and esophageal electrodes during inspiratory resistive loading. They observed differences in terms of the frequency shift of the EMGdi power spectrum and reported that, for some electrode pairs on the surface of the chest, frequency shifts were not seen, yet were clearly present in the recordings from other surface electrode pairs, as well as from the signals obtained with the esophageal electrode. With respect to the detection of fatigue, these authors suggested that

"there is a serious disadvantage to using only chest surface electrodes instead of esophageal electrodes". Sharp et al (1993) evaluated the EMGdi CF values in quadriplegic patients with both surface electrodes, and esophageal electrodes. These patients were selected in order to exclude EMG contamination of surface recordings by intercostal muscle activity. Lower CF values were consistently observed from the surface recordings than the esophageal recordings. The authors proposed that the major factor accounting for the differences in frequency content between esophageal and surface recordings of the EMGdi is the low-pass filtering effect of chest wall tissues. In agreement with Repko et al (1989), they concluded that "thoracic surface recordings of EMGdi do not accurately reflect frequency information" of the diaphragm, and hence, are not recommended for the detection of diaphragmatic fatigue.

4.4.1. Factors which influence esophageal recordings of EMGdi

In addition to all the factors described in Chapter 3, Sections 3.6. and 3.7. which can influence the EMG signal and its power spectrum, the EMGdi in humans obtained with esophageal electrodes is under the influence of various other factors including the electrocardiogram (ECG), the electrical activity associated with esophageal peristalsis, and electrode motion artifacts.

(i) The electrocardiogram

Due to the proximity of the esophageal electrode to the heart, the EMGdi is contaminated by the unavoidable presence of a large and variable ECG signal. Compared to the EMGdi, the ECG represents a high-power, but low-frequency signal. The power spectrum of the ECG signal overlaps that of the EMGdi, as seen in Figure 4.5., which demonstrates EMGdi power spectrums (and CF values) obtained for the ECG (dashed-dotted line), and the diaphragm (solid line).

The interfering ECG needs to be reduced, or preferably removed before quantitative analysis of the EMGdi is possible. Over the years, several methods have been proposed to solve this problem. According to Evanich et al (1976), to remove a portion of a large ECG, one

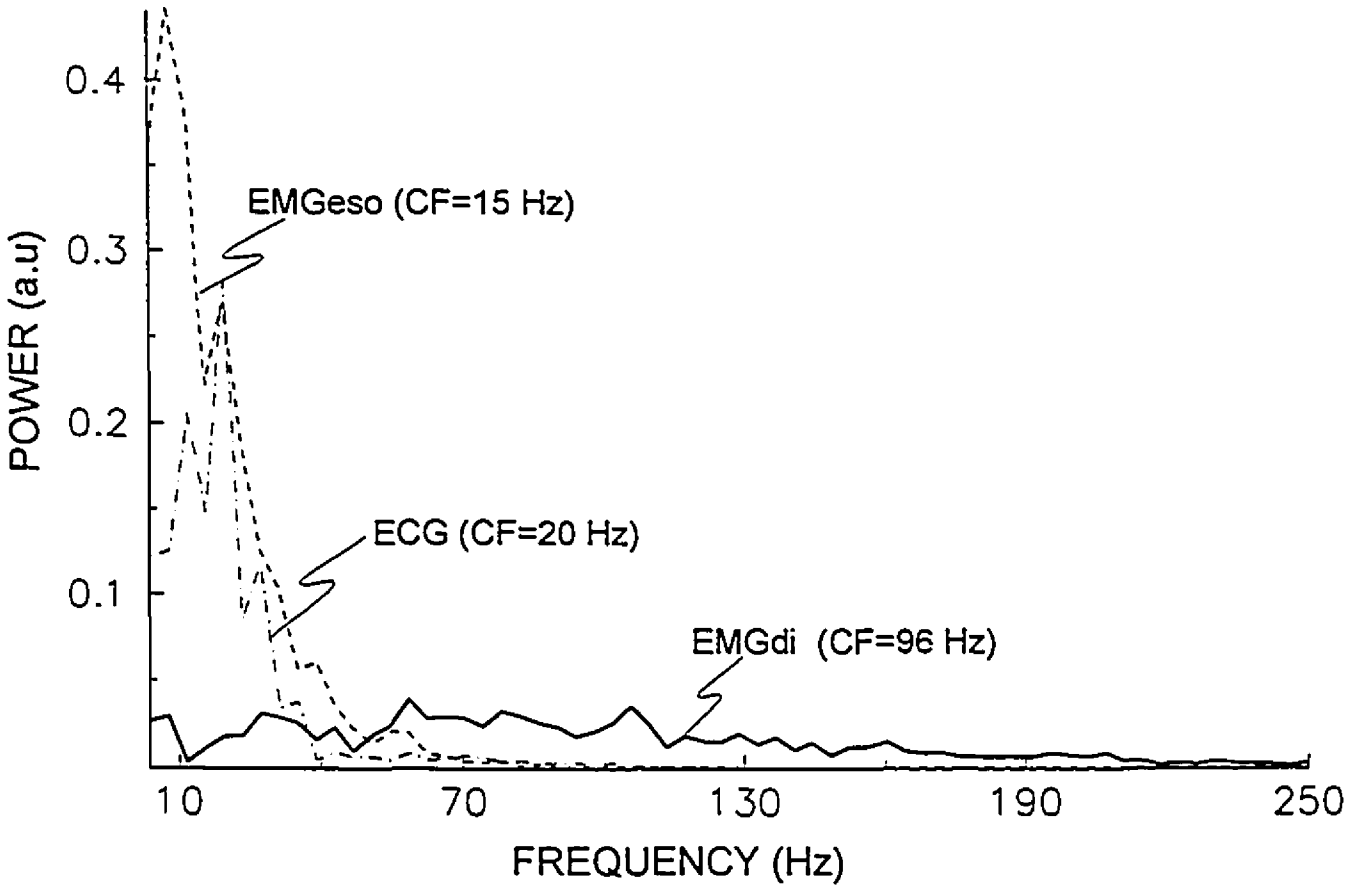

Figure 4.5. Power spectrums for ECG, EMGeso, and EMGdi

can clip a portion of the signal above a given voltage level (Lourenço & Mueller, 1967). In the past, this was considered adequate only when the amplitude of the EMGdi does not exceed that of the ECG. One objection to the use of clipping techniques relates to the fact that when the ECG signal is truncated to something approaching a square wave, new harmonics may be introduced, and will affect the distribution of power of the signal (Schweitzer et al, 1979). To remove more of the ECG signal, it has been suggested that one should filter the ECG from the EMGdi (Evanich et al, 1976). Schweitzer et al (1979) has demonstrated that a high-pass filter of 50-60 Hz is required before the power of the ECG signal can be filtered out completely. However, a significant amount of power related to the EMGdi power spectrum is located in this frequency range, and the information pertaining to the EMGdi will be lost. Thus, high-pass filtering is not recommended as a method to eliminate the influence of the ECG on EMGdi. Sharp et al (1993) have suggested that manually gating out and replacing the ECG signal by zeros is an adequate method to eliminate the ECG. However, such manual gating remains a tedious exercise. Most recently, Sinderby et al (1993) have proposed automatic computer algorithms to eliminate the ECG from the EMGdi. This software automatically selects EMGdi samples as a percentage of the ECG's R-R interval. This ensures that when the heart rate changes, as in cases of increases in lung volume or under conditions of inspiratory resistive breathing, that EMGdi sample selection can remain flexible, and automatic.

(ii) Esophageal peristalsis

Esophageal peristalsis is an involuntary contraction of the smooth muscle of the esophagus. The electrical activity emitted by the lower part of the esophagus (EMGeso) consists of repetitive spike-bursts that are high in amplitude and low in frequency (Tokita et al, 1970). The presence of EMGeso will therefore influence the power spectrum of the EMGdi, and its associated spectral estimates. An EMGeso power spectrum is plotted in Figure 4.5. (dashed line) along with the spectrum from EMGdi. The influence of EMGeso can be determined by evaluating the shape of the EMGdi power spectrum (Sinderby et al, 1993), since it contributes a large amount of power in the low frequency region.

(iii) Motion artifacts

Motion artifacts occur at the electrode-tissue interface and are due to the relative movement of the electrode and the tissues (Basmajian & De Luca, 1985). Esophageal electrodes are likely to move during respiratory maneouvres (even if they are fixed externally at the nose), particularly during exercise or under conditions of loaded breathing. Motion artifacts of this sort are low-frequency and high-power, and hence will contribute a significant amount of power to the low frequency range of the power spectrum. The frequency of these motion artifacts has been described to be below 20 Hz (Schweitzer et al, 1979). CF values of EMGdi will thus be underestimated when motion artifacts are present in the signal. The influence of motion artifacts can be eliminated either by high-pass filtering the signal, or by replacing the low frequency slope of the power spectrum by a prediction line (Sinderby et al, 1993).

(iv) Distance filtering

Another particular problem associated with using esophageal electrodes is that the distance between the electrodes and the diaphragm may be altered with displacement of the diaphragm during respiratory maneouvers. As described in Section 3.4.5. (and in Figure 3.4.), the distance dependent filter acts as a low-pass filter, such that the high-frequency components of the signal are lost, and the total power of the signal is reduced (Lindström & Pétersen, 1983). This filter is very powerful, and displacements of only a few mm from the muscle will affect the recorded signal. Several investigators have observed the effect of the distance filter on the EMGdi (in terms of total power), as recorded with esophageal electrodes (Daubenspeck et al, 1989; Fischer & Mittal, 1990; Gandevia & McKenzie, 1986; Grassino et al, 1976; Kim et al, 1978).

To minimize the distance filtering effect, one approach was to anchor the electrodes at the gastro-esophageal junction by inflating, in the stomach, a balloon located at the end of the electrode (Delhez & Petit, 1966; Grassino et al, 1976; Kim et al, 1978; Taylor, 1960). Any

movement of the crural part of the diaphragm would be followed by the electrodes, thus maintaining a constant relationship between the diaphragm position and the electrodes. In order to anchor the balloon securely, a counter weight must be applied at the nose.

It is questionable if balloon stabilization is sufficient to control for the distance dependent filtering effect. The lower esophageal sphincter has been shown to move independently of respiratory maneouvers during swallowing or esophageal peristalsis (Clark et al, 1970; Johnson, 1968; Winans, 1972), suggesting that balloon stabilization does not necessarily guarantee a fixed position with respect to the diaphragm at all times. Önal et al (1979) stated that the existence of high intraluminal pressures at the gastroesophageal junction (Winans, 1972) suggest that anchoring of the esophageal electrodes in man is unnecessary, because this high pressure should prevent significant displacement of a thin indwelling catheter. They found no differences in EMGdi obtained with and without balloon stabilization during CO_2 rebreathing, and concluded that "the use of a stabilizing gastric balloon at best offers no advantage over securing the catheter at the nose once the site of maximum activity is determined" (along their three electrode pairs).

4.4.2. The effect of lung volume and chest wall configuration

It has also been suggested that lung volume and chest wall configuration can alter the EMGdi (Bellemare & Bigland-Ritchie, 1984; Bolton et al, 1992; Daubenspeck, 1989; Delhez & Petit, 1966; Gandevia & McKenzie, 1986; Hubmayr et al, 1989; Mead, 1973; Schweitzer et al, 1979; Swenson & Rubenstein, 1992; Taylor, 1960).

The amplitude of the diaphragm compound muscle action potential (CMAP), as recorded by surface electrodes, has been shown to either increase (Bellemare & Bigland-Ritchie, 1984; Bolton et al, 1992; Daubenspeck et al, 1989; Gandevia & McKenzie, 1986; Hubmayr et al, 1989; Mead, 1973), decrease (Swenson & Rubenstien, 1992; Hubmayr et al, 1989), or remain unchanged (Gea et al, 1991) with increasing volume from FRC to TLC. These conflicting results are most likely due to differences in the methods of phrenic nerve stimulation, and due to the recording techniques, that is, differences in the size, spacing, and

positions of the (active and reference) electrodes with respect to the diaphragm.

Esophageal recordings of the diaphragm CMAP have also been demonstrated to be influenced by lung volume (Daubenspeck et al, 1989; Delhez & Petit, 1966; Gandevia & McKenzie, 1986; Mead, 1973). Mead (1973) demonstrated that when the phrenic nerves were stimulated transcutaneously and bilaterally, they found systematic increases in the diaphragm CMAP as sensed by the esophageal electrodes. This occurred both when lung volume was increased and when, at a constant lung volume, the abdomen was expanded and the rib cage simultaneously compressed. (But later, they realized that they had inconstant, submaximal stimulation and that no evidence as to the reliability of the esophageal electrodes could be deduced from the experiments). Gandevia & McKenzie (1986) similarly observed increases in the area and amplitude of the diaphragm CMAP with increasing lung volume, and concluded that esophageal recordings of diaphragmatic EMG are unreliable because, under conditions of constant "neural drive" (i.e. supramaximal phrenic nerve stimulation), the EMG signals obtained were altered. Their balloon-stabilized electrode consisted of one single pair of electrodes, placed 5 cm apart. Daubenspeck et al (1989) attempted to further minimize the effect of lung volume on the EMGdi with a new approach. Their idea was to use a multiple electrode array in order to minimize distance filtering effects which occur during diaphragmatic excursion. In this study, the electrode was not anchored with a balloon, but was fixed externally at the nose. These authors rectified and integrated the EMG signals from each of the (seven) pairs of electrodes and summed up the values from each of the pairs to give an approximation to the total activity over the span of the array. With this new approach, they found that lung volume was only responsible for a relatively small increase in the evoked CMAP amplitude.

Lack of uniformity in recording and stimulation techniques has produced confusing and unreliable results with respect to the effect of lung volume on the diaphragm CMAP, whether measured by surface or esophageal electrodes. Studies in animals have demonstrated that the effect of lung volume on the diaphragm CMAP is highly dependent on the positioning of the electrodes (Mead, 1973; Grassino et al, 1976; Kim et al, 1978; Lantzy et al, 1991). Therefore, the studies performed in humans, particularly those using esophageal electrodes,

should be interpreted with caution.

With respect to voluntary contractions of the human diaphragm, the topic of this thesis, few reports are available which have investigated the effect of lung volume and chest wall configuration on the CF of EMGdi. Schweitzer et al (1979) demonstrated an increase in CF by 20 Hz during the first two seconds of tidal breathing, which then remained at a plateau. He attributed his findings to the progressive recruitment of fibers with faster conduction velocities. Weinberg et al (1993) observed increasing CF values during a progressive inspiration, and found these results to be due to a progressive reduction of low-frequency motion artifact influence as the inspiration progressed.

Hence, a study examining the effect of lung volume and chest wall configuration on the CF of the EMGdi during voluntary contractions is required, especially for the purpose of determining whether or not esophageal recordings of EMGdi are reliable in the evaluation of diaphragmatic fatigue. The next chapter describes the experimental work that was performed in order to evaluate the effects of chest wall configuration on the CF of the EMGdi as obtained in human subjects during voluntary activity.

CHAPTER 5

EXPERIMENTAL WORK:

EFFECTS OF CHEST WALL CONFIGURATION AND ELECTRODE POSITIONING ON HUMAN DIAPHRAGMATIC EMG.

5.1. INTRODUCTION

In humans, the diaphragm electromyogram (EMGdi) is often recorded by esophageal electrodes positioned at the level of the gastro-esophageal junction. Past studies have implied that the electrical activity recorded is mainly from the crural portion of the diaphragm (Agostoni et al, 1960; Petit et al, 1960; Dubois et al, 1963). Several investigators have observed that the time and frequency domain measurements of EMGdi are influenced by lung volume and chest wall configuration (Daubenspeck et al, 1989; Delhez & Petit, 1966; Gandevia & McKenzie, 1986; Schweitzer et al, 1979). These reports have introduced doubts concerning the reliability of using esophageal electrodes as a diagnostic tool for diaphragmatic fatigue.

5.1.1. Voluntary activity and EMGdi

With respect to the frequency domain analysis of voluntary contractions of the human diaphragm, Schweitzer et al (1979) reported that EMGdi center frequency (CF) values increased during the first two seconds of a tidal inspiration. Weinberg et al (1993) demonstrated that the changes in CF values they observed during an inspiration to total lung capacity (TLC) were related to motion artifacts and to insufficient signal to noise ratios. When these variables were controlled for, the coefficient of variation of the changes in CF values with lung volume was reduced from 40% to 10%. EMGdi signal quality is thus an important factor to consider when interpreting the results from studies describing the effect of lung volume on voluntary EMGdi. For example, esophageal recordings of EMGdi are subject to contamination by the electrocardiogram (ECG), motion artifacts (Schweitzer et al, 1979), noise (Arvidsson et al, 1984), and esophageal peristalsis (Sinderby et al, 1993). These artifacts, however, can

today be detected and excluded from the EMGdi analysis by computer software (Sinderby et al, 1993).

5.1.2. Electrically evoked EMGdi

With respect to studies involving electrically evoked EMGdi in humans, Gandevia & McKenzie (1986) observed a systematic increase in the amplitude and area of the diaphragm compound muscle action potential (CMAP) with increasing lung volume, following unilateral supramaximal stimulation of the phrenic nerve. These authors concluded that esophageal measurements of EMGdi are unreliable as an index of neural drive because, under conditions of constant "drive" (supramaximal stimulation), the EMGdi signals obtained were altered. They suggested that one of the sources of the volume related artifact was the change in the distance between the diaphragm and the electrodes. Later, Daubenspeck et al (1989) attempted to minimize the effect of lung volume on EMGdi by using a multiple electrode array, which could account for the axial displacement of the diaphragm with respect to the electrodes. In this study, the area of the CMAPs recorded from seven pairs of electrodes were summed in order to give an approximation of the total activity over the span of the array. Their findings generally agreed with those of Gandevia & McKenzie (1986), however the relationship between lung volume and the area of the CMAPs was found to be quite modest.

5.1.3. The muscle-to-electrode distance filter (MEdist filter)

Increasing the muscle-to-electrode distance (MEdist) has been described both theoretically and experimentally, to influence EMG recordings (Lindström, 1970; Gath & Stalberg, 1976; Gath & Stalberg, 1978; Andreassen & Rosenflack, 1978; De la Barrera et al, 1994; Fuglevand et al, 1992; Gydikov & Gatev, 1982). The effect of increasing the MEdist can be compared to a low-pass filter, the cut-off frequency of which is inversely proportional to the observation distance (Lindström, 1973). Hence, EMG signals obtained at increasing MEdist will be reduced in amplitude and in frequency as the high frequency components are filtered out. In the present paper, the effect of MEdist on the EMGdi signal will be referred to as MEdist

filtering.

It has been observed that increasing the distance between the diaphragm and the esophageal electrodes influences the amplitude of the EMGdi signal (Fischer & Mittal, 1990; Daubenspeck et al, 1989; Gandevia & McKenzie, 1986; Önal et al, 1979; Kim et al, 1978; Grassino et al, 1976), but no discussion was provided regarding the frequency charateristics of the signal.

5.2. PURPOSE OF THE STUDY

The aims of the present study were, 1) to evaluate the frequency domain characteristics of the MEdist filter in the region of the crural diaphragm, and hence the effect of MEdist filtering on the EMGdi CF values, by using a multiple array esophageal electrode. 2) To take advantage of MEdist filtering in order to locate the position of the diaphragm with respect to the multiple electrode array. 3) To quantify the effect of changes in chest wall configuration and lung volume on the center frequency, while minimizing the effect of MEdist filtering and while controlling for signal quality.

We were interested in studying voluntary contractions of the diaphragm (i.e. the diaphragm interference pattern) in order to evaluate whether esophageal electrodes are reliable, for example, in measurements of CF for diaphragmatic fatigue.

5.3. METHODS

5.3.1. Signal acquisition

EMGdi was measured via an array of eight stainless steel rings mounted on a Swan-Ganz catheter, forming seven sequential electrode pairs with an inter-electrode distance of 10 mm, similar to that described by Daubenspeck et al (1989). A schematic representation of the electrode is presented in Figure 5.1. The most caudal pair of rings was referred to as "electrode pair 1", and the most cephalad pair of rings "electrode pair 7". A latex balloon was located at the caudal end of the electrode and was inflated only at the beginning of the

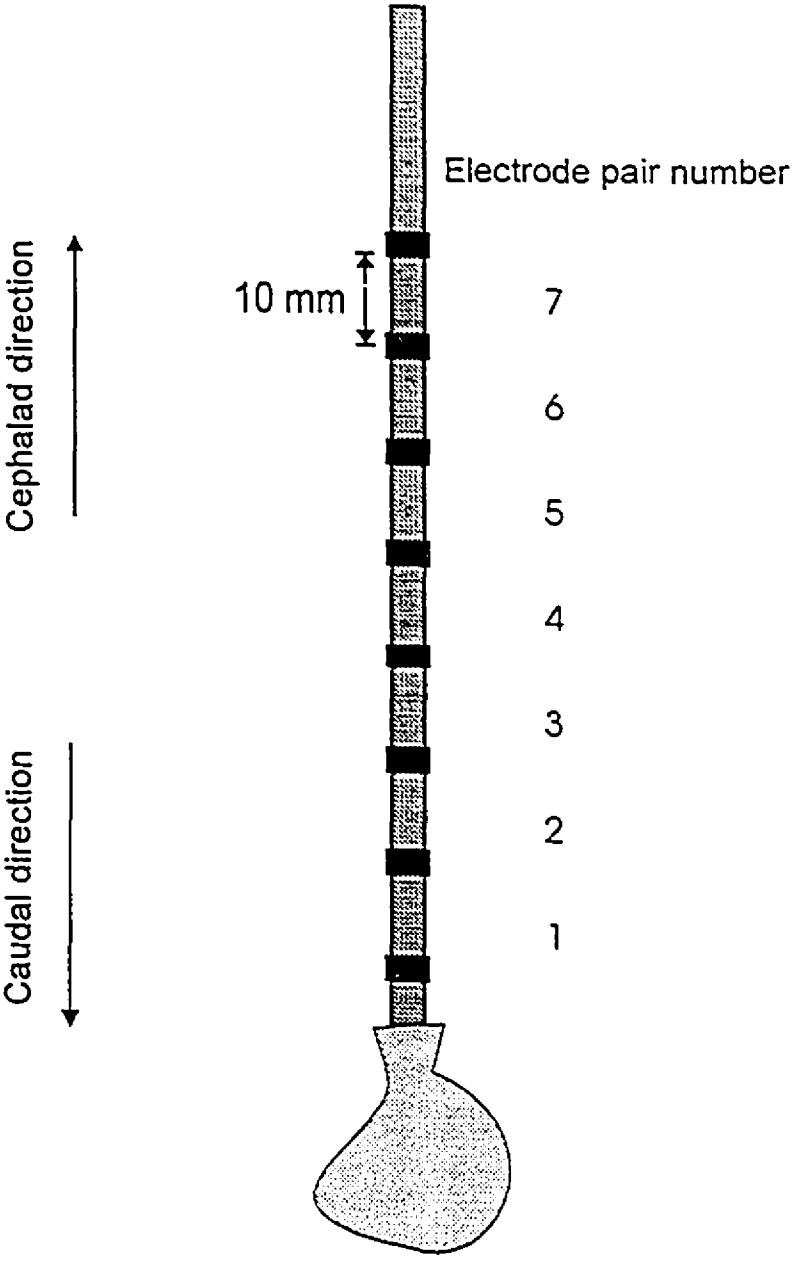

Figure 5.1. Schematic representation of the esophageal electrode used in the present study

experiment in order to position the electrode.

EMGdi signals from each of the seven pairs of rings were amplified (Burr-Brown, INA101), high-pass filtered at 17 HZ and low-pass filtered at 500 Hz (Frequency Devices: 774BT-3, 740BT-3). All EMGdi signals were displayed and monitored on a storage oscilloscope (Gould, Model 1604). A two lead differential ECG was obtained from electrodes placed on the sternum, vertically, and 10 cm apart (Graphic Controls, FC24). The ECG signals were amplified, high-pass filtered at 16 HZ and low-pass filtered at 32 HZ (TECA electromyograph, Model TE 4, White Plains, N.Y.). The seven EMGdi signals and the ECG signal were recorded onto an eight channel analog magnetic tape (Hewlett-Packard Instrumentation Recorder, 3968A). The tape recorder was calibrated to ensure similar gains of adequate amplitude that would not saturate for any recorded channel during an active TLC manoeuvre. All EMGdi and ECG signals were acquired from the tape recorder and digitized by an A/D converter (Data translations 2801), with 12-bit resolution, at a sampling frequency of 1000 Hz.

5.3.2. Evaluation of chest wall configuration

Chest wall configuration was assessed throughout the experiment by the method of Konno and Mead (1967) (Figure 5.2.). Two Respiratory Inductive Plethysmography bands were used (Respitrace®, Ambulatory Monitoring, Inc. White Plains, N.Y.). The rib cage (RC) band, was placed around the upper portion of the thorax, vertically centered over the nipples, while the upper edge of the abdominal (AB) band was placed around the abdomen at the level of the umbilicus. The RC signals were amplified and displayed on the vertical axis, and the AB signals on the horizontal axis of a storage oscilloscope (Tektronix, 5103N).

5.3.3. Experimental protocol

Five normal male subjects were studied while seated in an upright arm chair. Respitrace® bands were positioned on the subjects and secured in place by tape. Subjects were trained to perform iso-volume manoeuvres and relaxation curves with visual feedback from the oscilloscope. Once familiar with the isovolume and relaxation manoeuvres, subjects practiced

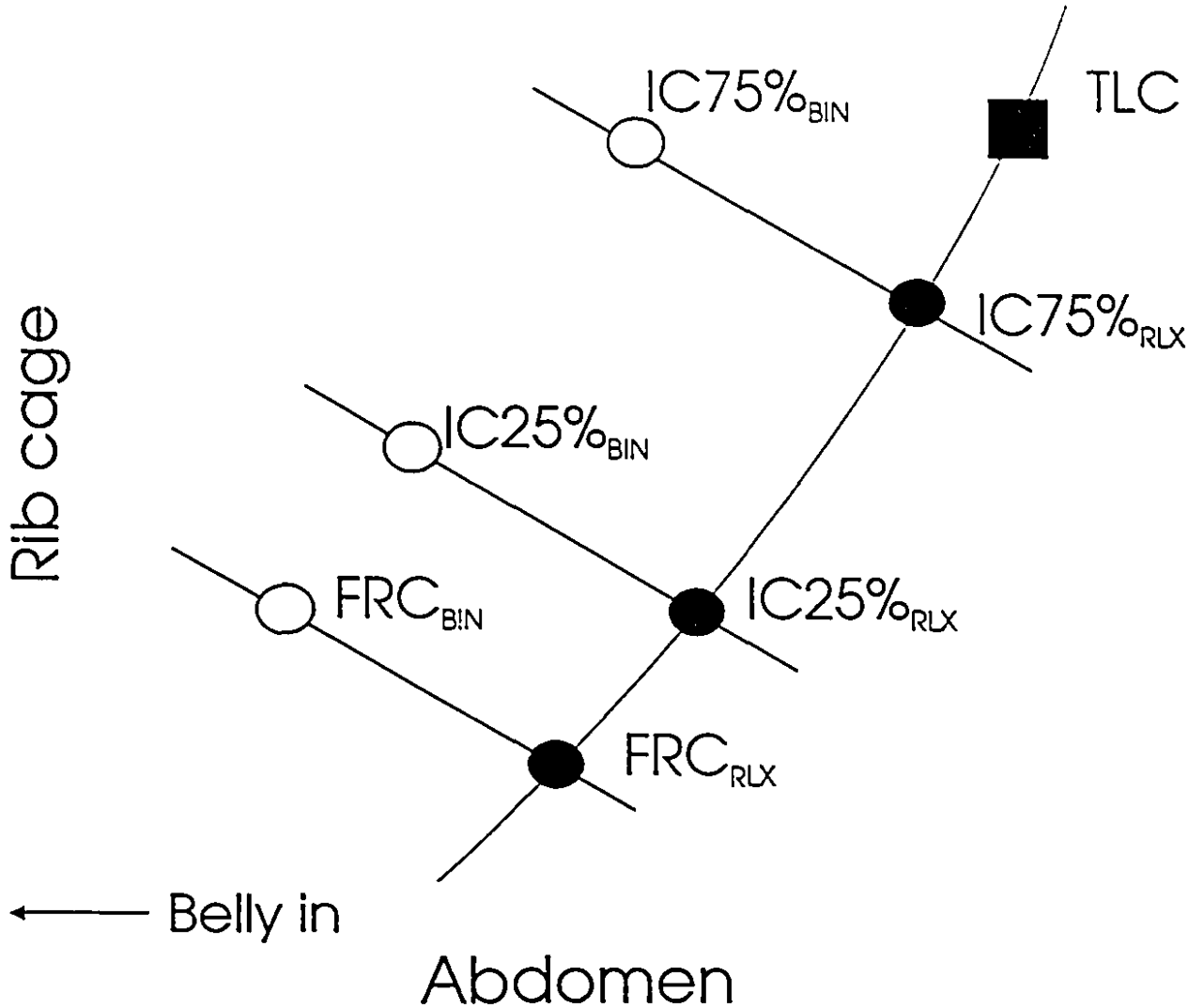

Figure 5.2. Konno & Mead diagram (y axis= rib cage displacement, x axis= abdominal displacement) showing the seven unique chest wall configurations at which the subjects performed the isometric contractions. Points FRC_{RLX}, $IC25\%_{RLX}$, $IC75\%_{RLX}$, and TLC (solid symbols), represent four lung volumes along the relaxation curve at FRC, 25% of IC, 75% of IC, and TLC, respectively. Points FRC_{BIN}, $IC25\%_{BIN}$ and $IC75\%_{BIN}$ (open symbols) represent chest wall configurations at these same lung volumes when the diaphragm is lengthened by a belly-in manoeuvre. It was not possible for subjects to accomplish a belly-in manoeuvre at TLC. Note: points FRC_{BIN} and FRC_{RLX} represent the same lung volume but represent different chest wall configurations (as predicted by Konno and Mead), and hence, different diaphragm configurations, and lengths.

reaching defined points on the newly obtained Konno and Mead diagram (Figure 5.2.).

Following anesthesia (Lidocaine 1%) of the nasal mucosa, the esophageal electrode was passed through the nose into the esophagus. When the electrode was positioned in the stomach, a 5 cm long, 3 cm in circumference balloon was inflated and anchored at the gastro-esophageal junction. Subjects were then instructed to perform an active total lung capacity (TLC) manoeuvre at which point, the electrode was fixed securely at the nose. The balloon was then deflated, and remained so until the end of the test.

With the esophageal electrode in place, subjects were asked to perform a relaxation curve from TLC to functional residual capacity (FRC) and a series of iso-volume manoeuvres at FRC, 25% of inspiratory capacity (IC), at 75% of IC, and at TLC (Figure 5.2.). To ensure that posture and the position of the Respitrace® bands remained constant, these manoeuvres were repeated throughout the experiment.

It was our interest to examine static contractions of the diaphragm at four different lung volumes along the relaxation curve, FRC on the relaxation curve (FRC_{RLX}), 25% of IC on the relaxation curve, ($IC25\%_{RLX}$), 75% of IC on the relaxation curve ($IC75\%_{RLX}$), and TLC on the relaxation curve (TLC). Furthermore, we examined static contractions of the diaphragm at three isovolume increases in diaphragmatic length, FRC with belly in (FRC_{BIN}), 25% of IC with belly in ($IC25\%_{BIN}$), and 75% of IC with belly in ($IC75\%_{BIN}$). We arbitrarily decided that the belly-in manoeuvres should be close to 75% of maximum inward AB displacement. It was not possible to accomplish a belly-in manoeuvre at TLC.

The seven pre-determined chest wall configurations that were evaluated are illustrated in a Konno and Mead diagram in Figure 5.2. (For each subject, the Konno-Mead diagram was drawn with a wax pencil on the screen of a storage oscilloscope). In order to reach a pre-determined point in the Konno and Mead diagram (marked on the oscilloscope), subjects reconfigured their RC and AB with the glottis open. With training, subjects were able to reach the designated points instantaneously, with a few minor adjustments to the RC and/or AB configurations if necessary. While keeping the beam of the scope at the target point, i.e. while maintaining a fixed RC and AB CSA, they performed a mild, non-fatiguing, inspiratory effort

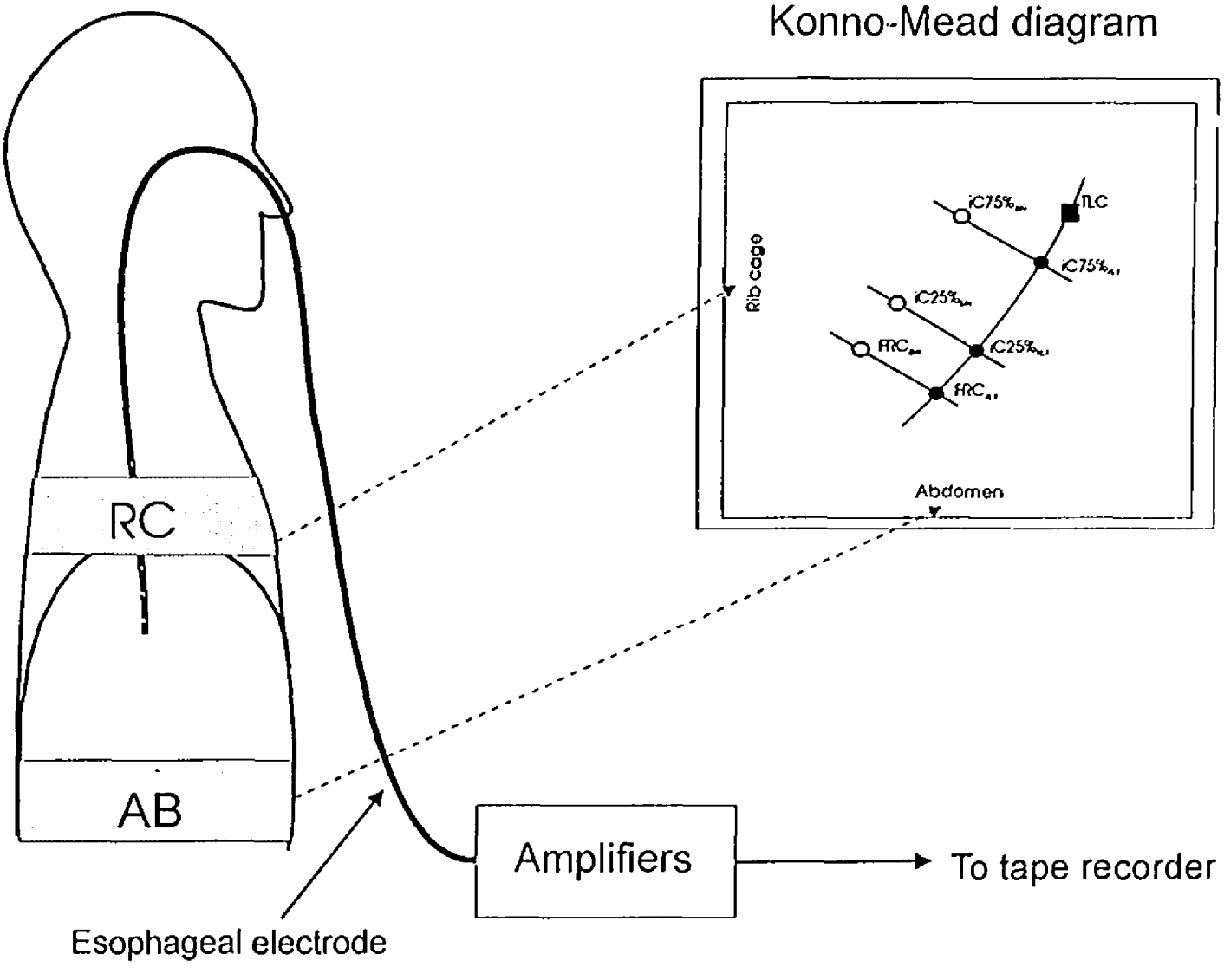

Figure 5.3. Experimental Set-up

against closed airways. Under these conditions, the diaphragm was assumed to contract with minimal shortening (quasi-isometric). Subjects held the voluntary contractions for approximately ten seconds, and the manoeuvres were repeated randomly, five times for each chest wall configuration. EMGdi signals from all contractions were evaluated for evidence of fatigue, and if fatigue was present, as detected by later spectral analysis, those signals were excluded from the analysis. The experimental set-up is presented in Figure 5.3.

5.3.4. Signal analysis

To allow for objective analysis, EMGdi signals were automatically selected with computer software which, based upon pre-determined criteria, made an evaluation of signal quality (Sinderby et al, 1993a). A schematic representation of the computer algorithms is presented in Figure 5.4.

This computer software automatically locates the QRS components from the ECG signal and thus allows one to select EMGdi samples free of cardiac activity. The size of the EMGdi segment is determined by the user and expressed as a percentage of the ECG's R-R interval (Figure 5.4., Step 1). On average, the raw EMGdi samples in the present study ranged from 250-300 ms in duration. According to Arvidsson et al (1984), EMG samples of this size are acceptable for signal analysis. From the raw signal, the DC levels and trends are removed by linear regression (Figure 5.4., Step 2). The first and last zero crossings of the time domain EMGdi signal are then determined (Figure 5.4., Step 3). To fit the samples for a Fast-Fourier transform of 1024 points, the tails of the EMGdi sample are padded (with the mean value of the sample) from the first and last zero crossings (Figure 5.4., Step 4). The time domain EMGdi sample is converted into the frequency domain by Fast-Fourier Transformation (Cooley & Tukey, 1965) (Figure 5.4., Step 5), and the power spectrums are calculated. The power spectrums obtained are then evaluated for various signal quality indices, namely, (1) the signal to motion artifact (SM) ratio (Sinderby et al, 1993a), (2) the signal to noise (SN) ratio (Arvidsson et al, 1984), (3) the drop in power of the spectrum (DP) ratio (Sinderby et al, 1993a), and (4) a spectral deformation (W) ratio (Arvidsson et al, 1984). Only signals of fulfilling the pre-

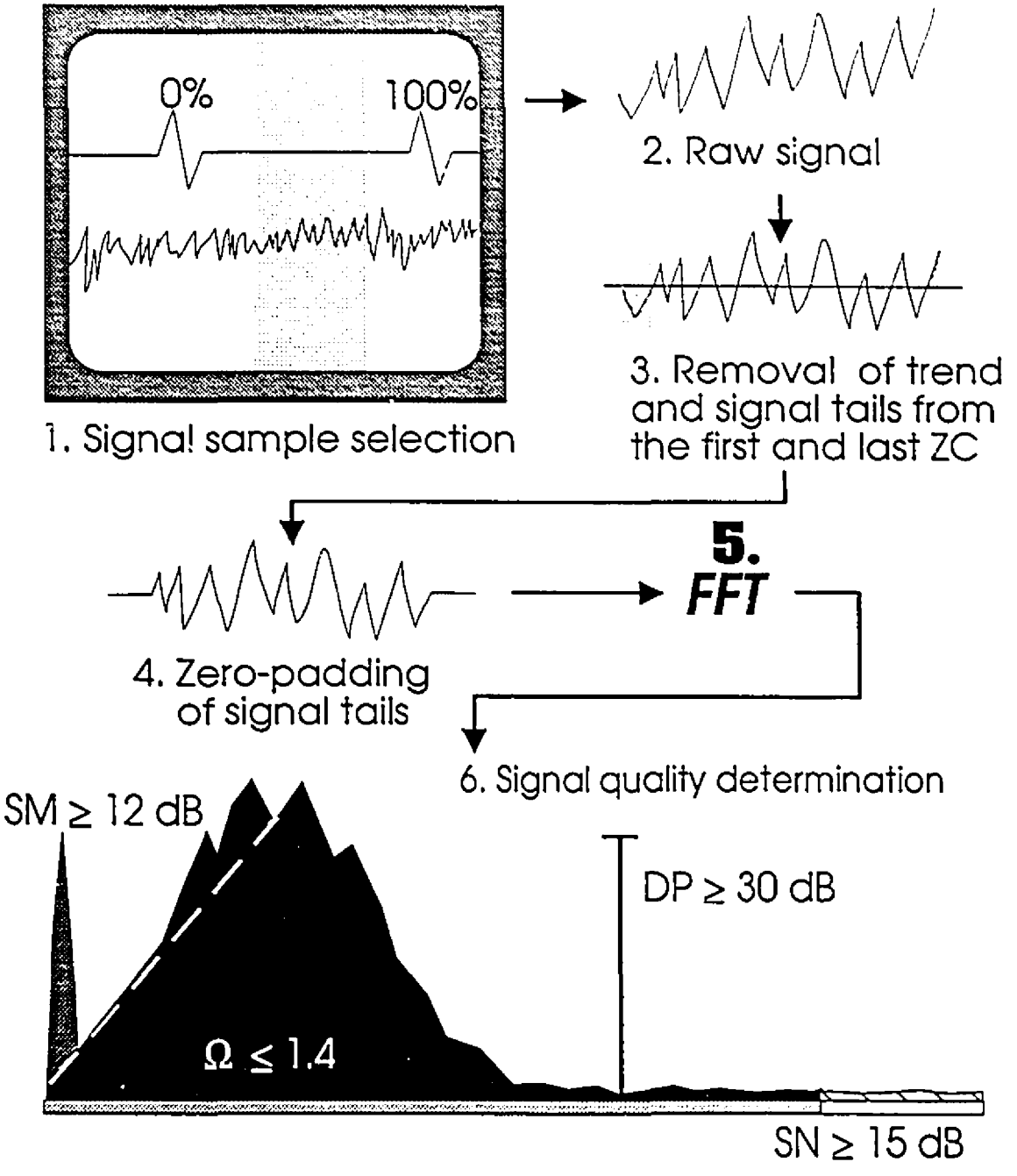

Figure 5.4. Schematic representation of the computer algorithms used in the EMGdi analysis. See text for details.

determined standards were included in the analysis (see below).

(i) The signal to motion artifact ratio (SM): In order to evaluate the influence of motion artifacts, two assumptions must be made: a) motion artifacts usually occur at frequencies below 20 Hz (Schweitzer et al, 1979), and b) in terms of the power spectrum, the influence can be considered linear from 2 to 20 Hz. The low frequency slope of the power spectrum can be predicted by a straight line from 0 HZ (the DC level in logarithmic scaling) to the peak power in the spectrum (see white dashed "prediction line" in power spectrum, Figure 5.4.). The SM ratio is then obtained by taking the power (area) of the entire spectrum, divided by the area under the spectral curve which falls above the prediciton line, for the first 20 Hz of the spectrum. The SM is expressed in dB, and is sensitive to low frequency motion artifacts.

(ii) The signal to noise ratio (SN): Noise is hereby defined as disturbances which are high-frequency in nature. Calculation of the SN ratio assumes that no EMGdi-related power occurs in the upper 20% of the power spectrum (see hatched area in power spectrum of Figure 5.4.). First, the power in the upper 20% of the spectrum is calculated. The total noise contribution is predicted by integrating the upper 20% area for all frequencies in the spectrum, and is displayed in Figure 5.4. by the dotted and white areas below the spectrum. The SN ratio is then obtained by dividing the area under the entire spectrum, by the area of the total noise. The SN ratio is expressed in dB, and is sensitive to high frequency noise.

(iii) The drop in power ratio (DP): This ratio is obtained by dividing the highest power of the spectrum (observed between 35 and 600 Hz), by the lowest power of the spectrum (within the same frequency range). The drop in power is indicated by the vertical line in the spectrum of Figure 5.4. The DP ratio is expressed in dB and is sensitive to reductions in "peaking" of the power spectrum in the 35 to 600 Hz range, where most of the EMGdi power is located.

(iv) Spectral deformation index (Ω): As the name implies, this index is sensitive to changes in the shape and symmetry of the power spectrum, and is derived mathematically by the following formula:

$$\Omega = (M_2/M_0)^{1/2}/(M_1/M_0),$$

where M_2, M_1, and M_0 represent the spectral moments of order 2, 1 and 0, respectively. Spectral moments (M) of order n are obtained by:

$$M_n = \sum_{0}^{f} \text{power} * (\text{frequency})^n,$$

where f is the highest frequency in the spectrum. The Ω ratio is expressed in relative units.

It has been determined that the following combination of the above-described indices allows for an error of CF values in the range of -5 to +10 Hz: SM>=12 dB, SN>=15 dB, DP>=30 dB, and Ω,<=1.4, and were the acceptance levels that were used in the present study.

The EMGdi signals obtained from all static contractions were evaluated for quality based on calculations of the above described indices. The computer software automatically excludes any EMGdi segments that do not satisfy the pre-determined ratios, as described above. Following evaluation of signal quality, an average power spectrum was calculated for the five contractions performed at each of the chest wall configurations.

In the present study, CF was chosen as the numeric value to characterize the power spectrum. For signals that passed signal quality determination, CF was calculated as the spectral moment of order one (M_1) divided by that of order zero (M_0), where the spectral moments are calculated as above. All subjects' EMGdi signals from the seven pairs of electrodes, and at each of the chest wall configurations were analyzed separately. At each of the chest wall configurations, a mean CF value was calculated for the five contractions.

5.3.5. Determination of MEdist filtering and the position of the diaphragm with respect to the multiple electrode array

The MEdist filter acts on the EMG signal as a low-pass filter, filtering out the high frequency components of the spectrum. The rate of decrease in power in the high frequency range is referred to as the high-frequency slope. With increasing distance away from the

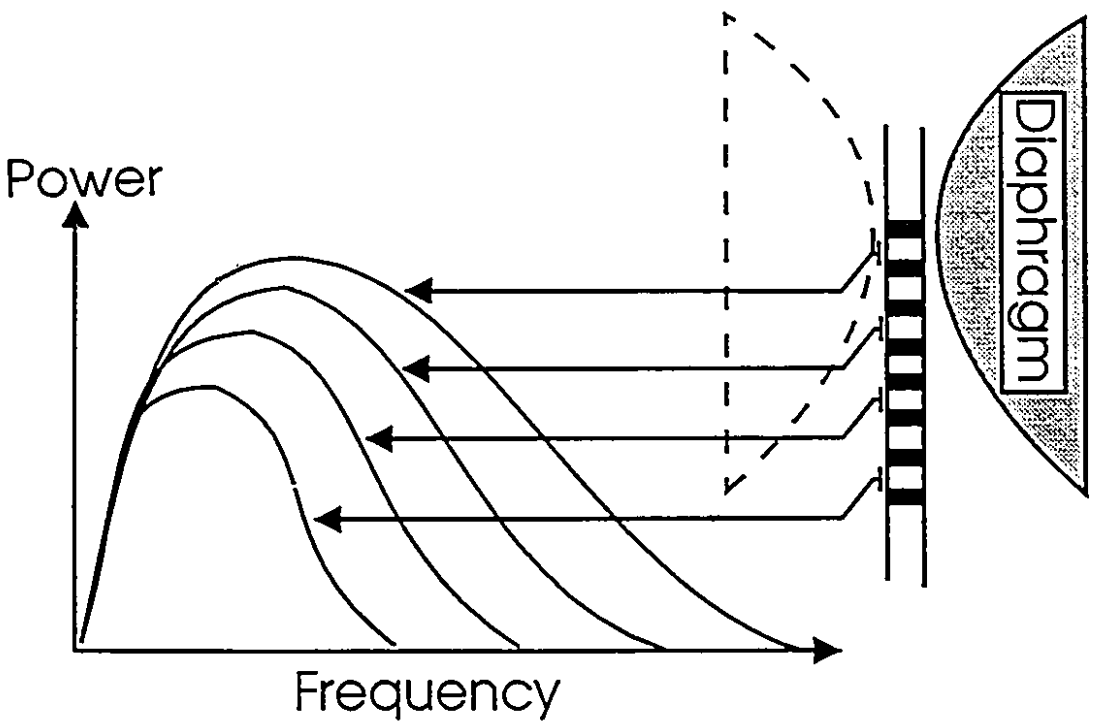

Figure 5.5. Schematic representation of the hypothesis proposed in this study. According to signal theory, as the muscle-to-electrode distance increases, the high frequency components of the power spectrums are filtered out.

muscle, the rate of decrease of the high frequency slope of the power spectrum becomes progressively steeper (Lindström, 1973). Thus, with changes in MEdist, the rate of decrease in power should be quantifiable for the EMGdi power spectrums obtained from the different electrode pairs along the array. The model upon which this hypothesis is based is presented in Figure 5.5.

Based on this theory, determination of the pair of electrodes closest to the diaphragm was achieved by examining the power spectrums obtained simultaneously for all electrode pairs, and by selecting the power spectrum which is the least filtered by MEdist. This was allowed by successive comparison of power spectrums. In order to compare the rates of the drop in power between two power spectrums (i.e. the high frequency slope), the difference in power between two spectrums was calculated (in dB) in the frequency range of 75 Hz to 150 Hz. This range was selected because it is well below the cut-off frequency usually observed for EMGdi recordings with esophageal electrodes which have an interelectrode distance of 10 mm. The slope of the difference in power between two spectrums was calculated by linear regression analysis.

The comparison of power spectrums started at the most caudal pair of electrodes (whose signals were of acceptable quality), and continued until the most cephalad pair of electrodes (whose signals were of acceptable quality). After the comparison between any two power spectrums, the one with the lowest loss of high frequency power was passed on for comparison with the power spectrum obtained from the next pair of electrodes, until all spectrums involved had been compared. The remaining power spectrum (i.e. the one with the lowest rate of drop in power), and the electrode pair it was obtained from, was assumed to represent the electrode pair that was least affected by the MEdist filter, and thus was closest to the diaphragm. From now on, this electrode pair will be referred to as the "optimal pair" of electrodes.

5.4. RESULTS

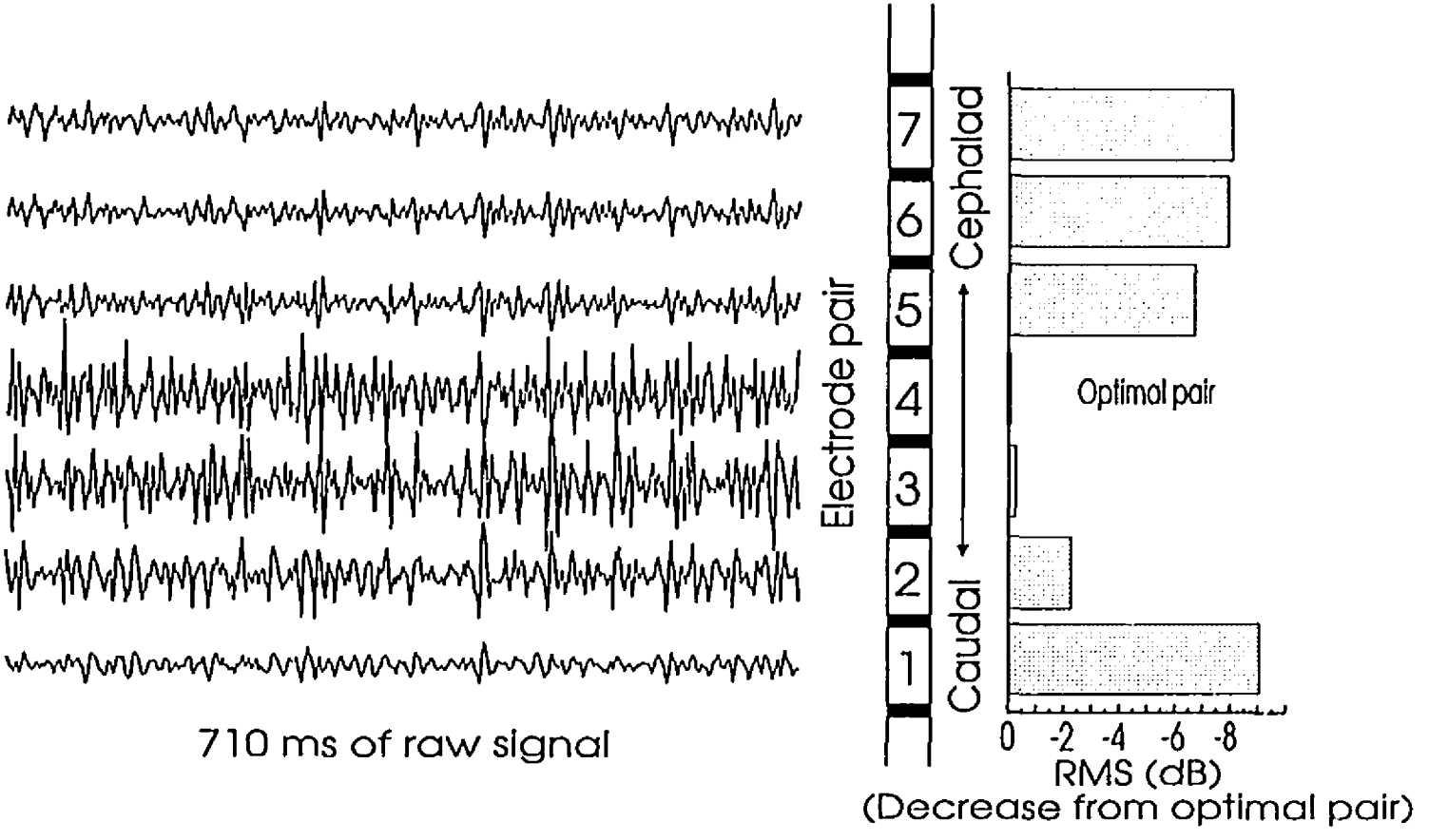

Figure 5.6. Left: Simultaneous tracings of EMGdi signals (710 msec) from each of the seven pairs of electrodes, during a static contraction at $IC75\%_{aux}$ for one subject. This signal was obtained between two consecutive ECGs. By visual inspection alone, one can see that the amplitude of the signal is higher at electrode pairs 2, 3 and 4, and progressively decreases away from these pairs of electrodes. This EMGdi sample was selected between two consecutive ECGs. Right: Bar graphs demonstrate the loss of signal power (in dB) with respect to the optimal pair of electrodes, in this case pair 4.

5.4.1. The effect of the MEdist filter on esophageal recordings of EMGdi

(i) The effect of MEdist filter on EMGdi amplitude

Simultaneous tracings of EMGdi signals from all electrode pairs revealed that the amplitude of the signal was higher at one specific pair of electrodes, and progressively decreased away from this pair of electrodes (Figure 5.6., left). Spectral analysis revealed that the EMGdi obtained from this pair of electrodes was the one least filtered by distance, and was thus the optimal pair of electrodes. As well, the total power, or RMS (dB), of the EMGdi was less for signals obtained from electrode pairs at increasing distances away from the optimal pair. The decrease in RMS (in dB) from the optimal pair of electrodes is displayed in Figure 5.6., right. The reduction in total power was smaller for electrode pairs adjacent to the optimal. Signals obtained at electrode pairs 20 mm and more away from the optimal pair showed progressively stronger reductions in total power with increasing distance. Recurrently, it was observed that the power at the optimal pair of electrodes was actually slightly lower than that of its neighbouring pairs.

(ii) The effect of MEdist filter on EMGdi power spectrums

The rate of decrease in power in the frequency range of 75 to 150 Hz was consistently more pronounced the further away from the optimal pair the signals were recorded. An example of this phenomena is illustrated in Figure 5.7., for subject #5, during a contraction at FRC_{RLX}. This graph shows the averaged power spectrum obtained from the optimal pair, and the averaged power spectrums obtained from three electrode pairs of increasing distance away from the optimal pair in the caudal direction (10, 20 and 30 mm away). The four power spectrums are superimposed in order to display the reduction in total power, and the progressive loss of high frequency power as the MEdist increases. The vertical lines in the main graph of Figure 5.7. indicate the frequency range where the MEdist filter function was calculated (75 to 150 Hz). The upper right graph shows the same four power spectrums blown-up for this frequency range. The straight lines were obtained by linear regression analysis, and

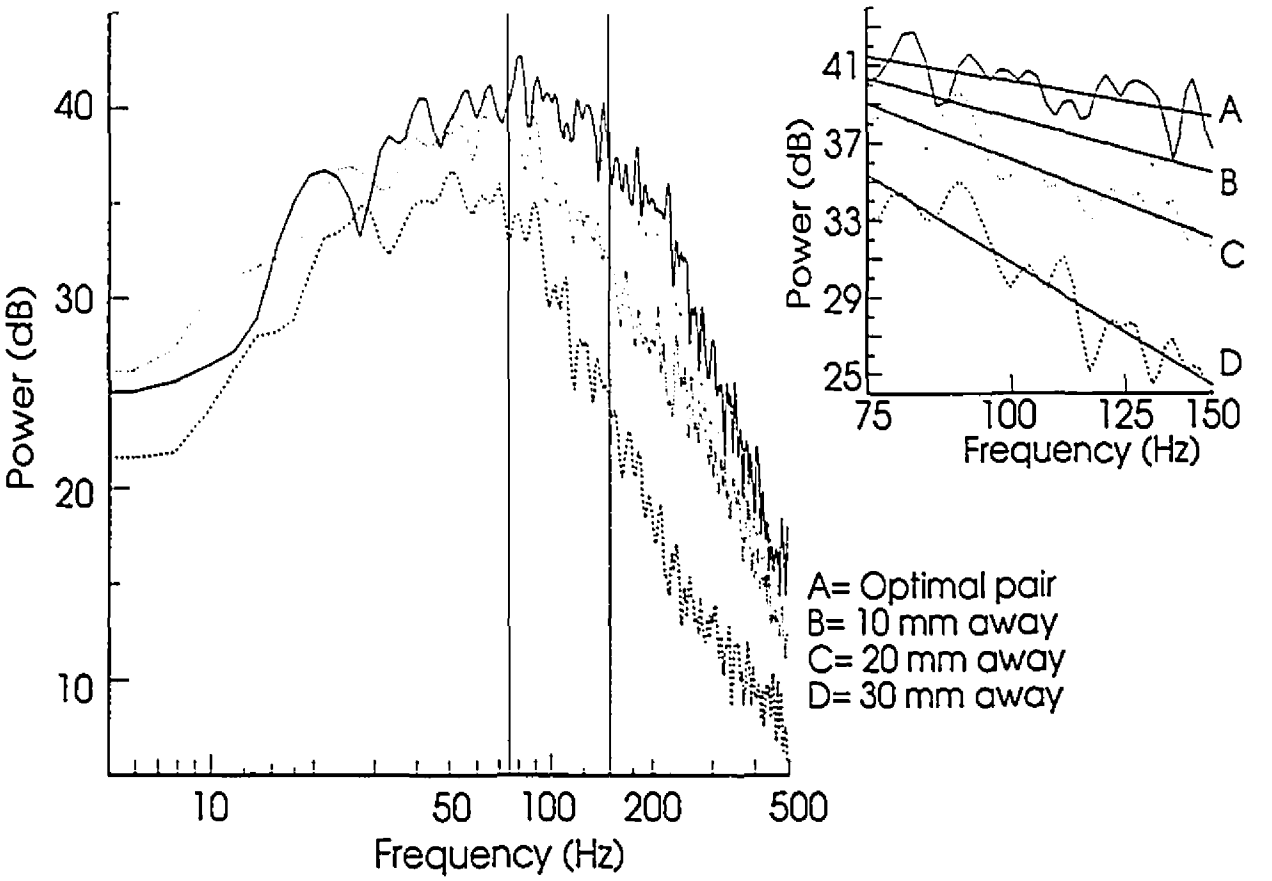

Figure 5.7. Main graph: Averaged EMGdi power spectrums (n=30) obtained simultaneously at the optimal pair of electrodes (thick solid line), and from the three pairs of electrodes caudal to the optimal, at 10 mm away (dotted line), 20 mm away (dashed line), and 30 mm away (dot-dashed line). These average power spectrums contain approximately 3 seconds of information, from one subject, performing a static contraction at FRC_{RLX}. Note 1) the reduction in total power of the spectrum, and 2) the steeper high frequency slope, as the distance increases away from the optimal pair. The vertical lines indicate the frequency range where the MEdist filter function was calculated (75 Hz to 150 Hz). Right inset: This graph shows the same four power spectrums blown-up for the frequency range of interest for the MEdist filter function. The straight lines were obtained by linear regression analysis, and demonstrate the rate of decrease of the high frequency slope, i.e. the rate of decrease in power as a function of frequency. Note for the most distant pair of electrodes (30 mm away from the optimal), that the slope of the high frequency portion of the spectrum is the steepest.

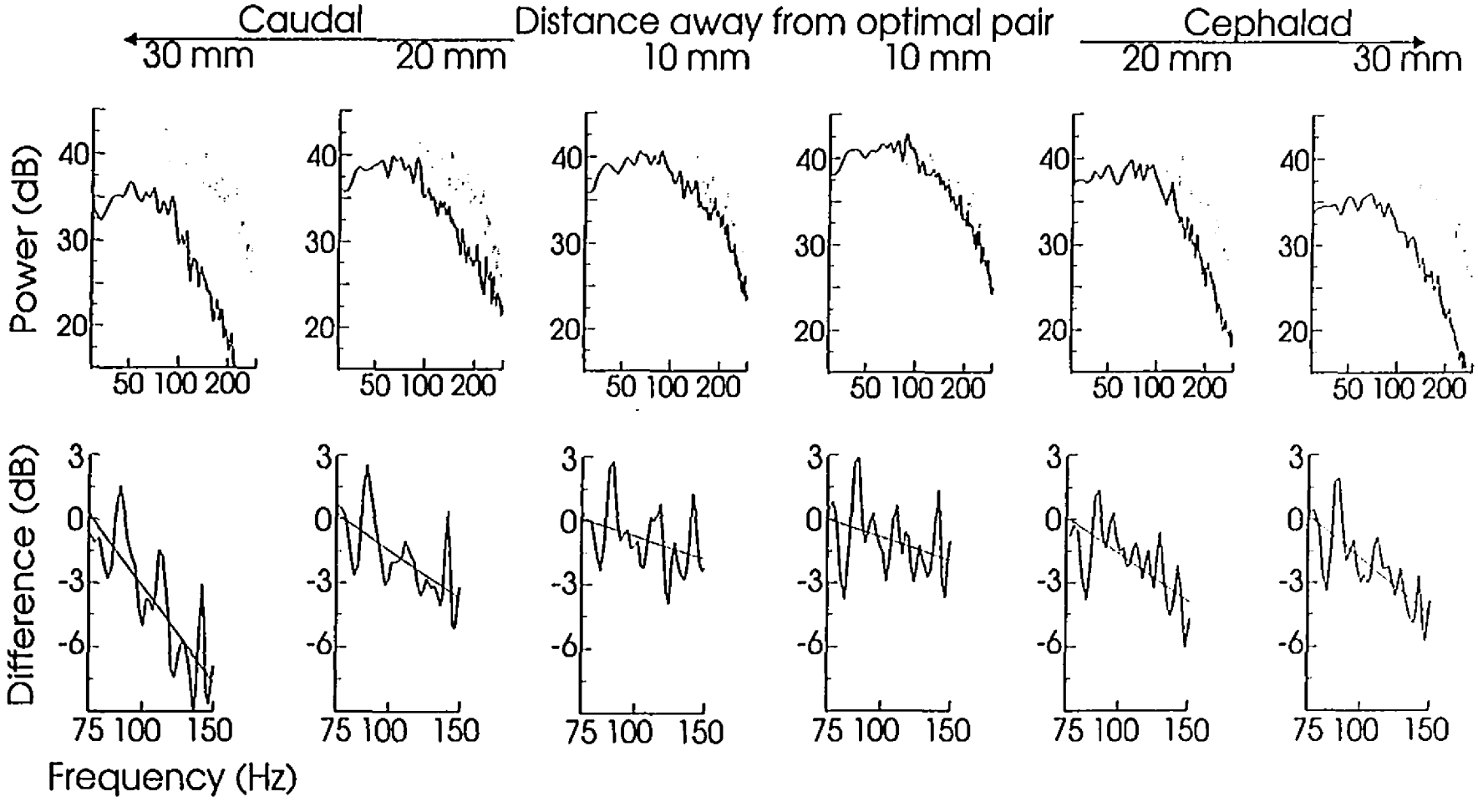

Figure 5.8. Average power spectrums and MEdist filter function obtained from all of the electrode pairs in relation to the optimal. All data are from EMGdi signals obtained during a static contraction at FRC_{ALV}, in one subject. Top row: Average power spectrums obtained from the optimal pair (dotted line), and for electrode pairs 10, 20, and 30 mm away (thick solid lines), in the caudal and cephalad directions. The reduction in power between the power spectrum from the optimal pair and the spectrums from the more peripheral electrode pairs (in dB for the frequency range of 75 Hz to 150 Hz) is plotted in the graph directly underneath for each electrode pair position.

demonstrate the rate of decrease in power as a function of frequency, and their respective intercepts, for signals obtained from the optimal pair and the pairs 10, 20 and 30 mm away, in the caudal direction.

The MEdist filter was more pronounced at increasing distances away from the optimal pair, and was different for signals obtained in the caudal and cephalad directions. In the caudal direction, the MEdist filter (in the 75 to 150 Hz frequency range) was determined to be -2.3 (± 1.67), -4.62 (± 3.13), and -6.3 (± 2.94) dB/octave, for electrode pairs 10, 20, and 30 mm away from the optimal pair, respectively. The corresponding values for the cephalad direction were determined to be -1.75 (± 1.68), -3.52 (± 1.64), and -4.17 (± 2.26) dB/octave for electrode pairs 10, 20, and 30 mm away from the optimal pair, respectively. This is exemplified in Figure 5.8., which depicts the signals' power distribution between 30 and 300 Hz (top row) for all electrode pairs (solid lines) compared to the optimal pair, in this case electrode pair 4 (dotted line), for the same subject and conditions as in Figure 5.7.

Below each power spectrum in Figure 5.8. (bottom row), is a representation of the differences in power obtained from the studied and the optimal pair of eiectrodes. The difference in power was calculated in dB for the frequency range of 75 Hz to 150 Hz. To allow quantification of the MEdist filter, the difference in power at 75 Hz was adjusted to zero.

(iii) The effect of MEdist filter on CF values

As is expected from the above described MEdist filter, CF values decreased in all subjects with increasing distance away from the optimal pair, in both the caudal and cephalad directions. Regardless of chest wall configuration, the rate of decrease in CF values, as determined by linear regression analysis, on either side of the optimal pair of electrodes, remained relatively unaltered. This is exemplified for one subject in Figure 5.9. showing CF values (mean ± SD) obtained with increasing distance away from the optimal pair for all different chest wall configurations. For any chest wall configuration, across all seven pairs of electrodes, there was always one pair of electrodes for which CF was the highest. Inspection of the power spectrums between 75-150 Hz confirmed that this was the optimal (least distance-

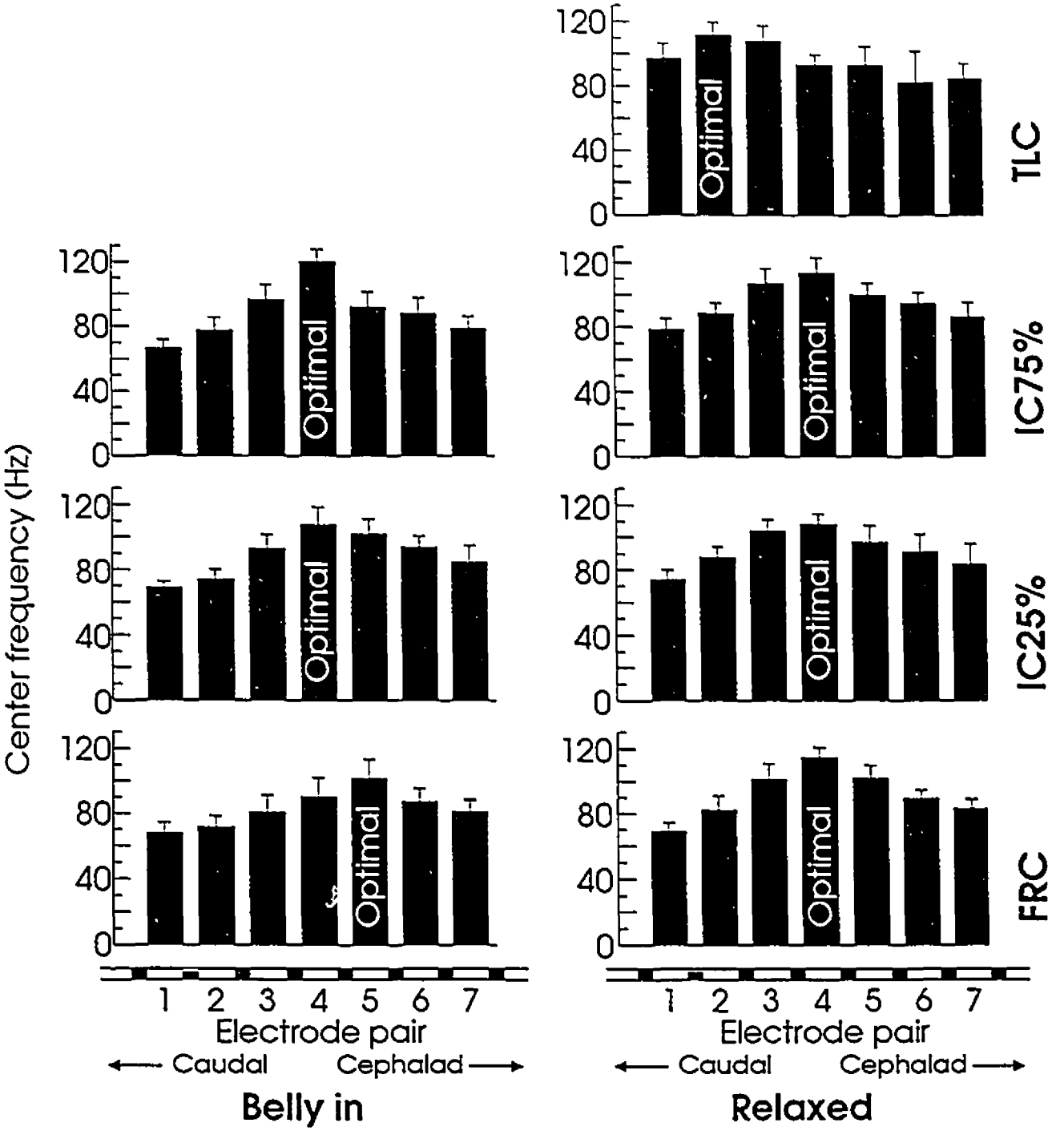

Figure 5.9. Each bar graph represents the CF values (mean ± SD) (y axis) for each of the seven electrode pairs (x axis), obtained during the isometric contractions at each of the different chest wall configurations, for subject #5. Note that at each chest wall configuration, across all electrode pairs, there was always one electrode pair where CF values were the highest. Inspection of the power spectrums indicated that this electrode pair was the optimal pair, and is marked in the respective graphs. CF values then decreased as a function of distance away from the optimal pair of electrodes.

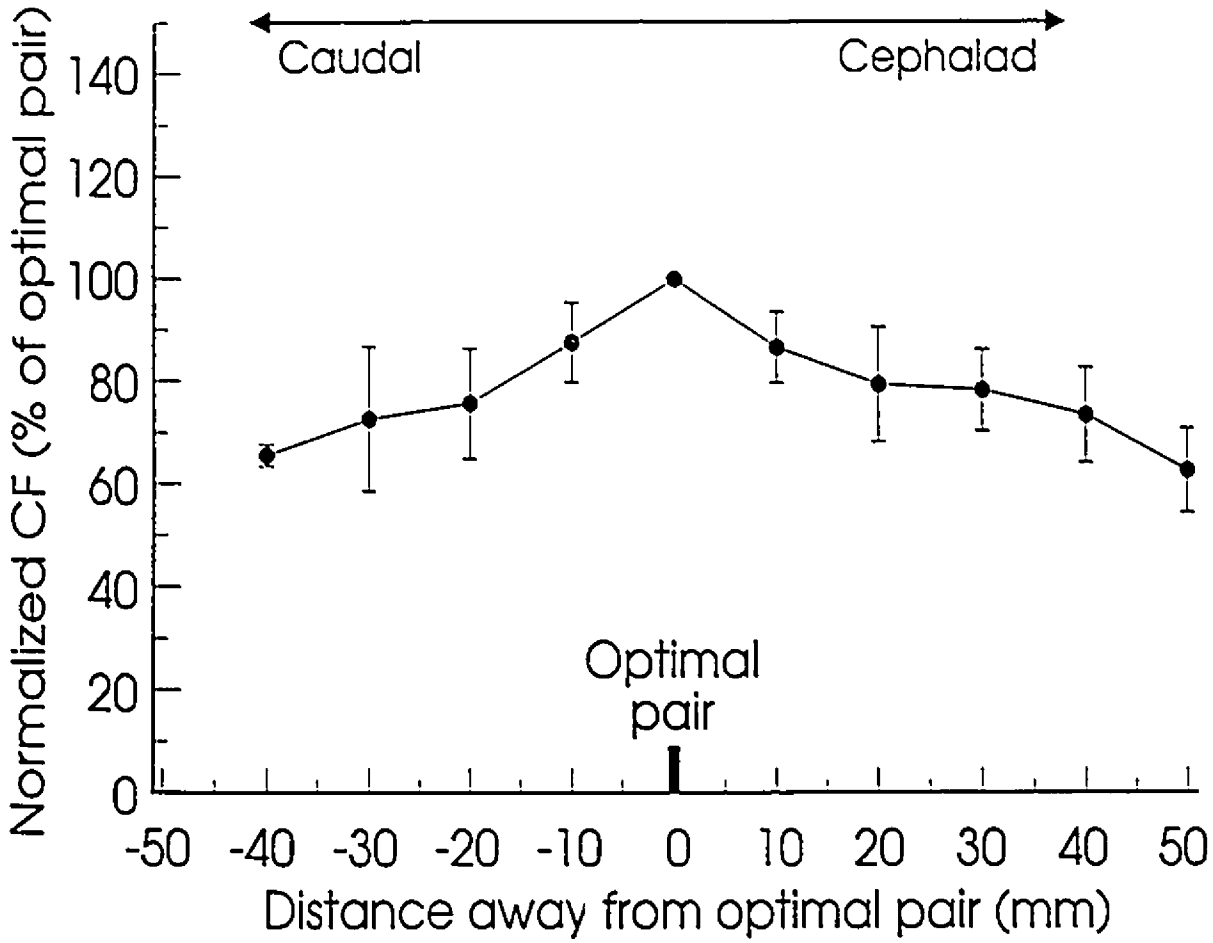

Figure 5.10. Center frequency (y axis) decreases as a function of distance (x axis) away from the optimal pair (0 mm) both in the caudal direction (i.e. towards the stomach), and in the cephalad direction (i.e. towards the esophagus). CF values are normalized for the value obtained at the optimal pair, and represent data from all five subjects, and from all of the chest wall configurations.

filtered) pair of electrodes, and is marked in the respective graphs of Figure 5.9. For contractions at each chest wall configuration, CF values progressively decreased at similar rates depending on whether the caudal or cephalad directions were evaluated. However, the rate of decrease in CF values in the caudal direction was steeper than that for the cephalad direction.

The mean decrease in CF values with respect to the optimal pair, for the group of five subjects at all chest wall configurations, was 0.84% /mm (r=0.76) and 0.65% /mm (r=0.73), in the caudal and cephalad directions, respectively, as shown in Figure 5.10. An important observation in this study was that the quality of the EMGdi signal decreased as a function of distance away from the optimal pair of electrodes. The rate of EMGdi signal exclusion due to poor SM, SN, DP, and W ratios, was therefore much higher for electrode pairs located 30 mm and more away from the optimal pair.

5.4.2. Change in optimal pair position with changes in chest wall configuration

The change in position (i.e. the number) of the optimal pair (in turn due to the change in position of the diaphragm and/or the electrode), was evaluated for the different chest wall configurations. No consistent pattern was observed for changes in optimal pair position with changes in chest wall configuration.

5.4.3. Effect of chest wall configuration on EMGdi center frequency

The effect of changes in chest wall configuration on CF values obtained from the optimal pair are plotted for each subject individually in Figure 5.11., and is presented numerically in Table 5.1. The values presented are the mean CF values ± SD. Overall, there was no consistent pattern between CF values and chest wall configuration. Depending on the subject studied, CF values could either increase, remain unchanged, or vary randomly, with changes in chest wall configuration.

When the subjects are evaluated as a group, there was no effect of chest wall configuration on mean CF values (Figure 5.12.). Along the relaxation curve, CF values

TABLE 5.1.

	FRC_{RLX}	$IC25\%_{RLX}$	$IC75\%_{RLX}$	TLC	FRC_{BIN}	$IC25\%_{BIN}$	$IC75\%_{BIN}$
Subject # 1	58 ± 7.8	65 ± 9.5	73 ± 9.1	70 ± 10.6	65 ± 15.2	64 ± 7.5	[illegible]
Subject # 2	96 ± 12.8	105 ± 11.1	118 ± 6.5	105 ± 13.6	95 ± 3.3	104 ± 7.3	100 ± 5.0
Subject # 3	89 ± 10.3	96 ± 9.2	96 ± 9.0	112 ± 10.1	94 ± 2.2	92 ± 7.7	103 ± 11.0
Subject # 4	105 ± 7.0	115 ± 8.0	110 ± 9.6	108 ± 1.3	114 ± 6.3	107 ± 6.3	101± 3.7
Subject # 5	115 ± 7.3	108 ± 7.7	114 ± 11.4	112 ± 9.6	102 ± 14.4	108 ± 13.0	120 ± 9.3
Mean ± 95% CI	92.64 ± 26.6	97.69 ± 24.3	99.70 ± 19.9	101.45 ± 21.9	94.07 ± 22.4	94.98 ± 22.8	106.48 ± 11.36

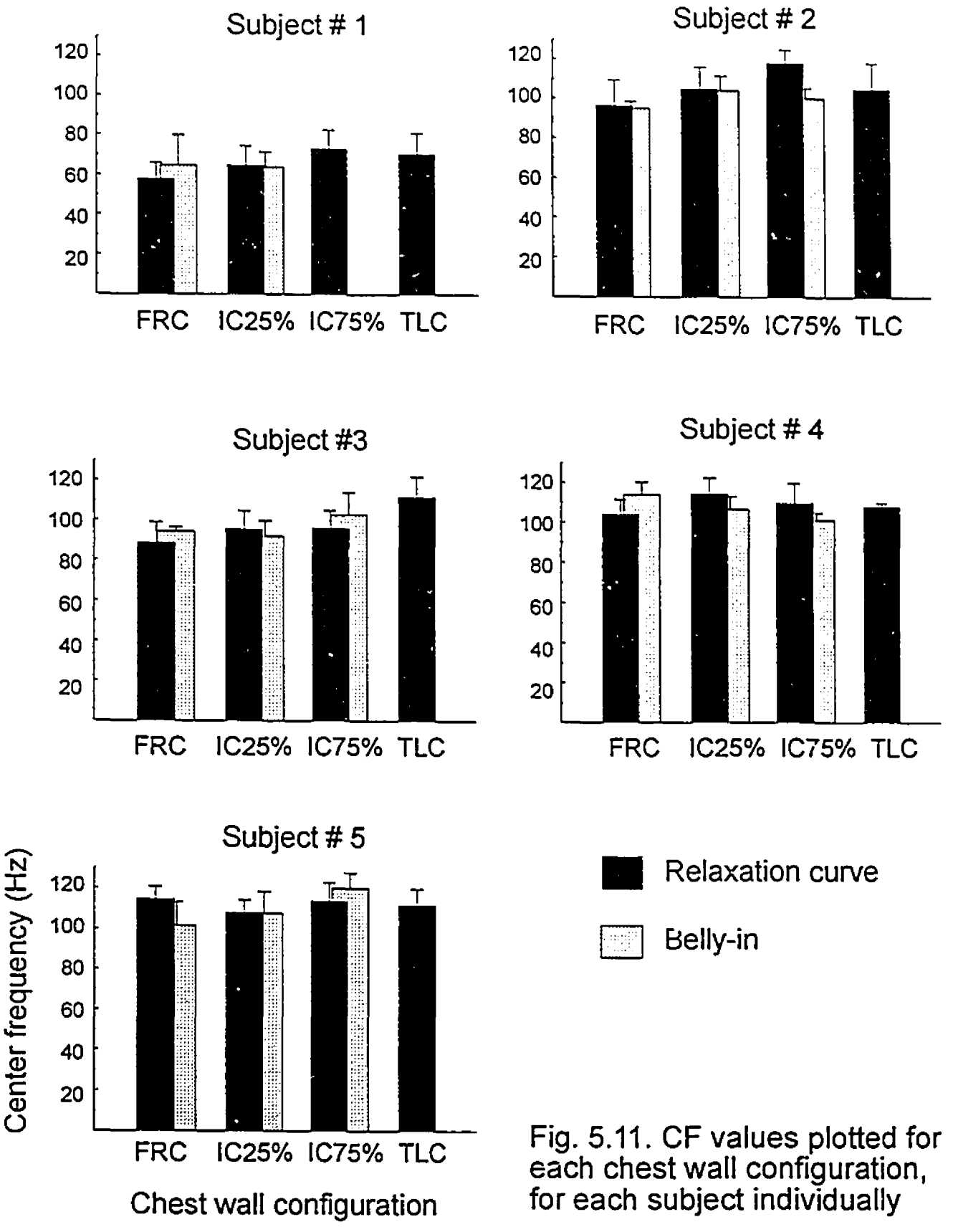

Fig. 5.11. CF values plotted for each chest wall configuration, for each subject individually

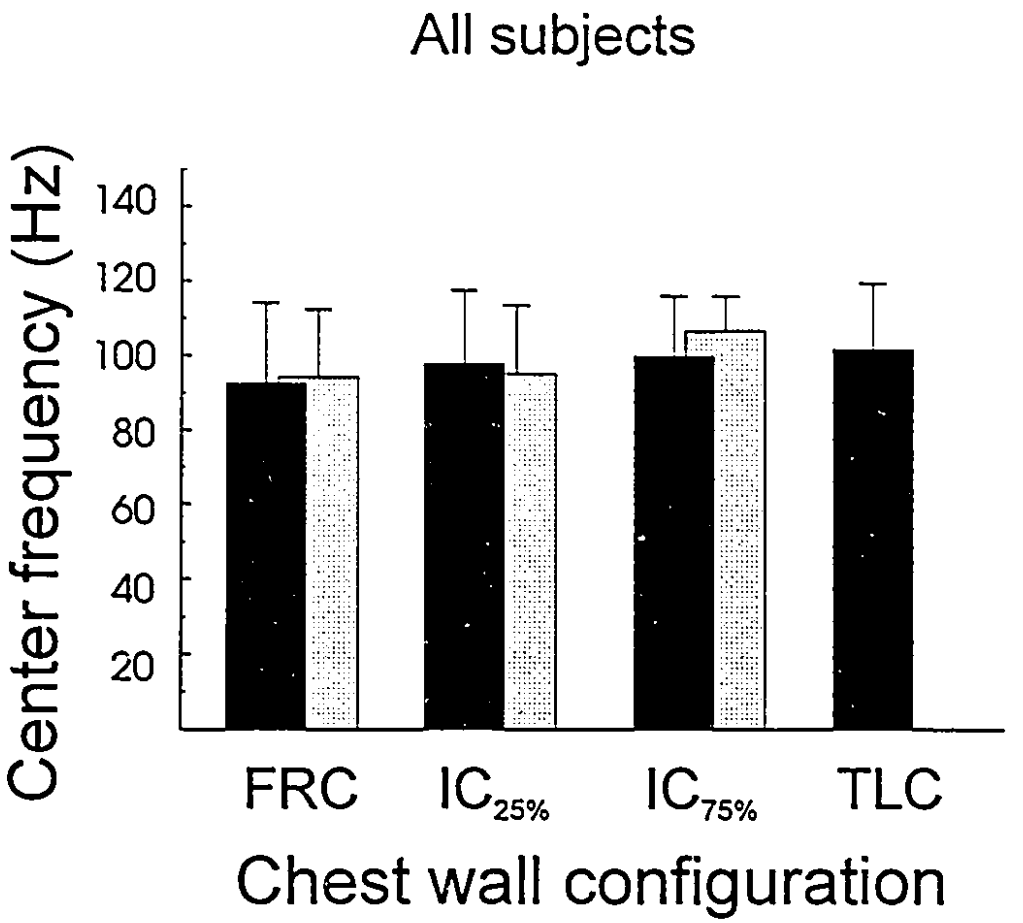

Figure 5.12. CF values (y axis) plotted as a function of chest wall configuration (mean ± SD) for all five subjects

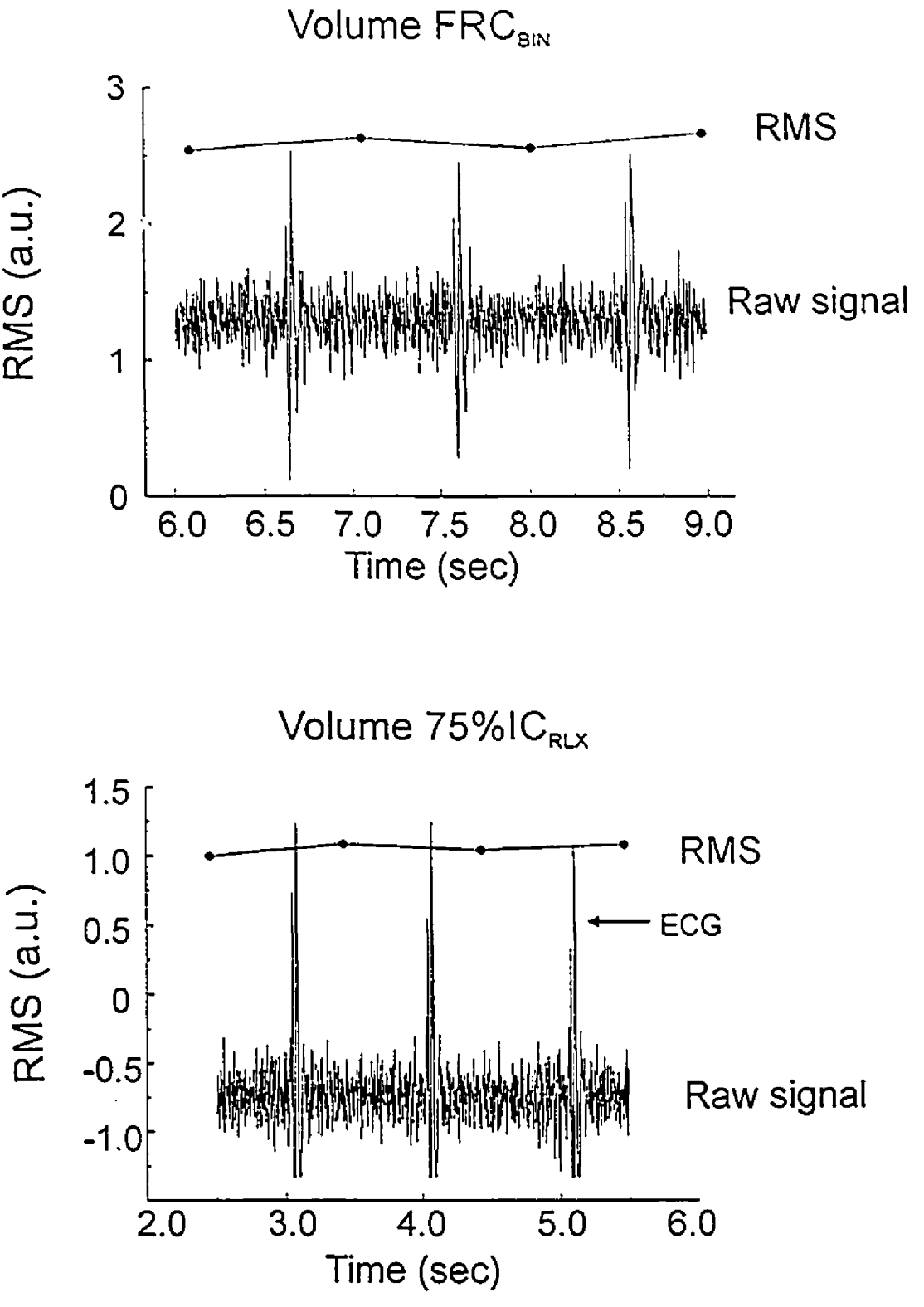

Figure 5.13. Raw signals of EMGdi for FRC_{BIN} (top) and 75% IC_{RLX} (bottom) with respective RMS values (y axis) as a function of time (x axis)

increased on average by 10 Hz from FRC_{RLX} to TLC, at the optimal pair of electrodes (Figure 5.12., solid bars). At any given volume, no consistent pattern was observed between CF values and diaphragm lengthening, as achieved by the belly-in manoeuvres (Figure 5.12., solid and hatched bars). As well, the effect of increasing lung volume during the belly-in manoeuvres showed a similar 10 Hz increase from FRC_{BIN} to $IC75\%_{BIN}$.

Of interest is that, at electrode pairs caudal or cephalad to the optimal pair, CF values could either increase, decrease, or fluctuate randomly with increases in lung volume along the relaxation curve.

Figure 5.13. demonstrates raw EMGdi signals (3 seconds in duration) and RMS values obtained in one subject during a static contraction at FRC_{BIN} (top graph) and IC75%RLX. Note the ECGs are included in the raw signal, but are excluded for calculations of RMS (1 second average).

5.5. DISCUSSION

The results of the present study indicate that there is a consistent muscle to electrode distance filtering effect (MEdist filter) which influences the EMGdi power spectrum and its associated center frequency (CF). This problem, however, can be controlled for by using a multiple array esophageal electrode, and by detecting the optimal pair of electrodes closest to the diaphragm from which to record and analyze the EMGdi signals. With the above method, we found no significant nor consistent effect of chest wall configuration and/or lung volume on EMGdi CF.

5.5.1. Evidence for the MEdist filter in esophageal recordings of EMGdi

In the present study, we have provided evidence that changes in MEdist can influence esophageal recordings of EMGdi. Our results are supported by studies which evaluated the effect of electrode positioning on measurements of EMGdi in the time domain. Fischer & Mittal (1990) reported that by pulling an esophageal electrode through the esophagus in a region where the diaphragm is located, they observed a successive increase in EMGdi amplitude as

the electrodes moved closer towards the diaphragm. The EMGdi amplitude then remained at a plateau over a distance of 2 cm, after which it successively diminished. Daubenspeck et al (1989) found that the EMGdi amplitude always peaked at one pair of electrodes along their multiple electrode array, and then tapered off in both directions with increasing distance from this point. They reported that shifts as small as 1 cm from the point of peak activity resulted in a substantial reduction of the signal amplitude. Önal et al (1979) described that during CO_2 rebreathing, the EMGdi amplitudes obtained with an anchored esophageal electrode were higher at electrode pairs 1.5-5.5 cm cephalad to the cardia, and then decreased further in the same direction. They concluded that electrode pairs located within 2 cm of the position of maximal activity could record EMGdi signals relatively accurately. In dogs, Kim et al (1978) reported that the diaphragm CMAP amplitude increased successively from the cardia to a point 4-6 cm more cephalad, from which point the amplitude of the diaphragm CMAP progressively decreased. Similarly, Grassino et al (1976) observed in cats that the CMAP amplitude was strongly affected by small adjustments in the position of the esophageal electrode. Results from the above decribed studies unanimously imply that the time domain, amplitude-based measurements of EMGdi are affected by increasing MEdist, however, no attempt was made to actually describe the MEdist filter, in either the time domain or the frequency domain.

The effect of the MEdist filter has been mathematically described for EMG signals obtained from single muscle fibers (Lindström, 1973). The mathematical model describes a damping factor which acts in a similar fashion to that of a low-pass filter, where the cut-off frequency and the high frequency slope of the power spectrum change as a function of distance away from the muscle fiber. These changes in the cut-off frequency and the high frequency slope of the power spectrum with increasing MEdist, can be described by so-called modified Bessel functions of the first order and second kind (Lindström & Magnusson, 1977). This theory has been verified experimentally for single muscle fibers by Andreasson and Rosenfalck (1978). For interference pattern EMG signals obtained with surface electrodes, the summation of signals from varying depths within the muscle will increase the complexity of the MEdist filter description. However, the general theory of a successively steeper high frequency slope of

the spectrum with increasing MEdist is still valid for the frequency range that we evaluated (75 Hz to 150 Hz) (Lindström & Broman, 1974).

The results obtained in the present study (Figure 5.6.) agree with those describing a decrease in signal amplitude with increasing distance away from the diaphragm. With the intention of defining the MEdist filter effect, we decided to expand our analysis into the frequency domain. The frequency domain analysis of EMGdi (Figures 5.7. and 5.8.) confirmed the previous theoretical and experimental reports of a steeper high frequency slope of the spectrum with increasing distance away from the muscle, and provided additional support for the existence of the MEdist filter in esophageal recordings of EMGdi.

As expected from the MEdist filter effect, CF values decreased as a function of distance away from the electrode pair that showed the highest CF values (Figures 5.9. and 5.10.). It is highly possible that the CF values obtained for the most peripheral electrode pairs may have been slightly overestimated due to the decreased SN ratio observed at this electrode pair position, and hence the slope of the decrease in CF with distance may be underestimated. It was observed that the MEdist filter effect, and the concomitant decrease in CF values with distance, were different for the caudal and cephalad directions. One of the basic assumptions often made in descriptions of the MEdist filter is that the tissues surrounding the muscle are electrically homogeneous, isotropic, and dissipative (Lynn et al, 1978). However, Geddes & Baker (1967) found considerable differences in resistivity between bone, blood, fat, and muscle. This may be one explanation for the different decreases in CF with distance for the two directions. It is also possible that the differences are due to the different orientations of the electrode pairs along the array with respect to the direction of the muscle fibers in the crural diaphragm.

Thus, the general observations of the MEdist filter in the EMGdi recordings from the present study include, 1) a progressive decrease in signal amplitude away from the pair(s) of electrodes where the amplitude was the highest (Figure 5.6.), 2) a progressively steeper high frequency slope away from the pair(s) of electrodes with the least steep high frequency slope of the spectrum (Figures 5.7. and 5.8.), and 3) a progressive decrease in CF values away from

the pair(s) of electrodes with the highest CF value (Figures 5.9. and 5.10.). These observations provide overwhelming evidence that the electrode pair(s) which records the least distance filtered signal, (as observed in 1, 2, and 3 above), must be closest to the diaphragm. Thus, with the existence of the MEdist filter, we can detect the position of the diaphragm with respect to the electrode array, and we can justify the notion of an "optimal" pair of electrodes from which to record and analyze EMGdi signals.

5.5.2. Factors which may influence the choice of the optimal pair

It has been theoretically described that bipolar recordings of EMG and hence, the MEdist filter, are influenced by innervation zones (Lindström, 1973). EMG recordings obtained with electrodes positioned over an innervation zone produce a reduction in the total power of the signal, with a shift of the power spectrum to higher frequencies. The magnitude of the MEdist filter will thus depend on how much the electrode pair is offset with respect to the center of the innervation zone (Lindström & Broman, 1974). EMGdi signals obtained in the present study may have been influenced by innervation zones underlying the optimal pair of electrodes, because we recurrently observed that the power spectrums obtained from the optimal pair had a reduction in total power of the signal and an increased contribution of power in the high frequency region, when compared to its neighbours. In such cases, however, the optimal pair of electrodes would still be locating the diaphragm.

Calculation of the MEdist filter could as well have been affected by the bipolar electrode transfer function (Lindström, 1970b). (A transfer function is defined is an expression linking the output of an instrument to its input). The bipolar electrode transfer function introduces so-called "dips" into the power spectrum, which are due to cancellation of power at a specific frequency and its harmonics. The frequencies at which the dips occur are proportional to the muscle fiber action potential conduction velocity (CV) and to the interelectrode distance (2d), according to the formula $CV = 2df_{dip}$, where f_{dip} is the frequency at which the first dip occurs. Power spectral "dips" will only occur if the electrodes are aligned in the direction of the muscle fibers, and in an area free of innervation zones. Due to the complicated anatomy of the crural

diaphragm, it is unlikely that the electrodes were aligned in the direction of the muscle fibers and in an area free of innervation zones. Hence, the presence of dips in the power spectrums is as well unlikely. Observation of the obtained power spectrums in this study did not reveal the presence of dips. If the electrodes had been aligned in the direction of the muscle fibers and in an area free of innervation zones, dips would still not have influenced the selection of the optimal pair because with an interelectrode distance of 10 mm, as in this study, the first dip would have been located at 300-500 Hz, assuming a mean muscle fiber CV of 3 to 5 m/s (Lindström, 1970b). The frequency interval chosen to determine the optimal pair of electrodes was 75 to 150 Hz and is thus well away from the frequencies at which dips related to the bipolar electrode transfer function would be present.

5.5.3. Multiple electrode arrays: finding the optimal pair of electrodes provides specific information about EMGdi

The idea of using a multiple electrode array in order to cover the span of diaphragm excursion was originally proposed by Daubenspeck et al (1989). Their method was to average the signals over all pairs of electrodes, contrary to our approach which aimed to find the electrode pair along the array from which to obtain a signal most representative of diaphragm activity.

Anatomical descriptions indicate that the crural portion of the diaphragm covers 2-3 cm of the esophagus (Skinner, 1972), and thus, 2-3 electrode pairs along our electrode array. This is clearly in agreement with the amplitudes of the raw EMG signals obtained from the seven pairs of electrodes (Figure 5.6.). From Figure 5.8., it can be seen that the MEdist filter effect is relatively small for electrode pairs 10 mm away from the optimal pair, in both the caudal and cephalad directions. At electrode pairs located 20 mm and more away from the optimal, the MEdist filter effect is much more pronounced, suggesting, with support from anatomical descriptions, that the diaphragm no longer covers these electrode pairs. One could therefore assume that 2-3 cm, and hence 2 to 3 electrode pairs of the electrode array, will receive EMGdi signals of acceptable quality. With a further increase in MEdist, the SN and SM ratios will

progressively decrease and the signals recorded will be less representative of diaphragm activity, and more representative of noise. This was evident in the present study by a higher exclusion rate of signals with poor quality from the more peripheral pairs of electrodes. Thus, if signals are averaged from all seven electrode pairs, as in Daubenspeck et al's study (1989), at least four of the pairs (out of seven) used in the summation of their signals will contain information that is influenced by poor signal to noise, signal to motion ratios, and by the MEDist filter, and will thus only provide gross estimations about EMGdi. To summarize, from the MEdist filter described in this study, in conjunction with anatomical descriptions of the diaphragm, we can believe that for electrode pairs 20 mm or more away from the optimal pair, one of the rings from the pair is likely to be off the muscle. These signals should thus not be considered for analysis since more adequate ones can be obtained closer to the muscle.

When using a multiple array esophageal electrode to obtain one signal most representative of diaphragm activity, it is crucial to cover the whole span of diaphragmatic displacement and/or electrode displacement, which can occur with changes in lung volume. Wade (1954) reported, from fluoroscopic measurements, that diaphragmatic displacement was 1.5 cm during quiet respiration and between 7 to 13 cm during deep respiration. Daubenspeck et al (1989) described the diaphragm descent during resting breathing to be approximately 2 cm, with no tendency for their esophageal electrode to move along with the diaphragm while it was secured to the nose. Gandevia & McKenzie (1986) also performed fluoroscopy and found that when a stabilizing balloon was used, the electrode moved through a vertical distance of about 8 cm between RV and TLC. Thus, a multiple array electrode which is not stabilized by a balloon, should cover about 7-13 cm, as predicted by Wade (1954). Schweitzer et al (1979) have suggested, however, that pressures up to 30 cm H_2O in the high pressure zone of the lower esophageal sphincter are alone sufficient to "anchor" an esophageal electrode catheter in this region. In the present study, the change in optimal pair position with changes in chest wall configuration never exceeded 4 cm, and could have been due to movement of the diaphragm and/or the electrode. In accordance with Schweitzer et al's (1979) suggestions, it is possible that a flexible electrode catheter can move along with the esophagus/diaphragm

during changes in chest wall configuration, even when the electrode is fixed to the nose. This may be allowed for by buckling of the flexible catheter in the pharynx and the esophagus. Regardless of whether the diaphragm or the electrode moves, the method of choosing the least distance-filtered electrode pair allows accurate recording of EMGdi.

The use of balloon stabilization in order to control for increases in MEdist is questionnable. Balloon stabilization may maintain the position of the electrodes with respect to the esophagus, but not necessarilly to the diaphragm. Based on fluoroscopic measurements, Gandevia & McKenzie (1986) reported that axial movement of the esopagheal electrode with changes in lung volume was "less than, but directly proportional" to the vertical displacement of the diaphragmatic dome. This implies that balloon stabilization does not maintain the electrode position with respect to the diaphragm. In fact, several authors have demonstrated that the gastro-esophageal junction moves 1-3 cm cranially during swallowing, suggesting that the esophagus is capable of moving, independent of respiratory manoeuvres (Johnson, 1968; Clark, 1970), but a concominant movement of the diaphragm was not commented on. Use of a multiple electrode array however, precludes the use of balloon stabilization, and is not affected by movement of the esophagus, as the optimal pair of electrodes closest to the diaphragm can be determined.

5.5.4. The effects of chest wall configuration and/or lung volume on EMGdi

The last of our aims was to determine the effect of chest wall configuration on the EMGdi CF values, while controlling for both the MEdist filter and EMGdi signal quality. This part of the study was prompted by reports suggesting that esophageal recordings of EMGdi are unreliable due to an "artifact" created by changes in lung volume. Schweitzer et al (1979), who investigated the intrabreath EMGdi in normal subjects, found that CF values increased over the first 1 to 2 seconds of inspiration by 20 HZ. Gandevia & McKenzie (1986) reported that diaphragm CMAPs increase in area and amplitude with lung volume and extrapolation of his presented data indicates that this was associated with a decrease in action potential duration, suggesting a shift of the power spectrum to higher frequencies. In both of these studies, the

electrode was anchored with balloons at the gastresophageal junction, and was assumed to track the movement of the diaphragm. As mentioned previously, the use of stabilizing balloons does not necessarily guarantee that the electrodes are not affected by changes in the distance to the diaphragm. Therefore, these studies cannot be regarded as entirely reliable because of the detrimental effects that MEdist filtering will have on the signal.

Daubenspeck et al (1989), without the use of a balloon stabilized electrode, still observed changes in CMAP amplitude with changes in lung volume. In this case, however, there was no evaluation of signal quality obtained from each of the seven pairs of electrodes. Therefore, the authors could not determine from the summed values, which of the seven pairs of electrodes were most influenced by lung volume. This leads us to ask, if the signals from all electrode pairs were influenced by lung volume, or was only one particular pair of electrodes influenced? The results from the present study demonstrate that CF changes with lung volume were not consistent for different electrodes, and thus an average across all electrode pairs would produce erroneous results. In our study, signals recorded at 10 mm or more away from the optimal pair, and still accepted for signal quality, usually increased in CF values with increasing lung volume, whereas CF values from the optimal pair, and 10 mm cephalad to the optimal pair showed no change with lung volume.

In the present study, there was no consistent effect of changes in lung volume and diaphragm length on the EMGdi CF at the optimal pair of electrodes, however a 10 Hz increase was observed from FRC_{RLX} to TLC for the group. It has been proposed that the diaphragm behaves in a sphincter-like fashion during deep inspiration (Klein et al, 1993). Such squeezing of the esophagus around the catheter would reduce MEdist filtering, subsequently producing higher CF values during higher lung volumes. Thus, the changes in CF values observed with lung volume at the optimal pair may have been due to changes in the radial distance around the electrode, as the esophagus squeezed the electrode during the contractions of the diaphragm at high lung volumes.

One could speculate that the increase in CF observed at the optimal pair was caused by movement of the esophagus, being pushed towards (closer to) the diaphragm during

increases in lung volume (or during the belly-in manoeuvres). As well, the possibility that changes in chest wall configuration produce changes in the orientation of the electrode array with respect to the fiber direction or the innervation zones cannot be excluded. For human investigations of EMGdi, no methods are yet available to determine the fiber direction of the crural diaphragm, nor the location of innervation zones with respect to the esophageal electrode, and thus, these influences were not controlled for in the present study.

The possibility that the changes in CF values with lung volume were due to poor signal quality can be excluded. Signal disturbances caused by noise, electrode motion, the ECG, and esophageal peristalsis were automatically excluded from the analysis. With the automatic analysis used, in the present study, the maximum underestimation of CF caused by motion artifacts has been calculated to be less than 5% (Sinderby et al, 1993). Similarly, any increases in CF observed at the optimal pair are not likely due to increased levels of noise because the maximum overestimation of CF due to noise levels is 10% (Sinderby et al, 1993). In this study, the random variations of CF values obtained during changes in chest wall configuration were within the combined range of 15%. Overall, we believe that the changes observed are most likely not physiological in nature, but are more related to the recording location and the influence of electrode proximity to the diaphragm, innervation zones, and/or orientation with respect to the muscle fiber direction.

Assuming EMGdi signal quality and the MEdist filter effect were adequately controlled for, changes observed in EMGdi with diaphragm shortening could be explained for by concepts derived from the physiology of nerve fibers. Based on the cable theory of electrical conduction in non-myelinated nerve fibers (Hodgkin & Rushton, 1946), muscle action potential conduction velocity (CV) is expected to increase with muscle shortening, due to its dependence on fiber diameter. When signals are ideal, frequency parameters used to quantify the EMG power spectrum always appear together with CV as a quotient, which implies that any changes in CV will be reflected by a proportional shift of the EMG power spectrum (Lindström, 1973). Thus, when CV increases with muscle shortening, as predicted by the cable theory, CF values will also increase. The increase in CV should be associated with a decrease in signal power

because the action potential spends a shorter amount of time on the muscle fiber membrane, giving off less energy/power. As previously mentioned, several authors have either indicated or implied that during diaphragm shortening, there is a power spectral shift to higher frequencies (Schweitzer et al, 1979; Weinberg et al, 1993; Gandevia & McKenzie, 1986), and that CMAP amplitude increases (Gandevia & McKenzie, 1986; Daubenspeck et al, 1989). Thus, the simultaneous occurence of power spectral shifts to higher frequencies and increases in signal power, as seen during diaphragm shortening, cannot be supported by the cable theory of electric conduction.

Controversies surrounding the effect of muscle length on the CMAP amplitude have provided further doubt as to whether the cable theory alone can account for the changes observed in CV/CF. Gydikov & Kosarov (1973) observed an increase in CMAP amplitude with increasing length and also described a concomitant reduction in CV, as is predicted by theory. Goldman (1964), in studying compound nerve action potentials, reported no changes in either CV nor action potential amplitude with changes in nerve length. In contrast, Martin (1954) saw increases in CMAP amplitude with increasing muscle length, but observed no changes in CV.

The conclusion must therefore be that previously reported systematic changes in power distribution, or total power, with changes in lung volume, are not necessarily due to changes in CV as predicted by the cable theory, but rather to the influence of the MEdist filter, innervation zones, or the changing orientation of the electrodes with respect to the direction of the crural musculature. This is further supported by the results of the present study, where non-contaminated signals were selected at electrode pairs where the MEdist filter effect was minimal, and did not reveal any consistent changes in CF values with changes in chest wall configuration. One therefore has to assume that such previously described changes are due to other factors, such as electrode configuration (including balloon stabilization), electrode positioning, and signal quality, rather than to volume effects in themselves.

The present method of determining the location of the diaphragm along an electrode array provides a more reliable way of obtaining EMGdi signals. This is especially important when using spectral analysis to detect diaphragmatic fatigue. For example, if we were to test

for diaphragmatic fatigue during exercise, large excursions of the diaphragm may place the diaphragm away from the electrodes, and the decreases in CF values due to the distance filter could easily be misinterpreted as fatigue. Thus, it is important to use a multiple array electrode which covers the span of diaphragmatic excursion, and to be able to select the least distance-filtered pair of electrodes from which to record and analyze the EMGdi signals. In addition, controlling for signal quality is of utmost importance as artifacts related to motion and noise can easily effect the EMGdi power spectrum.

Use of a multiple electrode array no longer necessitates tracking of the diaphragm's movement with a stabilizing balloon at the gastroesophageal junction, because our method allows us to "track" the diaphragm's movement by looking for the optimal pair of electrodes which are closest to the muscle. Detecting the optimal pair of electrodes is thus a method which is independent of either diaphragm or electrode displacement, assuming the multiple electrode array has the appropriate configuration, and covers the required distance.

CHAPTER 6

CONCLUSION

The overall objective of this study was to develop a reliable method to record the diaphragm electromyogram with an esophageal electrode. The specific aims of the work were to (1) quantify the muscle-to-electrode distance filter (MEdist) with a multiple array esophageal electrode, (2) develop a method which can trace the position of the diaphragm along a multiple array esophageal electrode, and (3) to evaluate the changes in center frequency (CF) with changes in chest wall configuration, while controlling for MEdist filtering effects and signal quality.

The results of this study confirmed that esophageal recordings of the diaphragm electromyogram (EMGdi) are severely affected by the muscle-to-electrode distance (MEdist). Evidence for this was provided by the following observations, which are in accordance with theory: (1) As the distance between the diaphragm and the electrodes increased, there was a reduction in signal amplitude. (2) The effect of increasing the distance between the electrodes and the diaphragm was that of a low-pass filter, and resulted in a filtering out of the high frequency components of the EMGdi power spectrum. (3) Spectral measurements, such as CF, were gradually reduced as the distance between the electrodes and the diaphragm increased. The diaphragm-to-electrode distance filter was found to affect CF by an approximate 1 Hz decrease in CF per mm displacement away from the diaphragm. By taking advantage of the MEdist filter, the pair of electrodes which was the least filtered by distance could be determined (the "optimal pair"), and was assumed to represent the position of the diaphragm. The method of selecting the optimal pair of electrodes has since been implemented into computer algorithms for on-line, automatic analysis of EMGdi.

By controlling for distance filtering effects and signal quality, there was no systematic effect of changes in chest wall configuration on CF values for the group of five subjects.

It is likely that the random fluctuations in CF values within a given subject were due to the influence of innervation zones underlying the optimal pair, as was occasionally indicated

by the reduction in power and a simultaneous increase in frequency at these electrodes. Hence, future work in this field requires scrutinization into the influence of the innervation zones in esophageal recordings of EMGdi in order to further reduce the stochastic variation.

REFERENCES

Agarwal, G.C., and Gottlieb, G.L. (1975) An analysis of the electromyogram by Fourier simulation and experimental techniques. IEEE Trans. Biomed. Eng. 22:225-229

Agostoni, E., Sant'Ambrogio, G., and Del Portillo Carrasso, H. (1960) Electromyography of the diaphragm in man and transdiaphragmatic pressure. J. Appl. Physiol. 15:1093-1097

Aldrich, T.K., Adams, J.M., Arora, N.S, and Rochester, D.F. (1983) Power spectral analysis of the diaphragm electromyogram. J. Appl. Physiol. 54:1579-1584

Alfonsi, E., Ricciardi, L., Arrigo, A., Lozza, A., Sandrini, G., Zandrini, C., and Moglia A. (1991) Local venous lactate changes and spectral analysis of surface EMG during fatiguing isometric efforts in intrinsic hand muscles. Funct. Neurol. 6:121-127

Anderson, C.R., and Stevens, C.F. (1973) Voltage clamp analysis of acetylcholine produced end-plate current fluctuations at frog neuromuscular junction. J. Physiol. (Lond.). 235:655

Andreassen, S., and Rosenfalck, A. (1978) Recording from a single motor unit during strong effort. IEEE Trans. Biomed. Eng. 25:501-508

Andreassen, S., and Rosenfalck, A. (1981) Relationship of intracellular and extracellular action potentials of skeletal muscle fibers. CRC Crit. Rev. Biomed. Eng. 6:267-306

Andreassen, S., and Arendt-Nielsen, L. (1987) Muscle fiber conduction velocity in motor units of the human anterior tibial muscle: a new size principle parameter. J. Physiol. (Lond.) 391:561-571

Arendt-Nielsen, L., and Mills, K.R. (1985) The relationshop between the mean power frequency of the EMG spectrum and muscle fiber conduction velocity. Electroenceph. Clin. Neurophysiol. 60:130-138

Arendt-Nielsen, L., Forster, A., and Mills, K.R. (1984) The relationship between muscle-fiber conduction velocity and force in the human vastus lateralis. J. Physiol. (Lond.), 353:6P

Arendt-Nielsen, L., and Zwarts, M. (1989) Measurement of muscle fiber conduction velocity in humans: techniques and applications. J. Clin. Neurophysiol. 6:173-190

Arvidsson, A., Grassino, A., and Lindström, L. (1984) Automatic selection of uncontaminated electromyogram as applied to respiratory muscle fatigue. J. Appl. Physiol. 56:568-575

Aubier, M., Farkas, G., DeTroyer, A., Mozes, R., and Roussos, C. (1981) Detection of diaphragmatic fatigue in man by phrenic nerve stimulation. J. Appl. Physiol. 50:538-544

Bahler, A.S., Fales, J.T., and Zierler, K.L. (1967) The active state of mammalian skeletal muscle. J. Gen. Physiol. 50:2239-2253

Bahler, A.S., Fales, J.T., and Zierler, K.L. (1968) The dynamic properties of mammalian skeletal muscle. J. Gen. Physiol. 51:369-384

Banus, M.G., and Zeltin, A. (1938) The relation of isometric tension to length in skeletal muscle. J. Cell. Comp. Physiol. 12:403-420

Banzett, R.B., Inbar, G.E., Brown, R., Goldman, M., Rossier, A., and Mead, J. (1981) Diaphragm electrical activity during lower negative torso pressure in quadriplegic men. J. Appl. Physiol. 51:654-659

Basmajian, J.V., and DeLuca, C.J. (1985) In: Muscles alive: their functions revealed by electromyography. Williams and Wilkins, Baltimore.

Basmajian, J.V. (1973) Electromyography. In: The structure and function of muscle, 2nd edition, Vol. III, Physiology and Biochemistry. G.H. Bourne (Ed.). Academic press, New York.

Bazzy, A.R., Korten, J.B., and Haddad, G.G. (1986) Increase in electromyogram low-frequency power in non-fatigued contracting skeletal muscle. J. Appl. Physiol. 61:1012-1017

Béliveau, L., Helal, J-N., Gaillard, E., Van Hoecke, J., Atlan, G., and Bouissou, P. (1991) EMG spectral shift and ^{31}P-NMR determined intracellular pH in fatigued human biceps brachii muscle. Neurology. 41:1998-2001

Bellemare, F., and Bigland-Ritchie, B. (1984) Assessment of human diaphragm strength and activation using phrenic nerve stimulation. Resp. Physiol. 58:263-277

Bellemare, F., and Grassino, A.E. (1982) Evaluation of human diaphragmatic fatigue. J. Appl. Physiol. 53:1196-1206

Bellemare, F., and Grassino, A.E. (1983) Force reserve of the diaphragm in patients with chronic obstructive pulmonary disease. J. Appl. Physiol. 55:8-15

Bigland-Ritchie, B. (1981) EMG and fatigue of human voluntary and stimulated contractions. In: Human muscle fatigue: Physiological mechanisms. Eds. Porter, H., and Whelan, J. London, Pitman Medical. pp. 130-156

Bigland-Ritchie, B.R., and Lippold, O.C.J. (1979) Changes in muscle activation during prolonged maximal voluntary contractions. J. Physiol. (Lond.) 292:14-15

Bigland-Ritchie, B., Donovan, E.F., and Roussos, C.S. (1981) Conduction velocity and EMG power spectrum changes in fatigue of sustained maximal efforts. J. Appl. Physiol. 51:1300-1305

Bilodeau, M., Arsenault, A., Gravel, D., and Bourbonnais, D. (1990) The influence of an increase in the level of force on the EMG power spectrum of elbow extensors. Eur. J. Appl. Physiol. 61:461-466

Bilodeau, M., Arsenault, A., Gravel, D., and Bourbonnais, D. (1991) EMG power spectra of

elbow extensors during ramp and step isometric contractions. Eur. J. Appl. Physiol. 63:24-28

Blinowska, A., Verroust, J., and Cannet, G. (1980) An analysis of synchronization and double discharge effects on low frequency electromyographic power spectra. Electromyogr. Clin. Neurophysiol. 15:346-354

Bolton, C.F. (1993) Clinical neurophysiology of the respiratory system. Muscle & Nerve. 16:809-818

Bolton, C.F., Grand'Maison, F., Parkes, A., and Shkrum, M. (1992) Needle electromyography of the diaphragm. Muscle & Nerve. 15:678-681

Botros, K.G., Bondok, A.A., Gabr, O.M., el-Eishi, H.I., and State, F.A. (1990) Anatomical variations in the formation of the human esophageal hiatus. Anatomischer Anzeiger. (Abstract) 171:193-199

Bradley, T.D., Chartrand, D.A., Fitting, J.W., Comtois, A., and Grassino. (1988) Effect of transdiaphragmatic partitioning on activation and fatigue of the diaphragm. Am. Rev. Res. Dis. 137:1395-1400

Brochard, L., Harf, A., Lorino, H., and Lemaire, F. (1989) Inspiratory pressure support prevents diaphragmatic fatigue during weaning from mechanical ventilation. Am. Rev. Res. Dis. 139:513-521

Brody, L., Pollock, M., Roy, S.H., De Luca, C.J., and Celli, B. (1991) pH induced effects on median frequency and conduction velocity on the myoelectric signal. J. Appl. PHysiol. 71:1878-1885

Broman, H. (1977) An investigation on the influence of a sustained contraction on the succession of action potentials from a single motor unit. Electromyogr. Clin. Neurophysiol. 17:341-358

Broman, H. and Lindström, L. (1974) A model describing the power spectrum of myoelectric signals. Part II: motor unit signal. Res. Lab. Med. Electr., Göteborg, Sweden, Tech. Rep. 8:74

Broman, H., Bilotto, G., and De Luca, C.J. (1985) Myoelectrical signal conduction velocity and spectral parameters: influence of force and time. J. Appl. Physiol. 8:1428-1437

Brooke, M.H. and K.K. Kaiser. (1970) Muscle fiber types; how many and what kind? Arch. Neurol. 23:369-379

Buchtal, F., and Engbaek, L. (1963) Refractory period and conduction velocity of the striated muscle fiber. Acta. Physiol. Scand. 59:199-219

Buchtal, F., and Madsen, A. (1950) Synchronous activity in normal and atrophic muscle. Electroenceph. Clin. Neurophysiol. 2:425-444

Buchtal, F., and Rosenfalck, A. (1966) Evoked action potentials and conduction velocity in

human sensory nerves. Brain Res. 3:1-122

Buchtal, F., Guld, C., and Rosenfalck, P. (1955) Propagation velocity in electrically activated muscle fibers in man. Acta. Physiol. Scand. 34:75-89

Buchtal, F., Guld, C., and Rosenfalck, P. (1957) Multielectrode study of the territory of a motor unit. Acta. Physiol. Scand. 39:83-104

Burke, R.E., Levine, D.N., Tsairis, P., and Zajac, F.E. (1973) Physiological types and histochemical profiles of motor units in cat gastrocnemius. J. Physiol. (Lond.). 234:723-748

Burke, R.E., Levine, D.N., and Zajac, F.E. (1974) Mammalian motor units: physiological-histochemical correlation in three types in cat gastrocnemius. Science 174:709-717

Bye, P.T.P., Esau, S.A., Walley, K.R., Macklem, P.T., and Pardy, R.L. (1984) Ventilatory muscles during exercise in air and oxygen in normal men. J. Appl. Physiol.56:464-471

Campbell, E.J.M. (1958) The respiratory muscles and the mechanics of breathing. Chicago: Year Book Publishers.

Carpenter, S., and Karpati, G. (1984) Normal organelles and constituents of skeletal muscle cells and their pathological reactions. In: Pathology of skeletal muscle. Churchill Livingstone Inc. New York.

Carey, J.M., and Hollinshead, W H. (1955) An anatomic study of the esophageal hiatus. Surg. Gyn. Obs. 100:196-200

Caskey, C.I., Zerhouni, E.A., Fishman, E.K., Rahmouni, A.D. (1989) Aging of the diaphragm: a CT study. Radiology. 171:385-389

Chaffin, D.B. (1973) Localized muscle fatigue - definition and assessment. J. Occup. Med. 15:346-354

Chandler, W.K., Rakowski, R.F., and Schneider, M.F. (1976) Effects of glycerol trreatment and maintained depolarization on charge movement in skeletal muscle. J. Physiol. (Lond.). 254:285-316

Clamann, H.P. (1993) Motor unit recruitment and the gradation of muscle force. Phys. Ther. 73:830-843

Clamann, H.P., Gillies, J.D., Skinner, R.D., and Henneman, E. (1974) Quantitative measures of output of motoneuron pool during monophasic reflexes. J. Neurophysiol. 37:1328-1337

Clark, J., and Plonsey, R. (1968) The extracellular potential field of the single active nerve fiber in a volume conductor. Biophys. J. 8:842

Clark, M.D., Rinaldo, J.A., and Eyler, W.R. (1970) Correlation of manometric and radiologic data from the esophagogastric area. Radiology. 94:261-270.

Clarke, R.S.J., Hellon, R.F.R., and Lind, A.R. (1958) The duration of sustained contractions of the human forearm at different muscle temperatures. J. Physiol. (Lond). 143:454-463

Close, R.E. (1972) The dynamic properties of mammalian skeletal muscle. Physiol. Rev. 52:129-97

Coërs, C., and Woolf, A.L. (1959) The innervation of muscle; a biposy study. Oxford: Blackwell

Cohen, C.A., Zagelbaum, G., Gross, D., Roussos, C., and Macklem, P.T. (1982) Clinical manifestations of inspiratory muscle fatigue. Am. J. Med. 73:308-316

Collis, J.L., Kelly, T.D., and Wiley, A.M. (1954) Anatomy of the crura of the diaphragm and the surgery of the hiatus hernia. Thorax. 9:175-189

Constantin, L.L. (1970) The role of sodium current in the radial spread of contraction in frog muscle fibers. J. Gen. Physiol. 55:703-15

Cooley, J.W., and Tukey, J.W. (1965) An algorithm for the machine calculation of complex Fourier series. Math. Comput. 19:297-301

Cullen, M.J., and Landon, D.N. (1988) The ultrastructure of the motor unit. In: Disorders of voluntary muscle, 5th edition. J. N. Walton (Ed.). Churchil Livingstone, New York.

Cummins, K.L., and Dorfman, L.J. (1981) Nerve fiber conduction velocity distribution: studies of normal and diabetic human nerves. Ann. Neurol. 9:67-74

Darnell, J., Lodish, H., and Baltimore, D. (1990) Molecular Cell Biology. 2nd edition. Scientific American Books Ltd. New York.

Daube, J.R. (1981) Quantitative EMG in nerve-muscle disorders. In: Neurology, Vol. 1: Clinical Neurophysiology, Chapt. 3. E. Stalberg, and R.R. Young (Eds.). Butterworths publishing Co., London

Daubenspeck, J.A., Leiter, J.C., McGovern, J.F., Knuth, S.L., and Kobylarz, E.J. (1989) Diaphragmatic electromyography using a multiple electrode array. J. Appl. Physiol. 67:1525-1534

De la Barrera, E.J., and Milner, T.E. (1994) The effects of skinfold thickness on the selectivity of the surface EMG. Electroenceph. Clin. Neurophysiol. 93:91-99

Del Castillo, J., and Katz, B. (1954) Quantal components of the end-plate potential. J. Physiol. (Lond.) 124:560-573

Delhez, L. (1965) Modalités chez l'homme normal de la réponse électrique des pilliers du diaphragme à la stimulation électrique des nerfs phréniques par des chocs uniques. Arch Int. Physiol. Bioch. 72:832-839

Delhez, L., and Petit, J.M. (1966) Données actuelles de l'électromyographie respiratoire chez

l'homme normal. Electromyography. 6:101-146

De Luca, C.J., and Forrest, W.J. (1973) Some properties of motor unit action potential trains recorded during constant force isometric contractions in man. Kybernetik. 12:160-168

De Luca, C.J. (1979) Physiology and mathematics of myoelectric signals. IEEE Tans. Biomed. Eng. 26:313-325

De Luca. C.J., LeFever, R., McCue, M., and Xenakis, A. (1982) Behavior of motor units in different muscles during linearly varying contraction. J. Physiol. (Lond.) 329:113-128

De Luca, C.J. (1984) Myoelectrical manifestations of localized muscular fatigue in humans. Crit. Rev. Biomed. Eng. 11(4):251-279

De Luca, C.J., and Merletti, R. (1988) Surface myoelectric signal cross-talk among muscles of the leg. Electroenceph. Clin. Neurophysiol. 69:568-575

Denier van der Gon, J.J., Gielen, C.C.A.M., ter Haar Romeny, B.M. (1982) Changes in recruitment threshold of motor units in the human biceps muscle. J. Physiol. (Lond.). 328:28P

Denny-Brown, D. (1949) Interpretation of the electromyogram. Arch. Neurol. Psych. 61:99-128

Derenne, J-P., Macklem, P.T., and Roussos, Ch. (1978) The respiratory muscles: mechanics, control and pathophysiology. Part I. Am. Rev. Res. Dis. 118:119-133

Desmedt, J.E. (1958) Methodes d'etude de la fonction neuromusculaire chez l'homme: Myogramme isometrique, electromyogramme d'excitation et topographie de l'innervation terminale. Acta. Neurol. Psychiatr. Belg. 58:977-1017

De Troyer, A., Sampson, M., Sigrist, S., and Macklem, P.T. (1981) The diaphragm: two muscles. Science. 213:237-238

De Troyer, A., Sampson, M., Sigrist, S., and Macklem, P.T. (1982) Action of costal and crural parts of the diaphragm on the rib cage in dog. J. Appl. Physiol. 53:30-39

De Troyer, A., Sampson, M., Sigrist, S., and Kelly, S. (1983) How the abdominal muscles act on the rib cage. J. Appl. Physiol. 54:465-469

De Troyer, A., and Loring, S.H. (1986) Action of the respiratory muscles. In: Handbook of Physiology, The Respiratory System. Section 3, Vol. III. Mechanics of breathing, Part 2. Ed. Fishman, A.P. American Physiological Society, Bethesda, MD.

De Troyer, A., and Estenne, M. (1988) Functional anatomy of the respiratory muscles. Clin. in Chest Med. 9:175-193

De Troyer, A. (1991) Respiratory muscles. In: The Lung: *Scientific foundations*. R.G. Crystal, J.B. West et al. (Eds.). Raven Press Ltd., New York.

Dick, T.E. Kong, F.G., and Berger, A.J. (1987) Recruitment order of diaphragmatic motor units obeys Hanneman's size principle. In: Respiratory muscles and their neural control. Eds: G.C. Sieck, S.C. Gandevia, and W.E. Cameron. New York, Liss. p.239-247

Draper, M.H., Ladefoged, P., and Whitteridge, D. (1957) Expiratory muscles involved in speech. J. Physiol. (Lond.). 138:17P-18P

Draper, M.H., Ladefoged, P., and Whitteridge, D. (1959) Respiratory muscles in speech. J. Speech. Res. 2:16-27

DuBois, P., Damoiseau, J., Defoanne, R., Troquet, J., Delhez, L., and Petit, J.M. (1963) Contrôle radiographique de la position des électrodes exploratrices de l'activité électrique du diaphragme par voie oesophagienne chez l'homme conscient. Acta. Tuberc. Pneumol. Belg. 5:456-462

Dulhunty, A.F., and Franzini-Armstrong, C. (1975) The relative contributions of the folds and caveolae to the surface membrane of frog skeletal muscle fibers at different sarcomere lengths. J. Physiol. (Lond.) 250:513-541

Eberstein, A., and Beattie, B. (1985) Simultaneous measurement of muscle conduction velocity and EMG power spectrum changes during fatigue. Muscle & Nerve. 8:768-773

Edstrom, L. and Kukelberg, E. (1968) Histochemical composition, distribution of fibers and fatigability of single motor units: anterior tibial muscle of the rat. J. Neurol. Neurosurg. Psychiatry. 31:424-433

Edwards, M.A. (1961) The anti-reflux mechanism: manometric and radiologic studies. Brit. J. Radiol. 34:474-487

Edwards, R.H.T., Hill, D.K., and Jones, D.A. (1975) Heat production and chemical changes during isometric contractions of the human quadriceps muscle. J. Physiol. (Lond.) 251:303-315

Edwards, R.H.T. (1981) Human muscle function and fatigue. In: Human muscle fatigue: Physiological mechanisms. Eds. Porter, H., and Whelan, J. London, Pitman Medical. pp.1-18

Edwards, R.H.T., and Faulkner, J.A. (1986) Respiratory Muscles: The thorax structure and function. In: The Thorax, Roussos, C. and Macklem P.T. (eds.) New York: Marcel Dekker. Part A., p.297

Elliott, G.F., Lowy, J., and Worthington, C.R. (1963) An X-ray and light diffraction study of the filament lattice of striated muscle in the living state and rigor. J. Mol. Biol. 6:295-305

Elliott, G.F., Lowy, J., and Milman, B.M. (1967) Low angle X-ray diffraction studies of living striated muscle during contraction. J. Mol. Biol. 25:31-45

Enad, J.G., Fournier, M., and Sieck, G.C. (1989) Oxidative capacity and capillary density of diaphragm motor units. J. Appl. Physiol. 67:620-627

Eisenberg, B.R., and Kuda, A.M. (1976) Discrimination between fiber populations in mammalian skeletal muscle using ultrastructure parameters. J. Ultrastruct. Res. 54:76-88

Ekstedt, J. (1964) Human single muscle fiber action potentials. Acta. Physiol. Scand. 61, Suppl. 226: 1-96

Ekstedt, J., and Stålberg, E. (1973) How the size of the needle electrodes leading-off surface influences the shape of the single muscle fiber action potential in electromyography. Comp. Progr. Biomed. 3:204-212

Elliot, A., and Offer, G. (1978) Shape and flexibiity of the myosin molecule. J. Molec. Biol. 123:505-519

Evanich, M.J., Lopata, M., and Lourenço, R.V. (1976) Analytical methods for the study of electrical activity in respiratory nerves and muscles. Chest. 70:158-162

Farkas, G.A., and De Troyer, A. (1987) The ventral rib cage muscles in the dog: contractile properties and operating lengths. Respir. Physiol. 68:301-309

Farkas, G.A., and Rochester, D.F. (1988) Functional characteristics of canine costal and crural diaphragm. J. Appl. Physiol. 65:2253-2260

Farkas, G.A., and Roussos, C. (1982) Adaptability of the hamster diaphragm to exercise and/ or emphysema. J. Appl. Physiol. 53:1263-1272

Fatt, P., and Katz, B. (1951) An analysis of the end-plate potential recorded with an intracellular electrode. J. Physiol. (Lond.). 115:320

Fatt, P., and Katz, B. (1952) Spontaneous threshold activity at the motor nerve ending. J. Physiol. (Lond.). 117:109

Fawcett, D.W. (1986) In: Bloom and Fawcett: A Textbook of Histology. Eleventh edition. W.B. Saunders Company. Philadelphia, PA. pp 265-310

Fex, J., and Krakau, E.T. (1957) Some experiences with Walton's frequency analysis of the electromyogram. J. Neurol. Neurosurg. Psychiat. 20:178-184

Fink, R., and Luttgau, H.D. (1976) An evaluation of membrane constants and potassium conductance in metabolically exhausted fibers. J. Physiol. (Lond.) 263:215-239

Fischer, M.J., and Mittal, R.K. (1990) Effect of intraesophageal electrode position on signal amplitude of the crural diaphragm electromyogram. J. Gastrointestinal. Motil. 2:184-189

Fitting, J.W., and Grassino, A.E. (1986) Exploration de la mobilité thoraco-abdominale et de la fonction des muscles respiratoires. Rev. Mal. Resp. 3:421-424

Fitts, R.H. (1994) Cellular mechanisms of muscle fatigue. Physiol. Rev. 74:49-94

Frank, G.B. (1958) Inward movement of calcium as a link between electrical and mechanical events in contraction. Nature. 182:1800-1801

Freund, H-J. (1983) Motor unit and muscle activity in voluntary motor control. Physiol. Rev. 63:387-436

Fuglevand, A.J., Winter, D. A., Patla, A.E., and Stashuk, D. (1992) Detection of motor unit action potentials with surface electrodes: influence of electrode size and spacing. Biol. Cyber. 67:143-153

Fuglsand-Frederiksen, A., and Ronager, J. (1988) The motor unit firing rate and the power spectrum of the EMG in humans. Electroenceph. Clin. Neurophysiol. 70:68-72

Gandevia, S.C., and McKenzie, D.K. (1986) Human diaphragmatic EMG: changes with lung volume and posture during supramaximal phrenic nerve stimulation. J. Appl. Physiol. 60:1420-1428

Ganong, W.F. (1991) Review of medical physiology. Fifteenth ed. Appleton & Lange, Norwalk, Connecticut, USA.

Gantchev, N., Kossev, A., Gydikov, A., and Gerasimenko, Y. (1992) Relation between the motor units recruitment threshold and their potentials propagation velocity at isometric activity. Electromyogr. Clin. Neurophysiol. 32:221-228

Gath, I., and Stalberg, E. (1975) Frequency and time domain characteristics of single muscle fiber action potentials. Electroenceph. Clin. Neurophysiol. 39:371-376

Gath, I., and Stalberg, E. (1976) Techniques for improving the selectivity of electromyographic recordings. IEEE. Trans. Biomed. Eng. 23:467-472

Gath, I., and Stalberg, E. (1978) The calculated radial decline of the extracellular action potential compared with *in situ* measurements in the human brachial biceps. Electroenceph. Clin. Neurophysiol. 44:547-552

Gea, J., Sauleda, J., Espadaler, J.M., Valls, A., Guiu, R., Aran, X., and Broquetas, J.M. (1991) Diaphragmatic activity due to magnetic stimulation of the brain during voluntary apneas performed at different lung volumes in healthy subjects (Abstract). Am. Rev. Res. Dis. (Suppl.) 143:A193

Geddes, L.A., and Baker, L.E. (1967) The specific resistance of biological material- a compendium of data for the biomedical engineer and physiologist. Med. & Biol. Comp. & Eng. 5:271-293

Geffen, L.B. (1964) Optimum length for contraction of rat circulated limb muscles. Arch. Int. Physiol. 72:825-834

Gerdle, B., Eriksson, N.E., and Hagberg, C. (1988a) Changes in the surface electromyogram during isometric shoulder forward flexions. Eur. J. Appl. Physiol. 57:1428-1437

Gerdle, B., Wretling, M-L., Henriksson-Larson, K. (1988b) Do the fiber type proportion and the angular velocity influence the mean power frequency of the electromyogram? Acta. Physiol. Scand. 134:341-346

Gerdle, B., Eriksson, N.E., and Brundin, L. (1990) The behavior of the mean power frequency of the surface electromyogram in biceps brachii with increasing force and during fatigue. With special regard to the electrode distance. Electromyogr. clin. Neurophysiol. 30:483-489

Goldman, D.E. (1943) Potential, impedance, and rectification in membranes. J. Gen. Physiol. 27:37-60

Goldman, L. (1964) The effects of stretch on impulse propagation in the median giant fiber of Lumbricus. J. Cell. Comp. Physiol. 62:105-112

Goodgold, J. (1984) Anatomical correlates of clinical electromyography. 2nd edition. Baltimore, MD. Williams and Wilkins.w

Goodgold, J., and Eberstein, A. (1983) Electrodiagnosis of neuromuscular disease. 3rd edition. Williams and Wilkins, Baltimore, MD.

Gordon, A.M., Huxley, A.F., and Julian, F.J. (1966) The variation in isometric tension with sarcomere length in vertebrate muscle fibers. J. Physiol. Lond. 184:170-192

Gordon, D.C., Hammond, C.G.M., Fischer, J.T., and Richmond, F.J.R. (1989) Muscle fiber architecture, innervation and histochemistry in the diaphragm of the cat. J. Morphol. 201:131-143

Grassino, A.E., Whitelaw, W.A., and Milic-Emili, J. (1976) Influence of lung volume and electrode position on electromyography of the diaphragm. J. Appl. Physiol. 40:971-975

Grassino, A.E., Goldman, M.D., Mead, J., and Sears, T.A. (1978) Mechanics of the human diaphragm during voluntary contraction: statics. J. Appl. Physiol. 44:829-839

Grassino, A.E., Gross, D., Macklem, P.T., Roussos, Ch., and Zagelbaum, G. (1979) Inspiratory muscle fatigue as a factor limiting exercise. Bull. Eur. Physiopath. Resp. 15:105-111

Grassino, A.E., Roussos, C., and Macklem P.T. (1991) Static properties of the chest wall. In: The Lung: *Scientific foundations*. R.G. Crystal, J.B. West, et al (Eds.). Raven Press Ltd. New York.

Gross, D., Grassino, A., Ross, W.R.D., and Macklem, P.T. (1979) Electromyogram pattern of diaphragmatic fatigue. J. Appl. Physiol. 46:1-7

Guyton, A.C. (1991) Textbook of medical physiology. 8th Ed. Saunders Co. Toronto, ON.

Gydikov, A., and Kosarov, D. (1973) Influence of various factors on the shape of the myopotentials in using surface electrodes. Electromyography. 13:319-343

Gydikov, A., Dimitrova, N., Kosarov, D., and Dimitrov, G. (1976) Influence of frequency and duration of firing on the shape of potentials from different types of motor units in human muscles. Experimental Neurology. 52:345-355

Gydikov, A., and Gatev, P. (1982) Human muscle fiber potentials at different radial distances from the fibers determined by a method of location. Exp. Neurol. 76:25-34

Gydikov, A., Kostov, K., Kossev, K., and Kosarov, D. (1984) Estimation of the spreading velocity and the parameters of the muscle potentials by averaging of the summated electromyogram. Electromyogr. Clin. Neurophysiol. 24:191-212

Hägg, G.M. (1981) Electromyographic fatigue analysis based on the number of zero crossings. Pfluegers Arch. 391:78-80

Hägg, G.M. (1992) Interpretation of EMG spectral alterations and alteration indexes at sustained contraction. J. Appl. Physiol. 73:1211-1217

Håkansson, C.H. (1956) Conduction velocity and amplitude of the action potential as related to circumference in the isolated frog muscle. Acta. Physiol. Scand. 37:14-34

Håkansson, C.H. (1957a) Action potential and mechanical response of isolated cross striated frog muscle at different degrees of stretch. Acta. Physiol. Scand. 39:199-216

Håkansson, C.H. (1957b) Action potentials recorded intra- and extracellularly from the isolated frog muscle fiber in Ringer's solution and in air. Acta. Physiol. Scand. 39:291-312

Hagberg, M., and Ericson, B-E. (1982) Myoelectric power spectrum dependence on muscular contraction level of elbow flexors. Eur. J. Appl. Physiol. 48:147-156

Hagberg, C., and Hagberg, M. (1988) Surface EMG frequency dependence on force in the masseter and the anterior temporalis muscles. Scand. J. Dent. Res. 96:451-456

Häkkinen, K., and Komi, P.V. (1983) Electromyographic and mechanical characteristics of human skeletal muscle during fatigue under voluntary and reflex conditions. Electroenceph. Clin. Neurophysiol. 55:436-444

Hanson, J. (1974) The effects of repetitive stimulation on the action potential and the twitch of rat muscle. Acta. Physiol. Scand. 90:387-400

Hary, D., Belman, M., Propst, J., and Lewis, S. (1982) A statistical analysis of the spectral moments used in EMG tests of endurance. J. Appl. Physiol. 53:779-783

Henneman, H. (1957) Relation between size of neurons and their susceptibility to discharge. Science. 126:1345-1346

Henneman, E., and Olson, C.B. (1965) Relations between structure and function in the design of skeletal muscle. J. Neurophysiol. 28:581-598

Hermens, H.J., Baten, C.T.M., Van Bruggen, T.A.M., Rutten, W.L.C., and Zilvold, G. (1991) Which parameters at motor unit level influence the median frequency of the surface EMG? In: Electromyographical Kinesiology. Anderson, P.A., Hobart, D.J., and Danoff, J.V. (Eds.). Elsevier Science Publishers, Amsterdam

Hilfiker, P. and Meyer, M. (1984) Normal and myopathic propagation of the surface motor unit action potentials. Electroenceph. Clin. Neurophysiol. 57:21-31

Hill, A.V. (1938) The heat of shortening and dynamic constants of muscle. Proc. R. Soc. London Ser. B. 126:136-195

Hill, A.V. (1949) The abrupt transition from rest to activity in muscle. Proc. R. Soc. London Ser. B. 136:399-420

Hill, D.K. (1957) Tension due to interaction between the sliding filaments in resting striated muscle: the effect of stimulation. J. Physiol. (Lond.). 199:637-684

Hodgkin, A. L., and Huxley, A.F. (1952) The dual effect of membrane potential on sodium conductance in the giant axon of the *Loligo*. J. PHysiol. (Lond.). 116:497-506

Hodgkin, A. L., and Rushton, W.A.H. (1946) The electrical constants of a crustacean nerve fiber. Proc. R. Soc. B. 133:449-479

Hodgkin, A.L. (1954) A note on conduction velocity. J. Physiol. 125:221

Holewijn, M. (1991) Temperature effects on EMG and muscle function. In: Electromyographical Kinesiology. Anderson, P.A., Hobart, D.J., and Danoff, J.V. (Eds.). Elsevier Science Publishers, Amsterdam

Homma, S., Iwata, K., Kusama, T., and Nakajima, Y. (1983) Effects of electrical constants on conduction velocity of action potentials measured with unidimensional latency-topography in frog skeletal muscle fibers. Jpn. J. Physiol. 33:711-720

Horita, T., and Ishiko, T. (1987) Relationships between muscle lactate accumulation and surface EMG activities during isokinetic contractions in man. Eur. J. Appl. Physiol. 56:18-23

Hubmayr, R.D., Litchy, W.J., Gay, P.C., and Nelson, S.B. (1989) Transdiaphragmatic twitch pressure: Effects of lung volume and chest wall shape. Am. Rev. Res. Dis. 139:647-652

Humphreys, P.W., and Lind, A.R. (1963) The blood flow through active and inactive muscles of the forearm during sustained handgrip contractions. J. Physiol. (Lond.). 166:120-135

Huxley, A.F, and Niedergerke, R. (1954) Interference microscopy of living muscle fibers. Nature. 173:971-973

Huxley, A.F, and Peachey, L.D. (1961) The maximum length for contraction in vertebrate striated muscle. J. Physiol. (Lond.). 156:150-165

Huxley, A.F, and Simmons, R.M. (1971) Proposed mechanism of force generation in striated muscle. Nature, (Lond.). 133:533-538

Huxley, H.E. (1957) The double array of filaments in cross striated muscle. J. Biophys. Biochem. Cytol. 3:631-648

Huxley H.E. (1985) The crossbridge mechanism of muscular contraction and its implications. J. Exp. Biol. 115:17-30

Huxley, H.E., and Brown, W. (1967) The low-angle x-ray diagram of vertebrate striated muscle and its behavior during contraction and rigor. J. Mol. Biol. 30:383-434

Huxley, H.E. and Hanson, J. (1954) Changes in the cross-striations of muscle during contraction and stretch, and their structural interpretation. Nature, Lond. 173:973-76

Inbar, G.F., Allin, J., and Kranz, H. (1987) Surface EMG spectral changes with muscle length. Med. & Biol. Eng. & Comput. 25:683-689

Inoue, F. (1955) Conduction velocity of action potential in a striated muscle fiber. Natur. Sci. Rep. Ochanomizu. 5:284-290

Jarcho, L.W., Berman, B., Dowben, R.M., and Lilienthal, J.L.Jr. (1954) Site of origin and velocity of conduction of fibrillary potentials in denervated and skeletal muscle. Am. J. Physiol. 178:129-134

Javaheri, S., Vinegar, A., Smith, J., and Donovan, E. (1987) Use of a modified Swan-Ganz pacing catheter for measuring P_{di} and diaphragmatic EMG. Pflugers. Arch. 408:642-645

Johnson, H.D. (1968) The cardia and hiatus hernia. Springfield, Illinois, Charles C. Thomas. pp 17-30.

Jones, D.A., Bigland-Ritchie, B., and Edwards, R.H.T. (1979) Excitation frequency and muscle fatigue: mechanical responses during voluntary and stimulated contractions. Exp. Neurol. 64:401-413

Jones, N.B., and Lago, P.J.A. (1982) Spectral analysis and the interference EMG. IEEE Proc. 129:673-678

Juel, C. (1988) Muscle action potential propagation velocity changes during activity. Muscle & Nerve. 11:714-719

Kadefors, R., Kaiser, E., and Pétersen, I. (1968) Dynamic spectrum analysis of myopotentials with reference to muscle fatigue. Electromyography. 8:39-74

Kahn, J.F., and Monod, H. (1989) Fatigue induced by static work. Ergonomics. 32:839-846

Kaiser, E., and Pétersen, I. (1963) Frequency analysis of muscle action potentials during

tetanic contraction. Electromyography. 3:5-17

Kandell, E., and Schwartz, J.H. (1985) Principles of Neural Science. 2nd edition. Elsevier Science Publishing Co., New York, NY

Kappert, H.F., Jonas, I., Schnell, K.D., and Rakosi, T. (1989) Frequency spectrum and integral value of electromyographic recording of the masseter and temporal muscles in correlation with muscle length. [German]. Deutsche Zahnarztliche Zeutschrift. (Abstract) 44: 908-10

Katz, B. (1948) The electrical properties of the muscle fiber membrane. Proc. Roy. Soc. B. 135:506-534

Katz, B. (1966) Nerve, Muscle, and Synapse. McGraw-Hill, New York.

Kelsen, S.G., Wolanski, T., Supinski, G.S., and Roessmann, U. (1983) The effect of elastase induced emphysema on diaphragmatic muscle structure in hamsters Am. Rev. Res. Dis. 127:330-334

Keynes, R.D., and Aidley, D.J, (1991) In: Nerve and Muscle. 2nd edition. Cambridge University Press.

Kim, M.J., Druz, W.S., Danon, J., Machnach, W., and Sharp, J.T. (1978) Effects of lung volume and electrode position on esophageal diaphragmatic EMG. J. Appl. Physiol. 45:392-398

Kimura, J. (1983) Electrodiagnosis in diseases of nerve and muscle. F.A. Davis Company, Philadelphia, PA.

Kirchberger, M.A. (1990) General Physiological Principles. In: Best and Taylor's Physiological Basis of Medical Practice. J.B. West (ed.). Williams & Wilkins, Baltimore, MD.

Klein, W.A., Parkman, H.P., Dempsey, D.T., and Fisher, R.S. (1993) Sphincter like thoracoabdominal high pressure zone after esophagogastrectomy. Gastroenterology. 105:1362-1369

Knappeis, G.G., and Carlsen, F. (1968) The ultrastructure of the M-line in skeletal muscle. J. Call. Biol. 38:202-211

Koepke, G.H., Smith, E.M., Murphy, A.J., and Dickinson, D.G. (1958) Sequence of action of the diaphragm and intercostal muscles during respiration: I. Inspiration. Arch. Phys. Med. Rehabil. 39:426-430

Koepke, G.H. (1960) The electromyographic examination of the diaphragm. Bull. Am. Assoc. Electromyogr. Electrodiagn. 7:8

Kogi, K., and Hakamada, T. (1962) Slowing of the surface electromyogram and muscle strength in muscle fatigue. Reports of Institute for Science of Labour Tokyo. 60:24-41

Koh, T.J., and Grabiner, M.D. (1992) Cross-talk in surface electromyograms of human hamstring muscles, J. Orthopedic Res. 10:701-709

Koh, T.J., and Grabiner, M.D. (1993) Evaluation of methods to minimize cross-talk in surface electromyography. J. Biomechanics. 26(Suppl):151-157

Komi, P.V., and Viitasalo, J.H.T. (1976) Signal characteristics of EMG at different levels of muscle tension. Acta. Physiol. Scand. 96:267-276

Kondo, S. (1960) Anthropological study on human posture and locomotion. Mainly from the viewpoint of electromyography. J. Fac. Sci. Univ. Tokyo V-II-2, 189

Konno, K., and Mead, J. (1967) Measurement of the separate volume changes in rib cage and abdomen during breathing. J. Appl. Physiol. 22:407-422

Körner, L., Parker, P., Almström, C., Herberts, P., and Kadefors, R. (1984) The relation between spectral changes of the myoelectric signal and the intramuscular pressure of human skeletal muscle. Eur. J. Appl. Physiol. 52:202-206

Kossev, A., Gerasimenko, Y., Gantchev, N., and Christova, P. (1991) Influence of the interpulse interval on the propagation velocity of the motor unit potentials. Electromyogr. Clin. Neurophysiol. 31:27-33

Kossev, A., Gantchev, N., Gydikov, A., Gerasimenko, Y., and Christova, P. (1992) The effect of muscle fiber length change on motor unit potentials propagation velocity. Electromyogr. Clin. Neurophysiol. 32:287-294

Kukulka, C., and Clamann, P. (1981) Comparison of the recruitment and discharge properties of motor units in human brachial biceps and adductor policis during isometric contraction. Brain Res. 219:44-55

Kwantny, E. Thomas, D.H., and Kwantny, H.G. (1970) An application of signal processing techniques to the study of myoelectric signals. IEEE Trans. Biomed. Eng. 17:303-313

Lago, P., and Jones, N.B. (1977) Effect of motor unit firing time statistics on the EMG power spectra. Med. Biol. Eng. Comput. 15:648-655

Landau, B.R., Akert, K., and Roberts, T.S. (1962) Studies on the innervation of the diaphragm. J. Comp. Neurol. 119:1-10

Langman, J. (1978) Coelomic cavity and mesenteries. In: Medical Embryology. Baltimore, MD. Williams & Wilkins, pp. 305-307

Lansing R., and Savelle, J. (1989) Chest surface recording of diaphragmatic potentials in man. Electroenceph. Clin. Neurophysiol. 72:59-68

Lantzy, A., O'Day, T.L., Vazquez, R.D., Guthrie, R.D., and Watchko, J.F. (1991) Diaphragmatic electromyogram power-spectral analysis as a function of reduced end-expiratory lung volume. Pediatr. Res. 30:606-609

Lateva, Z.C., Dimitrova, N.A., and Dimitrov, G.V. (1993) Effect of recording electrode position along a muscle fibre on surface potential power spectrum. Journ. Electromyogr. Kinesiol. 3:195-204

Lieberman, D.A., Faulkner, J., Craig, A., and Maxwell, L. (1973). Performance and histochemical composition of the guinea pig and human diaphragm. J. Appl. Physiol. 34:233-7

Lindström, L. (1970) On the frequency spectrum of EMG signals. Res. Lab. Med. Electr., Göteborg, Sweden, Tech.Rep. 7:70

Lindström, L. (1973) A model describing the power spectrum of myoelectric signals. Part I: single fiber signal. Res. Lab. Med. Electr., Göteborg, Sweden, Tech. Rep. 5:73

Lindström, L., Magnusson, R., and Pétersen, I. (1970) Muscular fatigue and action potential conduction velocity changes studied with frequency analysis of EMG signals. Electromyography, 10:341-356

Lindström, L., and Broman, H. (1974) A model describing the power spectrum of myoelectric signals. Part III: summation of motor unit signals. Res. Lab. Med. Electr., Göteborg, Sweden, Tech. Rep. 9:74

Lindström, L., and Kadefors, R. (1974) A model describing the power spectrum of myoelectric signals. Part IV: total power. Res. Lab. Med. Electr., Göteborg, Sweden, Tech. Rep. 10:74

Lindström, L., Kadefors, R., and Pétersen, I. (1977) An electromyographic index for localized muscle fatigue. J. Appl. Physiol. 43:750-754

Lindström, L., and Magnusson, R. (1977) Interpretation of myoelectric power spectra: A model and its applications. Proc. IEEE. 65:653-662

Lindström, L. and Petersen, I. (1981) Power spectra of myoelectric signals: motor unit activity and muscle fatigue. In: Neurology, Vol. 1: Clinical Neurophysiology, Chapt. 3. E. Stalberg, and R.R. Young (Eds.). Butterworths publishing Co., London

Lindström, L. and Pétersen, I. (1983) Power spectrum analysis of EMG signals and its applications. In: Computer-aided electromyography. Prog. Clin. Neurophysiol., Vol. 10. Ed. J.E. Desmedt. pp. 1-51, Karger, Basel.

Lippold, O.C.J. (1952) The relation between the integrated action potentials in human muscle and its isometric tension. J. Physiol. (Lond.). 117:492-499

Lippold, O.C.J., Redfearn, J.W.T., and Vuco, J. (1960) The electromyography of fatigue. Ergonomics. 3:121-131

Listerud, M.B., and Harkins, H.N. (1959) Variations in the muscular anatomy of the esophageal hiatus: based on the dissections of two hundred and four fresh cadavers. Western. J. Surg. 67:110-112

Lopez, J.R., Wanek, L.A., and Taylor, S.R. (1981) Skeletal muscle: length-dependent effects of potentiating agents. Science. 214:79-82

Loring, S.H., and Mead, J. (1982) Action of the diaphragm on the rib cage inferred from a force-balance analysis. J. Appl. Physiol. 53:756-760

Lourenco, R.V., and Mueller, E.P. (1967) Quantification of electrical activity in the human diaphragm. J. Appl. Physiol. 22:598-600

Low, A. (1907) The crura of the diaphragm and the muscle of Treitz. J. Anat. Physiol. 42:93-96

Luff, A.R. (1981) Dynamic properties of the inferior rectus, extensor digitorum longus, diaphragm and soleus muscles. J. Physiol. (Lond.) 313:161-71

Lynn, P.A., Bettles, N.D., Hughes, A.D., and Johnson, S.W. (1978) Influences of electrode geometry on bipolar recordings of the surface electromyogram. Med. Biol. Eng. Comput. 16:651-660

Lynn, P.A. (1979) Direct on-line estimation of muscle fiber conduction velocity by surface electromyography. IEEE Trans. Biomed. Eng. 26:564-571

Macklem, P.T., Gross, D., Grassino, A.E., and Roussos, Ch. (1978) Partitioning of inspiratory pressure swings between diaphragm and intercostal/accessory muscles. J. Appl. Physiol. 44:200-208

Martin, A.R. (1954) The effect of change in length on conduction velocity in muscle. J. Physiol. (Lond.) 125:215-220

Martonosi, A.N. (1982) Regulation of cytoplasmic calcium concentration by the sarcoplasmic reticulum. In: Disorsers of the motor unit. D.L. Schottland (Ed.). John Wiley & Sons. New York.

Masaki, T., Endo, N., Ebashi, S. (1967) Localization of 6s component of alpha-actinin at the Z band. J. Biochem. (Tokyo). 62:630-632

Masuda, T., and DeLuca, C.J. (1991) Recruitment threshold amd muscle fiber conduction velocity of single motor units. J. Electromyogr. Kinesiol. 2:116-123

Masuda, T., Miyano, H., and Sadoyama, T. (1983a) The propagation of motor unit action potential and the location of the neuromuscular junction investigated by surface electrode arrays. Electroenceph. Clin. Neurophysiol. 55:594-600

Masuda, T., Miyano, H., and Sadoyama, T. (1983b) The distribution of the myoneural junctions in the biceps brachii investigated by surface electromyography. Electroenceph. Clin. Neurophysiol. 56:597-603

Masuda, T., and Sadoyama, T. (1986) The propagation of single motor unit action potentials detected by a surface electrode array. Electroenceph. Clin. Neurophysiol. 63:590-598

Mathias, R.T., Levis, R.A., and Eisenberg, R.S. (1981) Electrical models of excitation-contraction coupling and charge movements in skeletal muscle. J. Gen. Physiol. 76:1-31

McCully, K.K., and Faulkner, J.A. (1983) Length-tension relationship of mammalian diaphragm muscles. J. Appl. Physiol. 54:1682-1686

McKenzie, D.K., and Gandevia, S.C. (1991) Skeletal muscle properties: diaphragm and chest wall. In: The Lung: *Scientific Foundations*. R.G. Crystal and J.B. West (Eds.). Raven Press Ltd., New York.

Mead, J. (1973) In: Loaded Breathing (Discussion) Eds. L.D. Pengelly, A.S. Rebuck, and E.J.M. Campbell. Longman Canada Limited. pp. 206-208

Mead, J. (1979) Functional significance of the zone of apposition of diaphragm to rib cage. Am. Rev. Res. Dis. 119:31-32

Mead, J., and Loring, S.H. (1982) Analysis of volume dispiacement and length changes of the diaphragm during breathing. J. Appl. Physiol. 53:750-755

Merletti, R., Sabbahi, M.A., and DeLuca, C.J. (1984) Median frequency of the myoelectric signal: effects of muscle ischemia and cooling. Eur. J. Appl. Physiol 52:258-265

Merletti, R., Knaflitz, M., and DeLuca, J.C. (1990) Myoelectric manifestations of fatigue in voluntary and electrically elicited contractions. J. Appl. Physiol. 69:1810-1820

Merletti, R., Knaflitz, M., and DeLuca, J.C. (1992) Electrically evoked myoelectric signals. Crit. Rev. Biomed. Eng. 19:293-340

Mills, K., and Edwards R. (1984) Muscle fatigue in myophosphorylase deficiency: power spectral analysis of the electromyogram. Electroenceph. Clin. Neurophysiol. 57:330-335

Milner-Brown, H.S., and Stein, R.B. (1975) The relationship between the surface electromyogram and muscular force. J. Physiol. (Lond.) 246:549-569

Moller, E. (1966) The chewing apparatus. Acta. Physiol. Scand. 69 (Suppl): 280, 229

Morimoto, S., Umazume, Y., and Masuda, M. (1980) Properties of spike potentials detected by a surface electrode in intact human muscle. Jpn. J. Physiol. 30:71-80

Morimoto, S., and Masuda, M. (1984) Dependence of conduction velocity on spike interval during voluntary muscular contraction in human motor units. Eur. J. Appl. Physiol. 53:191-195

Morimoto, S. (1986) Effect of length change in muscle fibers on conduction velocity in human motor units. Jpn. J. Physiol. 36:773-782

Moritani, T., Gaffney, F.D., Charmichael, T., and Hargis, J. (1985) Interrelationships among muscle fiber types, electromyogram, and blood pressure during fatiguing isometric contrac-

tion. In: Biomechanics IX-A. Winter D.A. (ed). Human Kinetics Publishers, III, pp. 287-292

Moritani, T., and Muro, M. (1987) Motor unit activity and surface electromyogram power spectrum during increasing force of contraction. Eur. J. Appl. Physiol. 56:260-265

Mortimer, J.T., Magnusson, R., and Petersén, I. (1970) Isometric contraction, muscle blood flow, and the frequency spectrum of the electromyogram. Proc. 1st nordic meeting on medical and biological engineering, Otaniemi, Finland, pp 142-144

Mortola, J.P., and Sant'Ambrogio, G. (1978) Motion of the rib cage and abdomen in tetraplegic patients. Clin. Sci. Mol. Med. 54:25-32

Moxham, J., Wiles, C.M., Newham, D., and Edwards, R.H.T. (1980). Sternomastoid function and fatigue in man. Clin. Sci. Mol. Med. 59:463-468

Moxham, J., Morris, A.J.R., and Spiros, G. (1981) Contractile properties and fatigue of the diaphragm in man. Thorax. 36:164-168

Mucke, R., and Heuer, D. (1989) Behaviour of EMG parameters and conduction velocity in contractions with different muscle temperatures. Biomed. Biochim. Acta. 48:459-464

Muller, N.G., Gulston, G., Cade, D., Whitton, J., Froese, A.B., Bryan, M.H., and Bryan, C. (1979) Diaphragmatic fatigue in the newborn. J. Appl. Physiol. 46:688-695

Murthy, K.R., Paul, N.L., and De Luca, C.J. (1991) Effects of motor unit synchronization and mean firing rate changes on myoelectric signal frequency spectrum. In: Electromyographical Kinesiology. Anderson, P.A., Hobart, D.J., and Danoff, J.V. (Eds.). Elsevier Science Publishers, Amsterdam

Naeije, M., and Zorn, H. (1982) Relation between EMG power spectrum shifts and muscle fiber action potential conduction velocity changes during local muscular fatigue in man. Eur. J. Appl. Physiol. 50:23-33

Naeije, M., and Zorn, H. (1983) Estimation of the muscle action potential conduction velocity in human skeletal muscle using the surface EMG cross-correlation technique. Electromyogr. Clin. Neurophysiol. 23:73-80

Nastuk, W.L., and Hodgkin, A.L. (1950) The electrical activity of single muscle fibers. J. Cell. Comp. Physio. 35:39-73

Newman, S., Road, J., Bellemare, F., Clozel, J.P., Lavigne, C.M., and Grassino, A.E. (1984) Respiratory muscle length measured by sonmicrometry. J. Appl. Physiol. 56:753-764

Newsome Davis, J. (1967) Phrenic nerve conduction in man. J. Neurol. Neorosurg. Psychiat. 30:420-426

Nishizono, H., Saito, Y., and Miyashita. (1979) The estimation of conduction velocity in human skeletal muscles in situ with surface electrodes. Electroenceph. Clin. Neurophysiol. 46:659-664

Norris, F.H., and Irwin, R.L. (1961) Motor unit area in a rat muscle. Am. J. Physiol. 200:944-946

Oetlicker, H., and Schumperli, R.A. (1982) Influence of sarcomere length, tonicity, and external sodium concentration on conduction velocity in frog muscle fibers. J. Physiol. (Lond) 332: 203-221

Okada, M. (1987) Effect of muscle length on surface EMG wave forms in isometric contractions. Eur. J. Appl. Physiol. 56:482-486

Önal, E., Lopata, M., and Evanich, J. (1979) Effects of electrode position on esophageal diaphragmatic EMG in humans. J. Appl. Physiol. 47:1234-1238

Önal, E., Lopata, M., Ginzburg, A.S., and O'Connor T.D. (1981) Diaphragmatic EMG and transdiaphragmatic pressure measurements with a single catheter. Am. Rev. Res. Dis. 124:563-565

Palacios, J.O., Alegria, F.A., and Posso, S.S. (1993) The influence of interelectrode distance on bipolar recording of sensory nerve action potential. A mathematical study. Electromyogr. Clin. Neurophysiol. 33:73-78

Palla, S., and Ash, M.M. (1981) Effect of bite force on the power spectrum of the surface electromyogram of human jaw muscles. Arch. Oral. biol. 26:287-295

Parker, P.A., and Scott, R.N. (1973) Statistics of the myoelectric signal from monopolar and bipolar electrodes. Med. and Biol. Eng. 11:591-596

Pataro, V.A., Piombo, H.S., Suarez, D.Z., and Acrish, M.W. (1961) Anatomic aspects of the esophageal hiatus: distribution of the crura in its formation. A study of sixty fresh human specimens. J. Int. Coll. Surg. 35:145

Payne, W.S., and Olsen, A. (1974) The esophagus. Lea & Febiger. Philadelphia, PA

Peachey, L.D., and Adrian, R.H. (1973) Electrical properties of the transverse tubular system. In: The structure and function of muscle, 2nd edition, Vol. III, Physiology and Biochemistry. G.H. Bourne (Ed.). Academic press, New York.

Person, P.A., and Kudina, L.P. (1968) Cross-correlation of electromyograms showing interference patterns. Electroenceph. Clin. Neurophysiol. 25:58-68

Person, R.S., and Mishin, L.N. (1964) Auto- and cross-correlation analysis of the electrical activity of muscles. Med. Electron. Biol. Engng. 2:155-159

Peter, J.B., Bernard, R.J., and Edgerton, V.R. (1972) Metabolic profiles of three fiber types of skeletal muscle in guinea pigs and rabbits. Biochemistry. 11:2627

Petit, J.M., Milic-Emili, G., and Delhez, L. (1960) Role of the diaphragm in breathing in conscious

normal man. J. Appl. Physiol. 15:1101-1106

Petrofsky, J.S. (1979) Frequency and amplitude analysis of the EMG during exercise on the bicycle ergometer. Eur. J. Appl. Physiol. 41:1-15

Petrofsky, J.S., and Lind, A.R. (1980a) Frequency analysis of the surface electromyogram during sustained isometric contractions. Eur. J. Appl. Physiol. 43:173-182

Petrofsky, J.S., and Lind, A.R. (1980b) The influence of the temperature on the amplitude and frequency components of the EMG during brief and sustained contractions. Eur. J. Appl. Physiol. 44:189-200

Petrofsky, J.S., Glaser, R.M., and Phillips, C.A. (1982) Evaluation of the amplitude and frequency components of the surface EMG as an index of muscle fatigue. Ergonomics. 25:213-223

Pette, D., and Vrbova, G. (1985) Neural control of phenotypic expression in mammalian muscle fibers. Muscle & Nerve. 8:676-689

Piper, H. (1912) Electrophysiologie muschliche muskeln. Basel: Springer-Verlag. 126.

Polgar, J., Johnson, M.A., Weightman, D., and Appleton, D. (1973) Data on fibre size in thirty-six human muscles, an autopsy study. J. Neurol. Sci. 19:307-318

Rack, P.M.H., and Westbury, D.R. (1969) The effects of length and stimulus rate on tension in the isometric cat soleus muscle. J. Physiol. 204:443-460

Rahn, H., Otis, A.B., Chadwick, L.E., and Fenn, W.O. (1946) The pressure-volume diagram of the thorax and lung. Am. J. Physiol. 146:161-178

Ralston, H.J., Inman, V.T., Strait, L.A., and Shaffrath, M.D. (1947) Mechanics of human isolated voluntary muscle. Am. J. Physiol. 151:612-620

Reid, M.B., Ericson, G.C., Feldman, H.L., and Johnson, R.L.Jr. (1987) Fiber types and fiber diameters in canine respiratory muscles. J. Appl. Physiol. 62:1705-1712

Repko, K.D., Greene, J.G., and Enderle, J.D. (1989) A comparison of esophageal and chest electrodes in studying the diaphragmatic EMG. Biomed. Sci. Instrum. 25:89-91

Reucher, H., Rau, G., and Silny, J. (1987a) Spatial filtering of non-invasive multielectrode EMG: Part 1-Introduction to measuring techniques and applications. IEEE Trans. Biomed. Eng. 34:98-105

Reucher, H., Rau, G., and Silny, J. (1987b) Spatial filtering of non-invasive multielectrode EMG: Part 2-Filter performance in theory and modelling. IEEE Trans. Biomed. Eng. 34:106-113

Ridgway, E.B., and Gordon, A.M. (1975) Muscle activation: effects of small length changes

on calcium release in single fibers. Science. 189:881-883

Rios, E., and Pizzaro, G. (1991) The voltage sensor of excitation-contraction coupling in skeletal muscle. Physiol. Rev. 71:849-908

Roberts, D.V. (1969) Simultaneous measurement of propagation velocity of action potential and contraction wave in frog striated muscle. J. Physiol. (Lond.) 147:62-63

Rochester, D.F. (1992) Respiratory muscles: structure, size, and adaptive capacity. In: Breathlessness (The Campbell Symposium) Eds. Jones, N.L., and Killian. Boehringer Ingelheim. pp.2-12.

Rourke, M., Erlandson, R.F., and Joynt, R.L. (1984) Quantitative analysis of computer simulated EMG interference patterns. Muscle & Nerve. 7:570-578

Roussos, C., and Macklem, P.T. (1982) The respiratory muscles. New Engl. J. Med. 307:786-796

Roy, S.H., DeLuca, C.J., and Schneider, J. (1986) Effects of electrode location on myoelectric conduction velocity and median frequency estimates. J. Appl. Physiol. 61:1510-1517

Saadeh, P.B., Sosner, J., and Wolf, E. (1987) Needle EMG of the diaphragm: a new technique. Arch. Phys. Med. Rehabil. 68:599

Sackner, J.D., Nixon, A., Davis, B., Atkins, N., and Scakner, M. (1980) Non-invasive measurement of ventilation during exercise using respiratory inductive plethysmography. Am. Rev. Res. Dis. 122:867-871

Sadoyama, T., and Miyano, H. (1981) Frequency analysis of surface EMG to evaluation of muscle fatigue. Eur. J. Physiol. 47:239-246

Sadoyama, T., Masuda, T., and Miyano, H. (1983) Relationships between muscle fiber conduction velocity and frequency parameters of surface EMG during sustained contraction. Eur. J. Appl. Physiol. 51:247-256

Sadoyama, T., Masuda, T., and Miyano, H. (1985) Optimal conditions for the measurement of muscle fiber conduction velocity using surface electrode arrays. Med. & Biol. Eng. & Comp. 23:339-342

Sadoyama, T., and Masuda, T. (1987) Changes of the average muscle fiber conduction velocity during a varying force contraction. Electroenceph. Clin. Neurophysiol. 67:495-497

Saitou, K., Okada, M., Sadoyama, T., and Masuda, T. (1991) Effect on surface EMG wave forms of electrode location with respect to the neuromuscular junctions: its significance in EMG-muscle length relation. In: Electromyographical Kinesiology. P.A. Anderson, D.J. Hobart, and Danoff, J.V. (Eds.). Elsevier Science Publishers B.V. Excerpta Medica, Amsterdam.

Salmons, S., and Sreter, F.A. (1976) Significance of impulse activity in the transformation of

skeletal muscle type. Nature (Lond.). 263:30-34

Sanchez, J., Medrano, G., Debesse, B., Riquel, M., and Derenne, J.P. (1985) Muscle fiber types in costal and crural diaphragm in normal men and in patients with moderate chronic respiratory disease. Bull. Res. Physiopatol. Respir. 21:351-356

Sant'Ambrogio, G., Frazier D.T., Wilson, M.F., and Agostoni, E. (1963) Motor innervation and pattern of activity of cat diaphragm. J. Appl. Physiol. 18:43-46

Sato, M. (1965) Some problems in the quantitative evaluation of muscle fatigue by frequency analysis of the electromyogram. J. Anthrop. Soc. Nippon. 73:20-27

Sato, H. (1976) Power spectral analysis of surface electromyograms during isometric contractions. J. Anthropol. Soc. Nippon. 84:1-14

Sato, H. (1982) Functional characteristics of human skeletal muscle revealed by spectral analysis of the surface electromyogram. Electromyogr. Clin. Neurophysiol. 22:459-516

Scherrer, J., and Bourguignon, A. (1959) Changes in the electromyogram produced by fatigue in man. Am. J. Phys. Med. 38:170-180

Schweitzer, T.W., Fitzgerald, J.W., Bowden, J.A., and Lynn-Davies, P. (1979) Spectral analysis of human diaphragm electromyogram. J. Appl. Physiol. 46:152-165

Seki, K., Miyazaki, Y., Watanabe, M., Nagata, A., and Narysawa, M. (1991) Surface electromyogram spectral characterization and motor unit activity during voluntary ramp contraction in men. Eur. J. Appl. Physiol. 63:165-172

Shankar, S., Gander, R.E., and Brandell, B.R. (1989) Changes in the myoelectric signal (MES) power spectra during dynamic contractions. Electroenceph. Clin. Neurophysiol. 73:142-150

Sharp, J.T., and Hyatt, R.E. (1986) Mechanical and electrical properties of the respiratory muscles. In: Handbook of Physiology, Section 3: The Respiratory System, Vol. III. Mechanics of Breathing, Part 2. Fishman, A.P., Macklem, P.T., Mead, J. (Eds.).

Sharp, J.T., Hammond, M.D., Aranda, A.U., and Rocha, R.D. (1993) Comparison of diaphragm EMG centroid frequencies: esophageal versus chest surface leads. Am. Rev. Res. Dis. 147:764-767

Shehata, R. (1966) The crura of the diaphragm and their nerve supply. Acta. Anat. 63:49-54

Sherington, C.S. (1925) Remarks on some aspects of reflex inhibition. Proc. R. Soc. Lond. (Biol). 97:519-45

Sieck, G.C. (1991) Diaphragm motor units and their response to altered use. Sem. Resp. Med. 12:258-269

Sieck, G.C., and Fournier, M. (1989) Diaphragm motor unit recruitment during ventilatory and non-

ventilatory behaviors. J. Appl. Physiol. 66:2539-2545

Sinderby, C.S. (1991) On diaphragmatic function and fatigue in cervical cord injury patients and prior polio infection patients. Thesis. University of Göteborg, Göteborg, Sweden. ISBN# 91-628-0282-8

Sinderby, C.S., Lindström, L., and Grassino, A. (1993a) Automatic EMG selection for diaphragmatic fatigue diagnosis (Abstract). Am. Rev. Res. Dis. (Suppl) 147:A697

Sinderby, C., Lindström, L., and Grassino, A.E. (1993b) Inter-electrode distance filtering function in measurements of diaphragmatic EMG (Abstract). Am. Rev. Res. Dis. (Suppl) 147:A697

Sinderby, C., Lindström, L., and Grassino, A.E. (1993) Action potential conduction velocity does not change with muscle length. Faseb Journal. 7:A221

Sinderby, C., Comtois, N., and Grassino, A.E. (1994) Influence of adjacent muscle cross-talk on the costal diaphragm electromyogram. Am. Rev. Res. Dis.(Abstract) 149:A131

Skinner, D.B. (1972) In: Gastroesophageal reflux and hiatal hernia. Eds. D.B. Skinner, R.H.R. Belsey, T.R. Hendrix, and G.D. Zuidema. Chap.2, Anatomy. Little Brown and Company, Boston.

Slater, C.R., and Harris, J.B. (1988) The anatomy and physiology of the motor unit. In: Disorders of voluntary muscle, 5th edition. J. N. Walton (Ed.). Churchil Livingstone, New York.

Sollie, G., Hermens, H.J., Boon, K.L., Wallinga-De Jonge, and Zivold, G. (1985a) The boundary conditions for measurement of the conduction velocity of muscle fibers with surface EMG. Electromyogr. Clin. Neurophysiol. 25:45-56

Sollie, G., Hermens, H.J., Boon, K.L., Wallinga-De Jonge, and Zivold, G. (1985b) The measurement of conduction velocity of muscle fibers with surface EMG according to the cross-correlation method. Electromyogr. Clin. Neurophysiol. 25:193-204

Solomonow, M, Baten, C., Smit, J., Baratta, R., Hermens, H., D'Ambrosia, R., and Shoji, H. (1990) Electromyogram power spectra frequencies associated with motor unit recruitment strategies. J. Appl. Physiol. 68:1177-1185

Stålberg, E. (1966) Propagation velocity in human muscle fibers in situ. Acta. Physiol. Scand. (Suppl.) 287, 70:2-112

Stephens, J.A., Garnett, R., and Buller, N.P. (1978) Reversal of the recruitment order of single motor units produced by cutaneous stimulation during voluntary muscle contraction in man. Nature. 272:362-364

Stolov, W.C., and Weiplepp, T.G. (1966) Passive length-tension relationship of intact muscle, epimysium and tendon in normal and denervated gastrocnemius of the rat. Arch. Phys. Med. Rehabil. 47:612-620

Stulen, F.B. and DeLuca, J.C. (1978) The relation between the myoelectric signal and physiological properties of constant force isometric contractions. Electroenceph. Clin. Neurophysiol. 45:681-689

Stulen, F.B., and DeLuca, C.J. (1981) Frequency parameters of the myoelectric signal as a measure of muscle conduction velocity. IEEE Trans. Biomed. Eng. 7:515-523

Swenson, M.R., and Rubenstein, R.S. (1992) Phrenic nerve conduction studies. Muscle & Nerve. 15:597-603

Sypert, G.W., and Munson, J.B. (1981) Basis of segmental motor control: motoneuron size or motoneuron type? Neurosurgery. 8:608-621

Tarkka, I.M. (1984) Power spectrum of electromyography in arm and leg muscles during isometric contractions and fatigue. J. Sports. Med. 24: 189-194

Taylor, A. (1960) The contribution of the intercostal muscles to the effort of respiration in man. J. Physiol. (Lond.) 151:390-402

Tesch, P.A., Komi, P.V., Jacobs, I., Karlsson, J., and Viitasalo, J.T. (1983) Influence of lactate accumulation on EMG spectrum during repeated concentric contractions. Acta. Physiol. Scand. 119:61-67

Testut, L. (1921) La traité d' anatomie humaine. Paris. Doin. édit. 5., pp. 874-886

Thornton, M.W., and Schweisthal, M.R. (1969) The phrenic nerve: Its terminal divisions and supply to the crura of the diaphragm. Anat. Rec. 164:283-290

Tokita, T., Tashiro, K., and Kato, K. (1970) Electromyography of the sophagus and its clinical applications. Acta. Otoralyng. 70:269-278

Trontjel, J.V. (1993) Muscle fiber conduction velocity changes with length. Muscle & Nerve. 16:506-512

Tusiewicz, K., Moldofsky, H., Bryan, A.C., and Bryan M.H. (1977) Mechanics of the rib cage and diaphragm during sleep. J. Appl. Physiol. 43:600-602

Van Boxtel, A., and Schomaker, L.R.B. (1984) Influence of motor unit firing statistics on the median frequency of the EMG power spectrum. Eur. J. Appl. Physiol. 52:207-213

Vander, A.J., Sherman, J.H. and Luciano, D.S. (1985). Muscle. In: Human Physiology: The Mechanisms of Body Function. Fourth Edition. McGraw-Hill, New York. pp 255-298.

van Harrevald, A. (1947) On the force and size of motor units in the rabbit's m. sartorious muscle. Am. J. Physiol. 151:96-106

Varguese, G., and Rogoff, J.B. (1983) Influence of interelectrode distance on antidromic sensory potentials. Electromyogr. clin. Neurophysiol. 23:297-301

Vergara, J., Tsien, R.Y., and Delay, M. (1985) Inosotol [1,4,5]-trisphosphate: a possible chemical link in excitation-contraction coupling in muscle. Proc. Natl. Acad. Sci. 82:6352-6356

Vestergaard-Poulsen, P. Thomsen, C., Sinkjaer, T., Stubgaard, M., Rosenfalck, A., and Henriksen, O. (1992) Simultaneous electromyogram and ^{31}P nuclear magnetic resonance spectroscopy- with application to muscle fatigue. Electroenceph. Clin. Neurophysiol. 85:402-411

Vigreux, B., Cnockaert, J.C., and Pertuzon, E. (1979) Factors influencing quantified surface EMGs. Eur. J. Appl. Physiol. 41:119-129.

Viitasalo, J.H.T., and Komi, P.V. (1977) Signal characteristics of EMG during fatigue. Eur. J. Appl. Physiol. 37:111-121

Viitasalo, J.H.T., and Komi, P.V. (1978) Interrelationships of EMG signal characteristics at different levels of muscle tension and during fatigue. Electromyogr. Clin. Neurophysiol. 18:167-178

Volpe, P., Salviati, G., Divirgilio, F., and Pozzari, T. (1985) Inosotol [1,4,5]-trisphosphate induces calcium release from the sarcoplasmic reticulum of skeletal muscle. Nature. 316:347-349

Vracko, R. (1974) Basal lamina scaffold- anatomy and significance for the maintenance of orderly tissue structure: a review. Am. J. Pathol. 77:314-347

Wade, O.L. (1954) Movements of the thoracic cage and the diaphragm in respiration. J. Physiol. 124:193-212

Walker, S.M. (1960) The relation of stretch and of temperature to contraction in skeletal muscle. Am. J. Phys. Med. Rehabil. 39:234-258

Weber, A., and Herz, R. (1963) The binding of calcium to actomyosin systems in relation to their biological activity. J. Biol. Chem. 238:599-605

Weinberg, J., Sinderby, C., Lindström, and Grassino, A. (1993) The role of diaphragm recruitment in EMG signal analysis (Abstract). Am. Rev. Res. Dis. (Suppl) 147:A698

Westbury, J.R., and Shaughnessy, T.G. (1978) Associations between spectral representation of the surface electromyogram and fiber type distribution and size in human masseter muscle. Electroenceph. Clin. Neurophysiol. 27:427-435

Williamson, B.R.J., Gouse, J.C., Rohrer, D.G., and Teates, C.D. (1987) Variation on the thickness of the diaphragmatic crura with respiration. Radiology. 163:683-684

Willison, R.G. (1964) Analysis of the electrical activity in healthy and dystrophic muscle in man. J. Neurol. Neurosurg. Psych. 27:386-394

Winans, C.S. (1972) Alteration of lower esophageal sphincter characteristics with respiration and

proximal balloon distension. Gastroenterology. 62:380-388

Winkler, T., Stalberg, E., and Haas, L.F. (1991) Uni- and bipolar surface recording of human nerve responses. Muscle & Nerve. 14:133-141

Wray, D.W. (1988) Neuromuscular transmission. In: Disorders of voluntary muscle, 5th edition. J. N. Walton (Ed.). Churchil Livingstone, New York.

Wyman, R.J. Waldron, I., and Wachtel, G.M. (1974) Lack of a fixed order of recruitment in cat motoneuron pools. Exp. Brain. Res. 20:101-114

Yaar, I., and Niles, L. (1992) Muscle fiber conduction velocity and mean power spectrum frequency in neuromuscular disorders and in fatigue. Muscle & Nerve. 15:780-787

Zipp, P. (1978) Effect of electrode parameters on the bandwidth of the surface EMG power density spectrum. Med. Biol. Comput. 116:537-541.

Zipp, P. (1982) Effect of electrode geometry on the selectivity of the myoelectric recordings with surface electrodes. Eur. J. Appl. Physiol. 50:35-40

Zwarts, M.J., Haenen, H.T.M., and Van Weerden, T.W. (1987) The relation between the average muscle fiber conduction velocity and EMG power spectra during isometric contraction, recovery, and ischemia. Eur. J. Appl. Physiol. 56:212-216

Zwarts, M.J., Van Weerden, T.W., Links, T.P., Haenen, H.T.M., and Oosterhuis, H.J.G. (1988) The muscle fiber conduction velocity and power spectra in familial hypokalemic periodic analysis. Muscle & Nerve. 11:166-173